

**MULTI-OBJECTIVE EVOLUTIONARY  
OPTIMIZATION OF PHOTOVOLTAIC GLASS  
FOR THERMAL, DAYLIGHT, AND ENERGY  
CONSIDERATION**

**A Thesis Submitted to  
the Graduate School of Engineering and Sciences of  
İzmir Institute of Technology  
in Partial Fulfillment of the Requirements for the Degree of**

**MASTER OF SCIENCE**

**in Architecture**

**by  
Aybüke TAŞER**

**April 2023  
İZMİR**

## ACKNOWLEDGMENTS

I want to express my deepest appreciation to my supervisor Prof. Tuğçe Kazanasmaz for her endless support, guidance, patience, and encouragement during the last three years. This thesis is enhanced by her precious presence. She helped me to build interdisciplinary and different perspectives into this study. I have always been intensely motivated by the dedication to her job.

I would like to present my gratefulness to my co-supervisor Assoc. Prof. Başak Kundakcı Koyunbaba has always assisted and inspired me with her strong background and technical support.

I want to express my gratitude to the members of the examining committee, Prof. Dr. Müjde Altın and Assist. Prof. Dr. Berk Ekici approved my M.Sc. thesis.

I would like to thank my lovely family, my mother, Yeşim Taşer, my father, Nuri Taşer, and my little brother, Emir Taşer, for their unconditional support throughout my whole academic life.

I want to express my thankfulness to my dearest friends and all my colleagues at the Izmir University of Economics, Faculty of Fine Arts and Design. I would like to extend my special gratefulness to Res. Assist. Filiz Özbengi Uslu, Gözde Damla Turhan, and Selen Çiçek for their emotional support. I also would like to present my endless appreciation to Prof. Ender Yazgan Bulgun, Assist. Prof. Emre Gönlügür, Assoc. Prof. Aslı Ceylan Öner, Assist. Prof. Athanasios Stasinopoulos and Assoc. Prof. Burkey Pasin for their support throughout this thesis and my academic life at the Izmir University of Economics.

I also would like to thank Assoc. Prof. Zeynep Durmus Arsan, Dr. Berk Ekici, and Assoc. Prof. Ahenk Yılmaz who have significantly contributed to building my architectural and academic career.

Lastly, I want to express my dearest thankfulness to my beloved Emir Emirbayer, who was the light to find motivation during tough times. This thesis would have been incomplete without your existence in my life.

# ABSTRACT

## MULTI-OBJECTIVE EVOLUTIONARY OPTIMIZATION OF PHOTOVOLTAIC GLASS FOR THERMAL, DAYLIGHT, AND ENERGY CONSIDERATION

As the industry has expanded and the population has increased recently, so have the World's energy consumption and greenhouse gas emissions. Buildings are responsible for almost 40% of this consumption and emissions. They should be designed following energy-efficient and sustainable strategies. One of the most practical methods for increasing building energy efficiency and reducing environmental effects is building-integrated photovoltaic systems, which use solar energy to generate electricity on-site. This thesis explores the potential of photovoltaic glass technology in an architecture studio at the Izmir Institute of Technology Campus in Izmir, Turkey. The initial part of the study uses simulation modeling and field measurements in three scenarios to test the benefits of this technology in terms of thermal and lighting energy consumption and comfort levels. Scenarios included amorphous silicon thin-film modules in three transmittance values modeled in existing windows. Research findings propose that photovoltaic glasses have the potential to balance the room's lighting loads in a range between 15.1-and 20.3%. They improved occupant thermal and visual comfort by preventing overheating and glare risks. They also decreased cooling loads. Then, the study uses a genetic optimization algorithm to explore the optimum potential of the system in terms of annual energy consumption and daylight performance. Design variables are the window-to-wall ratio (i.e., window size and location) and amorphous-silicon thin-film solar cell transmittance to generate optimum Pareto-front solutions for the case building. Optimization objectives are minimizing annual thermal (i.e., heating and cooling) loads and maximizing Spatial Daylight Autonomy. Optimized results of Low-E semi-transparent amorphous-silicon photovoltaic modules applied on the window surface show that the Spatial Daylight Autonomy is increased to 82% with reduced glare risk and higher visual comfort for the occupants. Photovoltaic modules helped reduce the room's seasonal and annual lighting loads by up to 26.7%. Compared to non-optimized photovoltaic glass, they provide 23.2% more annual electrical energy.

## ÖZET

### FOTOVOLTAİK CAMIN TERMAL, GÜN IŞIĞI VE ENERJİ BAKIMINDAN ÇOK AMAÇLI EVRİMSEL OPTİMİZASYONU

Son zamanlarda endüstri genişledikçe ve nüfus arttıkça, Dünya'nın enerji tüketimi ve sera gazı emisyonları da artmaktadır. Bu tüketim ve emisyonların yaklaşık %40'undan binalar sorumludur. Binalar, enerji verimli ve sürdürülebilir stratejiler izlenerek tasarlanmalıdırlar. Bina enerji verimliliğini artırmanın ve çevresel etkileri azaltmanın en yaygın yöntemlerinden biri, güneş enerjisini kullanarak yerinde elektrik üreten binaya entegre fotovoltaik sistemlerdir. Bu çalışma, İzmir, Türkiye'deki İzmir Yüksek Teknoloji Enstitüsü Kampüsü'ndeki bir mimarlık stüdyosunda fotovoltaik cam teknolojisinin potansiyelini keşfetmeyi amaçlamaktadır. Çalışmanın ilk bölümünde, bu teknolojinin termal ve aydınlatma enerjisi tüketimi ve konfor seviyeleri açısından faydalarını test etmek için üç senaryoda simülasyon modellemesi ve saha ölçümleri kullanılmaktadır. Senaryolar, mevcut pencerelerde modellenen üç geçirgenlik değerine sahip amorf silikon ince film modüllerini içermektedir. Araştırma bulguları, fotovoltaik camların odanın aydınlatma yüklerini %15.1 ile %20.3 arasında dengeleme potansiyeline sahip olduğunu göstermektedir. Aşırı ısınma ve parlama risklerini önleyerek kullanıcıların termal ve görsel konforunu iyileştirmekte ve soğutma yüklerini de azaltmaktadırlar. İkinci bölümde, sistemin yıllık enerji tüketimi ve gün ışığı performansı açısından optimum potansiyelini keşfetmek için bir genetik optimizasyon algoritması kullanılmaktadır. Tasarım değişkenleri arasında pencere-duvar oranı (pencere boyutu ve konumu) ve optimum Pareto verimliliği oluşturmak üzere amorf silikon ince film güneş pili geçirgenliği yer alır. Optimizasyon hedefleri, yıllık termal (ısıtma ve soğutma) yükleri en aza indirmek ve Mekansal Gün Işığı Otonomisini en üst düzeye çıkarmaktır. Pencere yüzeyine uygulanan düşük emisyonlu yarı saydam amorf silikon fotovoltaik modüllerinin optimize edilmiş sonuçları, Mekansal Gün Işığı Özerkliğinin %82'ye yükseltildiğini, parlama riskinin azaldığını ve bina kullanıcıları için daha yüksek görsel konfor sağladığını göstermektedir. Fotovoltaik modülleri, seçilen odanın mevsimsel ve yıllık aydınlatma yüklerini %26.7'ye kadar düşürmeye yardımcı olmaktadır. Son olarak, optimize edilmemiş fotovoltaik cama kıyasla yıllık %23.2 daha fazla elektrik enerjisi sağlamaktadırlar.

# TABLE OF CONTENTS

LIST OF FIGURES .....	viii
LIST OF TABLES .....	x
CHAPTER 1. INTRODUCTION .....	1
1.1. Theoretical Background & Problem Statement .....	1
1.2. Research Aim and Objectives .....	5
1.3. Structure of the Study .....	6
CHAPTER 2. LITERATURE REVIEW .....	7
2.1. Building Daylight Performance .....	7
2.1.1. Daylight Benefits .....	7
2.1.2. Daylight in Educational Buildings .....	8
2.1.3. Daylight Performance Metrics .....	9
2.1.4. Building Daylight Simulation .....	10
2.2. Building Energy Performance.....	11
2.2.1. Energy Performance Metrics.....	11
2.2.2. Building Energy Simulation.....	12
2.3. Building Performance Optimization .....	13
2.3.1. Optimization.....	13
2.3.2. Benefits of Optimization .....	14
2.3.3. Optimization Types .....	15
2.3.4. Optimization Methods and Algorithms.....	16
2.3.4.1. Evolutionary Algorithms.....	17
2.4. Building Integrated Photovoltaic Systems.....	18
2.4.1. Field of Application .....	18
2.4.1.1. Roof Applications .....	18
2.4.1.2. Façade (Wall) Applications.....	19
2.4.1.3. Glazing Applications.....	19

2.4.1.3. Shading System Applications .....	21
2.4.2. Production Technologies.....	22
2.4.2.1. First-Generation PV Cells.....	22
2.4.2.2. 2 <sup>nd</sup> Generation PV Cells (Thin-Film Solar Cells).....	24
2.4.2.3. Third Generation PV Cells.....	25
2.4.3. BIPV Types .....	29
2.4.3.1. Solar Cell Glazing.....	29
2.4.3.2. BIPV Module .....	30
2.4.3.3. BIPV Tile .....	30
2.4.3.4. BIPV Foil .....	30
2.4.4. Opportunities in the Market and Feasibility.....	31
2.5. Contributions from the Literature Review .....	31
CHAPTER 3. METHODOLOGY .....	40
3.1. Study Design.....	40
3.2. Case Building.....	41
3.3. Experimental Setting.....	44
3.4. Simulation Models .....	45
3.4.1. Daylight Simulation Model.....	45
3.4.2. Energy Simulation Model .....	46
3.5. Calibration.....	49
3.6. Multi-Objective Genetic Optimization .....	49
CHAPTER 4. RESULTS .....	53
4.1. Measurement Results .....	53
4.2. Calibration Results.....	55
4.3. Base Case Results .....	57
4.4. PV Glass Scenario Results.....	60
4.5. PV Glass Optimization Results.....	64
4.5.1. Pareto-front Analysis: Optimum Design Variables and Objectives .....	64

4.5.2. Optimum Daylight Performance Model: Highest sDA Solutions.....	69
4.5.3. Optimum Energy Performance Model: Lowest Thermal Load Solutions.....	71
CHAPTER 5. DISCUSSION AND CONCLUSION .....	73
REFERENCES .....	78
APPENDICES .....	95
APPENDIX A. COMPARATIVE ANALYSIS OF LITERATURE REVIEW.....	97
APPENDIX B. GRASSHOPPER SCRIPT FOR DAYLIGHT AND ENERGY SIMULATIONS .....	116
APPENDIX C. POINT-IN-TIME DAYLIGHT ANALYSIS OF BASE CASE UNDER CLEAR SKY WITH SUN AND OVERCAST SKY CONDITIONS .....	117
APPENDIX D. POINT-IN-TIME DAYLIGHT ANALYSIS OF 30% TRANSMITTANCE PV WINDOW UNDER CLEAR SKY WITH SUN AND OVERCAST SKY CONDITIONS.....	120
APPENDIX E. POINT-IN-TIME DAYLIGHT ANALYSIS OF 20% TRANSPARENT PV WINDOW UNDER CLEAR SKY WITH SUN AND OVERCAST SKY CONDITIONS .....	123
APPENDIX F. POINT-IN-TIME DAYLIGHT ANALYSIS OF 10% TRANSPARENT PV WINDOW UNDER CLEAR SKY WITH SUN AND OVERCAST SKY CONDITIONS .....	126

# LIST OF FIGURES

<b><u>Figure</u></b>	<b><u>Page</u></b>
Figure 2.1. (a) PV glass implementation on the façade of SwissTech Convention Center in Lausanne, Switzerland (Photo by Dr. Berk Ekici) (b) PV window application on the south façade of an education building in IZTECH Campus in İzmir, Turkey (c) PV implementation on the roof of EPFL building in Lausanne, Switzerland (Photo by Dr. Berk Ekici) (d) PV implementation on the roof of Schüco in Bielefeld, Germany (Photo by Dr. Onurcan Çakır) (e) PV canopy implementation on Tanjong Pagar Center by SOM Architects in Singapore by Solar Company OnyxSolar © (OnyxSolar 2022) (f) PV skylight implementation on Bell Works building in Holmdel, NJ (Solar Company: OnyxSolar ©) (OnyxSolar 2022) .....	20
Figure 2.2. PV production technologies .....	23
Figure 2.3. (a) Colored (orange) PV glass application in Block E, IZTECH Campus (b) Colored (blue) PV glass application in Block E, IZTECH Campus .....	25
Figure 2.4. Varied solar cell implementation on buildings.....	27
Figure 2.5. The number of annually published papers in 2002–2022 on BIPVs.....	32
Figure 2.6. The factors BIPV implementation depends on.....	33
Figure 2.7. BIPV systems implemented in countries.....	33
Figure 2.8. (a) Solar cell types used in studies (b) Climate types in studies. ....	35
Figure 2.9. Tools used in the studies .....	35
Figure 2.10. (a) Experimental conditions (b) Analysis type of the studies. ....	36
Figure 2.11. (a) Building types that BIPVs are implemented in studies (b) Evaluation criteria in studies.....	36
Figure 3.1. Method flowchart of the study .....	41
Figure 3.2. (a) Selected architecture faculty building (b) Interior of the architecture studio .....	42
Figure 3.3. (a) Köppen-Geiger Climate Specification system in World (b) Mediterranean climate indication according to Köppen Climate Specification .....	42
Figure 3.4. Hourly illumination of direct normal and global horizontal in lux .....	43
Figure 3.5. (a) Location of case building on the aerial view (b) Sun path diagram with the indication of the case building .....	43
Figure 3.6. Photos of inner and outer climate data loggers (1: indoor, 2: outdoor).....	44



<b><u>Figure</u></b>	<b><u>Page</u></b>
Figure 3.7. Location of inner and outer dataloggers with red circle and an indication of selected classroom in the yellow hatch.....	45
Figure 3.8. Grasshopper component script for the thermal and daylight simulations .....	49
Figure 3.9. Octopus interface.....	51
Figure 3.10. Illustration of window size change during the optimization process .....	52
Figure 4.1. Indoor and outdoor monitored data of temperature, relative humidity .....	55
Figure 4.2. Daily average temperatures per two calibration models: simulated/monitored indoor temperatures and outdoor temperatures .....	57
Figure 4.3. (a) Annual daylight autonomy results according to 500 lux threshold (b) Annual daylight autonomy results according to 2000 lux threshold.....	58
Figure 4.4. (a) Daily energy consumption for lighting during day-time on the clear sky with sun (b) Daily energy consumption for lighting during day-time on overcast sky.....	59
Figure 4.5. (a) Hourly energy consumption for heating of whole building (b) Hourly energy consumption for cooling the whole building. ....	59
Figure 4.6. The studio's annual daylight autonomy results in different transmittance a-Si thin-film photovoltaic modules.....	62
Figure 4.7. Hourly energy production results of 10% transmittance PV glass for South and East façades, respectively .....	63
Figure 4.8. a) Seasonal lighting load under a clear sky with sun condition and PV energy generation comparison (b) Seasonal lighting load under overcast sky condition and PV energy generation comparison .....	65
Figure 4.9. Pareto-front results of evolutionary algorithm .....	66
Figure 4.10. The base case, 30% transmittance PV glass, and three best-performed Pareto-front genomes' daylight autonomy results according to the 500 lux and 2000 lux thresholds .....	68
Figure 4.11. The hourly plot of heating and cooling energy consumption data and PV electrical energy generation data of the Pareto-front (1) solution .....	70

# LIST OF TABLES

<b><u>Table</u></b>	<b><u>Page</u></b>
Table 2.1. Comparison of different cell types regarding materials, efficiency, and appearance. ....	28
Table 2.2. Review of the optimization studies.....	36
Table 3.1. The weather conditions and locations of the selected building. ....	43
Table 3.2. Annual radiation and illumination weather data of Izmir, Turkey. ....	43
Table 3.3. The surface material specifications for the daylight simulations. ....	46
Table 3.4. Building material specifications .....	47
Table 3.5. Data input details and schedules for energy simulation model .....	48
Table 3.6. Optimization specifications for the Octopus multi-objective optimization algorithm.....	50
Table 3.7. Optimization specifications for the Octopus multi-objective optimization algorithm.....	52
Table 4.1. Monitored data on highest/lowest temperature and relative humidity .....	53
Table 4.2. Photovoltaic glass specifications (Source: Onyx 2021) .....	61
Table 4.3. Photovoltaic system electrical specifications (Source: Onyx 2021).....	61
Table 4.4. Seasonal lighting load and PV energy generation comparison .....	63
Table 4.5 Overall energy and daylighting data.....	63
Table 4.6. Pareto-front optimization genomes show each objective and variable in detail. ....	66
Table 4.7. Seasonal lighting load of the studio and PV glass electrical energy generation comparison. ....	68
Table 4.8. Overall energy and daylighting data.....	69
Table 4.9. Optimization genomes for highest sDA showing each objective and variable. ....	70
Table 4.10. Optimization genomes for the lowest total thermal loads showing each objective and variable in detail. ....	71
Table 4.11. Optimization solutions range for each objective and variable.....	72

# CHAPTER 1

## INTRODUCTION

### 1.1. Theoretical Background & Problem Statement

The World has been demanding more energy as the industry has grown recently. Significant environmental contamination has occurred by the widespread use of fossil fuels (IEA 2016: Nicoletti et al., 2015: Outgouga and Jamouli 2022). Thus, renewable energy has been developed competitively because of the shortage of energy (Meng et al., 2018). Building-integrated photovoltaic (BIPV) systems, which use solar energy to generate electricity on-site, have been recognized as possible practical ways to enhance energy saving of buildings and minimize environmental impact (EPIA 2011). With the help of BIPV technology, it is possible to use buildings as a source of electrical energy by embedding photovoltaic (PV) materials into the building envelope components (Peng, Huang, and Wu 2011).

PV systems use solar energy that is absorbed to generate electricity. BIPV is a novel type that has recently emerged on the market. They are connected to the parts of the building (i.e., roof, façade, slab, shading device) instead of a detached component away from the building envelope to meet some energy needs. Many researchers recommend using these systems for new buildings and renovating existing ones. As a relatively new application, semi-transparent PV (STPV) glazing has gained the interest of many researchers due to its capacity to generate energy and provide daylighting illumination (Meng et al., 2018).

Recent studies show that STPV cells might increase the building energy efficiency when applied to the glazing (Qiu and Hongxing 2020). It not only improves buildings' overall performance but can also enhance occupants' thermal and visual comfort. There are various types of semi-transparent thin-film solar cells in the industry. Each performs differently due to its various electrical and optical properties. Several studies have shown their potential, but it is noted in many research that amorphous silicon (a-Si) solar cells are preferable to other types of solar cells. According to the literature, it increases energy savings for heating and cooling loads (Martellotta, Cannavale, and Ayr 2017). There are three main research methods to assess the overall

performance of PV glazing technology. One may be the utilization of devices that can monitor the real-time performance of these systems. A study aims to understand the potential of PV glazing in terms of energy, daylight, and thermal performance using real-time measurement tools (Li et al., 2009). The brief results show that PV glazing and shading elements can decrease the building's electrical energy consumption and lighting load. A similar study proposed to test monocrystalline silicon solar cells' daylight and energy performance implemented on a PV shading device using field tests and a scale model (Lee 2019). Results proposed that architectural variables such as the incline angle and PV implemented area of the shading device significantly affect its performance. With digital tools' development, simulation-based software can be used in such research. They test the performance of any system without using such devices. One related study focuses on the energy, daylight, and aesthetic properties of façade-integrated PVs (FIPV) installed in different balconies in Trondheim, Norway (Xiang and Matusiak 2022). Simulation, survey, and mathematical methods for users to assess their overall performance. Results propose that side balconies are preferable in terms of daylight performance and energy generation, while partial balcony railings with complementary colors are more desirable in an aesthetical sense. It is noted in the study that FIPV and roof-integrated PVs can cover the energy need of an eleven-story building by up to 60%. Another study proposes a smart low-E PV glazing system containing a thermotropic layer that changes its visibility and optical properties to prevent overheating inside an office building in Nottingham, UK (Liu and Wu 2022). The specified PV is tested in thermal, electrical, and optical aspects. Brief results show that BIPV smart windows with different window-to-wall ratios, orientations, and transition temperatures affect the energy-saving potential of a building by up to 36.6% with higher visual comfort of occupants. A review study analyses different types of PV glazing, such as single and double glazing with or without ventilation. Studies in the literature are reviewed based on their energy generation and thermal performance. Study results indicate that conventional glazing can store more heat in the summer when compared with PV glazing. Also, PV glazing can contribute to the building's energy-saving capacity by reducing the cooling loads in hot climate regions (Yu et al., 2021). One study compares PV glass' energy and thermal performance with conventional glazing (Zhang et al., 2016). Conventional glazing types are single and double pane glazing for this study. The results demonstrate that semi-transparent solar cells applied on windows can decrease total annual electricity consumption by 16% and 18% in

temperate climates such as Hong Kong. PV glass improves a building's daylight performance and energy and thermal efficiency. One study discovered solar glazing could significantly enhance a façade's daylight performance. Also, they offered 26.5% of energy savings during the winter. According to one research, PV glasses could balance the lighting loads in a room between 15.1% and 20.3% (Taşer et al., 2022). They reduced the risk of overheating, cooling loads, and glare with enhanced occupant thermal and visual comfort. The third method emerges from the optimization approaches in that some studies have developed optimization models to generate optimum BIPV design. A study implemented an asymmetric concentrator PV glazing to the South façade of a building to enhance its energy generation and daylight performance. Experimental models have been created to assess its performance (Xuana et al. 2019). An optimization model has been developed to reduce the shading effect of each concentration array. The study variables are the gaps of concentrators, and the objectives are high optical quality, daylight, and energy performance. The optimization model indicates a suitable asymmetric concentrator PV glazing on the South façade of the building. A related study proposes assessing four different BIPVs' energy performance in three different climatic zones (Skandalos and Karamanis 2021). Thermal and visual comfort simulations are conducted through TRNSYS software. Results proposed that BIPV technology greatly impacts achieving zero-energy buildings. The optimization process has achieved an energy saving of up to 43%. The BIPV flexibility index is increased to 0.57 for varied climate regions. Indoor thermal and visual comfort are increased to 54% and 83%, respectively. An initiative study proposes an optimized model for façade integrated BIPVs in an office building in Gyeonggi-Do, Korea (Hwang, Kang, and Kim 2012). Brief study results show that BIPV can cover the need for building electricity in a range of 1-and 5% if optimization is applied to the performance objectives (Chae et al., 2014). BIPV systems are unique because they perform differently in varied climatic areas. One related work tests PV glass' thermal, energy, and daylight performance in diversified regions. It is suggested in the study that PV glass's optical characteristics should be optimized according to the climate. A similar study focused on optimizing different BIPV shading system configurations to maximize solar irradiation (Freitas and Brito 2015). It is found in the results that a tilted louver can produce up to 40% more electrical energy compared to a standard flat and vertical shading device. A recent study investigates the effect of different glazing types and window sizes on daylight performance and energy efficiency

for an office building in Algeria (Mesloub, Albaqawy, and Kandar 2020). Double-glazing PV modules with a 20% window-to-wall ratio are considered optimal PV windows. They provided 60% energy saving for the south façade.

Integrating new technology RESs into buildings with optimization algorithms was one of the possible sustainable solutions to increase building energy saving (Wijeratne et al., 2022). The optimization algorithm seeks to find the optimal solution. In a numerical sense, achieving the maximum or minimum value for different building variables is the procedure. Building performance optimization works with several design variables. Single or multi-objective optimization procedures are applied according to the number of objectives in the studies. Two methods can be preferred in multi-objective optimization problems. One is the weighted sum model, and the other is the Pareto front optimization method. Pareto optimization aims to find the trade-off or Pareto front between different building performance metrics or objectives. It seeks to dominate each genome objective (i.e., the solutions) (Evins 2013). Broadly two optimization methods used in the studies: conventional and computational optimizations. Both can be used for performative computational architecture (PCA). Conventional optimization methods analyze predefined design variables, while computational optimization methods work with optimization algorithms to achieve suitable building performance (Ekici et al., 2021). There is the evolutionary algorithm (EA) in the context of computational optimizations. It is also called population-based optimization. EAs work with populations of solutions to optimization problems. The population evolves into better candidates (Simon 2013). As a sub-class of evolutionary algorithms, there is a genetic algorithm (GA), a heuristic optimization method. It is a biological evolution's natural selection process (Galletly 1998). GA is based on biologically inspired variables, selection, mutation, and crossover to develop outstanding ideal generations for optimization tasks. The population generates an ideal solution as the GA arbitrarily selects good-performing solutions from the current population and employs them as parents to construct the next generation (MathWorks 2016). GA can solve complex design problems and multi-objective optimizations and eliminate failure rates due to simulation (Nguyen, Reiter, and Rigo 2014). Architectural decisions are significant in the design phase of buildings since they influence the building's performance (Sariyildiz 2012). Optimization algorithms provide practical guidance for the conceptual design of a project (Asadi and Geem 2015). They also allow for saving costs and time for architects by providing guidance. Simulations are

essential in most daylight and energy studies. Thus, the optimization process assesses many design decisions without simulating them manually.

## **1.2. Research Aim and Objectives**

Although studies in recent literature mainly concentrate on the efficiency of PV glass and their effect on the improvement of building performance, the target of this study is to discover the rate of coupling impact of PV glasses on an existing room in terms of heating, cooling and lighting loads together and visual comfort requirements in a comprehensive approach. We assume that this study is a trial renovation project, including shifting the existing glazing with the PV ones and revising the window areas. Thus, this thesis aims to understand whether the power generated from PV glasses can match the lighting loads of that room (studio) after renovation. It is significant since the optical modification in glasses alters the daylight passage inside. In this sense, the study contributes an original perspective to the literature. It uses digital and manual tools to analyze and validate the results and obtain broad conclusions on using this technology in such a building.

Therefore, the study intends to respond questions below:

1. What is the potential of PV glass in terms of energy, thermal, and daylight performance of educational buildings?
2. How are window-based parameters capable of thermal and daylight performance in PV glass-implemented buildings?

This study focuses on multiple energy efficiency and visual comfort aspects (i.e., daylight performance, energy consumption, and PV energy generation) rather than concentrating on a single performance object. Also, multiple architectural design decisions such as window size, location, and PV module transparency are widely explored using Octopus genetic optimization algorithm. For these reasons, the study concentrates on many aspects, optimizing an architecture studio of Izmir Institute of Technology Campus in İzmir, Turkey, for energy saving, energy generation, and enhancing daylight performance with visual and thermal comfort of occupants. The study seeks to understand the potential of PV technology based on the building's annual heating and cooling loads and the selected reference room's Spatial Daylight Autonomy (sDA).

### 1.3. Structure of the Study

Chapter 1 defines the research problem on a global scale and its possible solutions. The chapter mainly considers the theoretical background, problem statement, research motivations, research aim, and objectives.

Chapter 2 summarizes building daylight and energy performance, performance metrics, and simulation methods. The chapter then moves on to building performance optimization benefits, types, and tools. Building-integrated photovoltaic systems are introduced in this chapter. Fields of application, production technologies, types, and opportunities in the market are presented. Then, the summary of the BIPV-related studies and contributions from the literature are explained in this section.

Chapter 3 explains the methodology of the study. The study design, experimental setting of field measurements, simulation models, calibration, and optimization methods are described in this part.

Chapter 4 represents the results of the study. The chapter first presents the measurement and calibration results according to monitoring and simulation. Afterward, PV glass scenario results are presented and compared in detail. Finally, the optimization results of PV glass are indicated in this chapter.

Chapter 5 discusses the results and concluding remarks of the study. In this chapter, all results are interpreted in detail.

Some part of this thesis has been published in several journals and conference proceedings. *Chapter 2* (i.e., Literature Review) is published by the Journal of Solar Energy (Taşer, Koyunbaba, and Kazanasmaz 2023). *Chapter 4* (i.e., Headings 4.1.-4.4.) is published by IEEE Xplore (Taşer et al., 2022) *Chapter 3*, *Chapter 4* (i.e., Heading 4.5.), and *Chapter 5* are submitted to the Journal of Solar Energy for the consideration of publication.



## CHAPTER 2

### LITERATURE REVIEW

#### 2.1. Building Daylight Performance

##### 2.1.1. Daylight Benefits

The benefits of daylight can be divided into four categories: visual comfort, energy efficiency, occupant productivity, and health. Daylight is essential to human health in a built environment (Alhagla, Mansour, and Elbassuoni, 2019). The effect of natural light on human health is proven in many studies. According to one study, it has been confirmed that the availability of natural light significantly affects occupant health and productivity (Edwards and Torcellini 2002). Since it helps produce Vitamin D on the skin, it prevents many diseases.

It also influences occupant comfort and productivity (Fang 2017). It strongly enhances occupant mood and productivity in a working or learning space. One study proved that people prefer to work near window zones for more natural light (Joseph 2006). It is closely related to it improving their mood and motivation.

Additionally, it has been proved in many studies that daylight contributes to the energy savings of buildings. Windows are effective on heat gain and heat losses. Thus, they are responsible for a building's thermal and energy performance. The importance of selecting a proper glazing type for energy-saving is investigated in one study (Hee, Alghoul, Bakhtyar, et al., 2015). The glazing type and many parameters affecting daylight also influence the energy-saving potential of a building. Therefore, they need to be appropriately designed and well-understood.

Occupant discomfort may occur in terms of both visual and thermal. Poor daylight performance creates very dark and bright surfaces. It affects human perception, comfort, and productivity. Occupant productivity may decrease when there is not enough availability of daylight. The lack of natural light also increases a building's lighting loads. As a result, both money and energy would be wasted.

On the contrary, productivity similarly decreases due to excessive illumination (Day et al., 2019). Excessive illumination occurs due to the direct penetration of light

through interior space. When this happens, this causes discomfort for occupants due to glare. As a result of direct penetration of daylight, excessive heat gain also occurs. It heats interiors and increases energy loads (Francesca 2015).

This section categorizes daylight benefits under four headings: providing visual comfort, energy savings, occupant productivity, and occupant health. This study investigates energy-saving and visual comfort due to daylight performance.

### **2.1.2. Daylight in Educational Buildings**

Daylight is significant in every type of building, especially in educational ones. It is critical for the physical and psychological aspects of the educational process in a classroom (Galal 2019). Since classrooms are occupied mainly during the daytime, daylight influences students' concentration and success (Bayram and Kazanasmaz 2016). A successful educational building should enhance students' curiosity and learning motivation and make them feel physically and psychologically comfortable (Samiou, Doulos, and Zerefos 2022).

Regarding physical aspects, daylight significantly influences student health because it is associated with eyesight and biological parts of the human body (Kralikova, Dzunova, and Rusko 2020). Poor daylight performance may cause headaches and eye strain (Day et al., 2019). Windows are significant in this sense. They provide daylight and create a visual connection between indoors and outdoors. Outdoor views in working and learning environments may contribute to occupant health. One study aimed to understand the effect of daylight availability on thermal perception and the health of occupants (Jiang et al., 2022). It is found that occupants who have a window in their working environments feel more thermally comfortable. They have less stress and fatigue.

Daylight-related problems may occur due to lack of daylight, availability of excessive daylight, glare, flicker, and shadows. When a classroom lacks daylight, daylight performance influences student psychology (Liu et al., 2022). It has been proved in many studies that proper daylight performance can increase occupant productivity when they are processing work (Van Bommel 2006). One study found that students have higher productivity and satisfaction when accessing daylight. A correlation between daylight availability and student productivity is strongly seen in the

study (Day et al., 2019). A study noted that occupants with an adequately lit environment could have a better mood and well-being (Veitch et al., 2008). It is also found that they see their workplaces as more appealing. A similar study investigates occupant preferences using light availability in the space (Cuttle 1983). Results of the study present that 86% of occupants choose natural light instead of artificial light. Also, 99% of the occupants feel pleased and comfortable with a window in their working spaces. Occupant well-being and motivation are closely related to their comfort. Visual comfort allows individuals to comprehend the area and its items without effort, but visual discomfort makes it more challenging. Visual pain may occur due to glare. It causes eye strain and occupant dissatisfaction.

There are some factors of daylight performance. These are daylight illuminance level, daylight uniformity, glare risks, and light sources' color rendering index (Frontczak 2010). These factors influence students' visual comfort, health, productivity, and well-being. Thus, supplying an adequate lighting environment is essential for students to preserve their work. In this study, daylight illuminance level and glare risks are studied to provide visual comfort and decrease the thermal loads of the classroom.

### **2.1.3. Daylight Performance Metrics**

The researchers defined different performance metrics for daylight throughout the time. These are developed to evaluate the quantity of daylight on surfaces in interior spaces. There are static and dynamic daylight metrics (Nezamdoost and Van Den Wymelenberg 2017). Static daylight metrics calculate one point-in-time value. Illuminance and Daylight Factor are examples of static daylight metrics.

Illuminance measures the amount of light on a surface over the unit area. Illuminance is estimated in lux. It expresses the brightness of the surface (Fang 2017). There are recommended illuminance values for each type of building. For example, at least 300 lux illuminance value is required for educational buildings. These are determined by Illuminating Engineering Society (IES). The daylight factor is another type of static daylight metric. It is calculated as the ratio of indoor daylight illuminance to outdoor daylight illuminance. Its unit is a percentage (%). It changes due to several factors, such as building orientation, location, weather conditions, etc. (Ahmad et al., 2022).

More detailed annual metrics are developed to conduct a comprehensive daylight analysis throughout the time: Useful Daylight Illuminance (UDI) and Daylight Autonomy (DA). UDI defines upper and lower thresholds as “useful” illuminance (Kazanasmaz et al., 2016). UDI is a simple and effective evaluation because it divides the horizontal evaluation plane into useful and non-useful (Marins et al., 2019). DA only has a lower limit illuminance value. DA is a task-illuminance-based measure of daylight performance that is measured annually. DA has been replaced by sDA recently. sDA is “the percent of an analysis area that meets a minimum daylight illuminance level for a specified fraction of the operating hours per year” (IES 2012). This analysis type is beneficial for identifying proper illumination on a work plane during the year. Lastly, the area above-defined illuminance level for more than a desired percentage of time (hour) during a year is known as Annual Sunlight Exposure (ASE). It is helpful in terms of defining the visual discomfort risk (Mangkuto et al., 2018).

#### **2.1.4. Building Daylight Simulation**

Building performance can be assessed with several tools. Simulation-based ones are some of those tools. These are powerful and effective in evaluating the potential of architectural design decisions on the building’s performance (Brembilla, Drosou, and Mardaljevic, 2022). Although the actual building performance and simulation results may differ, building performance simulation tools seem reliable and easy to assess a building’s environmental impact.

Building daylight performance is significantly improved after Climate-Based Daylight Modelling (CBDM). It is developed during the 1990s (Mardaljevic 2000: Reinhart 2001). CBDM applies different intermediate sky models according to illuminance and irradiance values of weather files. The accurate sky models make it applicable to conducting a long-term daylight analysis and other building performance metrics (Wang, Wei, and Ruan 2021).

Researchers use many daylight performance simulation software. Most of them are illuminance-based metrics. Although many daylight simulation tools exist, some can calculate dynamic daylight metrics because they cannot perform annual-based tasks (Leccese et al., 2020). To do that, on-site illuminance measurements with data loggers are preferred. Dataloggers record data in specific time-interval, mostly hourly. These

data can calculate dynamic daylight performance metrics after monitoring is concluded. Although this seems a reliable method, it takes time and money. Thus, a recent and modern tool of daylight performance simulation is used in this study. Honeybee, a Radiance-based simulation plug-in of Grasshopper, directly connects with Rhino geometry to conduct a broad daylight and energy performance analysis. It can perform both point-in-time and annual task-based investigations. Therefore, it can estimate static and daylight performance metrics (Food4Rhino 2022). This thesis evaluates a dynamic daylight performance metric sDA and point-in-time illuminance via Honeybee v1.3.0 of Ladybug v1.3.0 plug-ins of Grasshopper.

## **2.2. Building Energy Performance**

It is noted that buildings' energy consumption covers at least 30% of the energy consumed in the World. The energy demand for buildings has increased significantly in the last decades. It is expected to grow more in the future. Building energy consumption is estimated to rise by 1.5% annually between 2012 and 2040 (Cao, Dai, and Liu 2016). Commercial buildings take great responsibility in this sense because they are responsible for most of the consumed energy of buildings. Retail and educational buildings, offices, hotels, and dining places are the highest energy consumers among commercial buildings (Broberg and Egüez 2018; Ntsaluba and Nwulu 2021). Building energy performance is significant in this sense. It needs to be adequately evaluated.

### **2.2.1. Energy Performance Metrics**

Some metrics are used to evaluate a building's energy performance. These are related to a building's consumed energy. Energy Use Intensity (EUI) is one of these metrics (Borgstein, Lamberts, and Hensen 2016). It is defined as the ratio of the annual energy consumption of a building to its gross floor area (EPA 2016). EUI can be classified as source EUI and site EUI. Source energy is the sum of raw fuel for managing the entire building. Site energy is the consumed heat and electricity energy by the whole building. Site energy is primarily seen in utility bills (EPA 2016a). There is also a method used in residential houses called end-use loads. It started to be used in the IECC and ANSI/RESNET/ICC Standard 301-2014 in 2015 (RESNET 2016). The

difference between these outcomes is that they initialize with the desired outcome (Fairey and Goldstein 2016).

If economic aspects of energy are significant for people, including energy cost analysis in building energy performance assessments is essential. This metric is called cost-weighted energy and is initialized by ASHRAE 90.1-1989. The type of fuel is effective in cost-weighted energy analysis. Some fuel types are cheap such as coal, and some are more expensive, like gas (Fairey and Goldstein 2016).

In sustainability goals, CO<sub>2</sub> emissions are significant. Energy sources emit CO<sub>2</sub> while they are consumed. Thus, emissions-weighted energy turned into a metric used in the studies by ASHRAE Standard 189.1 (Fairey and Goldstein 2016).

There are also rating systems to assess a building's energy performance. For instance, a HERS rating system was developed to determine dwellings' energy performance. Houses are rated between 0 and 100. 0 is attributed to a zero-energy building. By 2016, it was reported that approximately 2 million homes had a HERS rating. Rated dwellings were evaluated after their construction process had been completed. Air leakage and tightness of buildings are significant in the rating process (Fairey and Goldstein 2016). zEPI score is similar to the HERS rating system. Buildings are rated between 0 and 100. 0 identifies a zero-energy building.

### **2.2.2. Building Energy Simulation**

Several factors affect a building's energy use and energy metrics. These may be climatic conditions, building orientation, glazing area, occupancy schedules, occupant density, equipment used in buildings, surrounding building density, shading by trees, etc. All these factors can be tested in simulation models. A building can be three-dimensionally modeled and simulated to estimate its energy performance before, during, and after construction (Augenbroe, 2022).

There are some computational tools to estimate a building's energy consumption. These tools decrease time and money consumption for energy calculations. They are fast and easy to use by researchers. They have been developed a lot in recent years. These tools include EnergyPlus, OpenStudio, IES-VE, TRNSYS, and DOE-2. Some of these tools calculate the building's energy consumption and assess

its indoor environmental quality aspects like thermal/visual comfort and indoor air quality (Wang and Zhai 2016).

Among several tools, EnergyPlus is one of the most reliable and popular. It is an engine that can be used individually or as a plug-in with Grasshopper and OpenStudio. It is open-source and free software. EnergyPlus is a powerful tool for simulating complex and large models. It is developed together with the National Renewable Energy Laboratory (NREL), the U.S. Department of Energy (DOE), National Laboratories, Companies, and Academic institutions (Crawley et al., 2001). EnergyPlus can model complex HVAC and other mechanical systems and calculate heating, cooling, lighting, and ventilation loads by using actual weather data of the region (Bonnema, Leach, and Pless 2013; EnergyPlus 2015). In this study, OpenStudio and EnergyPlus, the extensions of a Grasshopper plug-in, are used.

## **2.3. Building Performance Optimization**

### **2.3.1. Optimization**

Architectural decisions are significant in the design phase of a building since they influence the building's performance (Sariyildiz 2012). Optimization algorithms provide practical guidance for the conceptual design of a project (Asadi and Geem 2015). Simulations are essential in most daylight and energy optimizations. Therefore, the optimization process must assess many design decisions without simulating them manually. In optimization studies, the general aim is to find the optimal solution. In a numerical sense, it is the procedure to achieve the maximum or minimum value of different building variables. Building performance optimization is greatly improved with the developments in parametric design and building performance simulation tools. Algorithmic optimization engines and building performance simulation tools are developed in the late 2000s (Nguyen, Reiter, and Riho 2014).

In optimization logic, there are mainly two different input variables and objectives. Variables are building components and properties such as window-to-wall ratio, geometry, transparency, insulation thickness, floor height, etc. Variables are architectural design decisions. Objectives include building performance criteria such as heating and cooling load, indoor air temperatures, sDA, DA, etc.

### **2.3.2. Benefits of Optimization**

The benefits of optimization are emphasized in many studies. One study highlights that computational optimization is beneficial, especially in the design phase (Evins 2013). It allows for saving costs and time for architects by providing guidance. In the study, the energy performance of a building is optimized with variables of the building envelope and mechanical systems. Another study reveals that energy-related objectives affect the optimization design (Ekici et al., 2019). This review paper noted that the best parameters to optimize the studies are the window-to-wall ratio, shading orientation, window sizes, and building geometry.

A relevant study aims to reduce Danish nearly-zero-energy residential buildings (nZEBs) by optimizing the variables related to daylight performance and thermal comfort (Vanhoutteghem, Skarning, Hviid 2015). The variables are size, orientation, and glazing properties of windows. The study's objective is to see the effects of the variables on heating load, daylight, and thermal performance of nZEBs. The authors use EnergyPlus for energy simulation and DAYSIM for daylight performance simulation. The final result indicates that a balance between thermal comfort and daylight performance of buildings has been achieved with an optimization logic. In addition, low U-values are preferred when large windows are used for heat gain to reduce heating demand. Several design options are suggested in the research for future designs.

Very initiative research proposes to develop optimized models for three different climate zones of the USA regarding daylight and energy performance of buildings (Yuan 2017). First, project variables are defined for the parametric modeling. Then, energy and daylight simulations are conducted for the three cases. The optimization stage is started after the simulation process. One multi-objective model and separate daylight and energy optimization models are created for each case. EnergyPlus and DAYSIM of Ladybug guided daylight and energy simulations, while Octopus, a plug-in of Grasshopper, is used for the optimization process. The final results advise separate optimized models of the same building for three different climatic conditions.

One study measures the efficacy of glazing properties, window size, and orientation on the building's heating and cooling loads and energy needs (Cesari et al., 2018). Glazing properties are defined as the g-value and U-value. Unlike other studies, the study uses only a simulation rather than an optimization method. Authors use Sketch



Up for 3D modeling, TRNSYS software for energy performance analysis, and the TRNBuild package for dynamic simulation. Initially, the building in Bologna, Italy, is modeled, and its energy performance is simulated. Then, commercially available glazing types in the market are defined, and their energy performance is affected. The study evaluates the energy performance of each variable in the simulation model and presents the best-performed ones in terms of heating and cooling load. The study proposes a manual optimization model for the selected building. Results show that narrower windows with proper window glazing can reduce the building's energy demand and heating and cooling loads. In addition, while the heating load depends on the g-value and U-value, the cooling load depends less on these values.

Another study focuses on optimizing the window-based parameters for better thermal comfort and daylight quality in a residential building in Australia (Chen, Hammad, and Kamardeen 2020). Variables are different window types, sizes, and placements. Multi-objective optimization with Revit in Dynamo conducted the research. As a result of the optimized model, an energy saving of %8.5 is provided.

### **2.3.3. Optimization Types**

Building performance optimization works with several design variables. These variables aim to be optimized for better building performance objectives. In the studies, there may be defined single or multi objectives. According to the number of objectives, single or multi-objective optimization procedures are applied. In multi-objective optimization problems, two methods can be preferred. One is the weighted sum model, and the other is the Pareto front optimization method. In the weighted sum model, various objectives are given varying weights, and the weighted objectives are added together to form a single cost function. In the second method, Pareto optimization aims to find the trade-off or Pareto front between different building performance metrics or objectives. It seeks to dominate other objectives together (Evins 2013). The solutions are divided into two dominant and non-dominated solutions in this method. Non-dominated solutions aim to retrofit different objectives at the same time. It means that no other solutions performed better in both performance metrics. Non-dominated solutions form the Pareto front. Dominated solutions retrofit one or some objectives more than others. Therefore, it dominates them. In multi-objective optimization

problems, the Pareto front method is significant because the aim is to improve different performance metrics. This thesis applies multi-objective optimization based on the Pareto front method.

Also, another optimization type may be defined in the “building” sense. Different reference buildings are selected in the studies to optimize their performance. Only one room is optimized in some portions, while the whole building aims to be optimized in other studies. So, a single or multi-zone optimization categorization is a significant one. For example, a multi-zone optimization is carried out in one study for a high-rise building in the Netherlands (Ekici et al., 2021). The study aims to optimize the entire structure by using three different algorithms. Shading devices, glazing types, and building geometry are the variables in the study. The objectives are daylight autonomy, annual sunlight exposure, and some energy standards. It is concluded that multi-zone optimization significantly improves high-rise buildings in urban zones. Another study aimed to minimize the thermal loads and maximize daylighting of a room (Futrell 2015). Four different optimization algorithms are studied in the research. These are compared according to their results’ efficiency. Results show that optimized models significantly improve the daylight and thermal performance of the room compared with the existing situation.

### **2.3.4. Optimization Methods and Algorithms**

There are broadly two different optimization methods used in the studies. These are conventional optimization and computational optimizations. Both can be used for performative computational architecture (PCA). Conventional optimization methods analyze predefined design variables, while computational optimization methods work with optimization algorithms to achieve suitable building performance. Optimization algorithms have been frequently used to deal with the complexity of the design challenge (Ekici et al., 2021). It is essential to define suitable algorithms for different optimization problems.

Different optimization algorithms have been developed throughout time. Other optimization algorithms are reviewed and classified as global and local methods in one study. These are stochastic or deterministic, derivative-based or derivative-free, heuristic or meta-heuristic, and bio-inspired or non-bioinspired methods. It is noted in

review studies that population-based stochastic algorithms are one of the most used algorithm types (Nguyen, Reiter, and Rigo 2014).

#### **2.3.4.1. Evolutionary Algorithms**

The evolutionary algorithm (EA) is also called population-based optimization. EAs work with populations of solutions to optimization problems. In each stage, the population evolves into better candidates. There are three main types of evolutionary algorithms. These are genetic algorithms (GA), evolutionary programming (EP), and evolution strategies (ESs) (Simon 2013).

A genetic algorithm (GA) is a heuristic optimization method. It is a sub-class of evolutionary algorithms. GA is the earliest and most used evolutionary algorithm. It is one of the preferred algorithms in computational optimization studies. It is a biological evolution's natural selection process (Galletly 1998). It modifies the solution population by including nature-based principles. GA is based on biologically inspired variables, including mutation, crossover, and selection, to develop high-quality optimal solutions to optimization problems. The population generates an ideal solution as the GA arbitrarily selects good-performing solutions from the current population and employs them as parents to construct the next generation (MathWorks 2016). GA can solve complex design problems and multi-objective optimizations and eliminate failure rates due to the simulation process (Nguyen, Reiter, and Rigo 2014).

Different tools that work with GAs are available. The most popular tools do not require advanced programming knowledge and have a user-friendly interface. For example, Rhino's Grasshopper parametric modeling tool has special plug-ins that work with GA. Galapagos and Octopus are two of these plug-ins. Galapagos can progress through single-objective optimization, while octopus can conduct multi-objective optimization. This study selects GA as an “optimization algorithm” according to the optimization problem.” The Octopus plug-in of Grasshopper is used to perform the optimization.

## **2.4. Building Integrated Photovoltaic Systems**

First, PV implementations were practiced in the 1980s. It is seen as high technology development. However, this system's cost and technical-related problems have emerged. Although the 1990s solved some problems, new technology is required for further solar industry development. With the developments of ZEB strategies, BIPV systems have gained popularity.

### **2.4.1. Field of Application**

Due to lower cost and easy application, BIPVs started to be implemented on building roofs, façades, glazing, and shading systems (Taveres-Cachat 2019). BIPV systems can generate electrical energy via the conversion of solar energy. Since they are attached to the building envelope, they also act as a thermal barrier between the building and the outdoor environment. They are beneficial since they reduce buildings' material, labor, and energy costs and provide an aesthetically pleasing view (Zhang et al., 2018). A detailed literature review is presented in Appendix A.

#### **2.4.1.1. Roof Applications**

For greater efficiency, PVs started to be first implemented on roofs (Knera 2015). PVs can be integrated as BIPV and building-attached photovoltaic (BAPV) systems. Although BAPV systems generate more electricity, BIPV systems provide a better overall building performance since they control the solar gain of the building. The available roof area for BIPV implementation is generally defined as 40% of the ground floor area. Most of the solar cells available in the industry can be used for BIPV roof applications (Ghosh 2020). However, first-generation PV cells are used mainly in roof BIPV applications. These include monocrystalline and multi-crystalline silicon PV cells. In BIPV roof applications, orientation and slope of the roof are the main parameters which affect performance, with south-facing and sloped roofs generally performing better. There is no airflow under PV modules in first-generation PV cells, which can be a disadvantage. Product types like BIPV foil, BIPV tile, BIPV module,

and solar cell glazing are suitable for roofs (Dim 2017). Studies show residential buildings have great potential for roof BIPV implementations (Defaix et al., 2012).

#### **2.4.1.2. Façade (Wall) Applications**

Since building facades cover more than roofs, façade BIPV implementations have gained popularity. Studies show that façade BIPV implementations significantly improve energy saving by 15% and 35% since they act as thermal barriers between indoor and outdoor environments (Jahanara 2013). When thin film and newly developed cells are used, the façade will allow daylight. If first-generation (i.e., silicon-based) cells are used, the façade will generally be opaque. BIPV façade systems contribute to the energy performance of the building and add an aesthetic appearance to the structure. One advantage of façade applications is their easy application process since they only require a mounting system with aluminum staples, brackets, and profiles (Chatzipanagi et al., 2016). There are two strategies for implementing PV on walls. PV can be implemented by mounting on an existing wall as a BAPV system or directly integrated into a building wall by replacing the wall with the PV as a BIPV system. BAPV systems include a gap between the building envelope and PV to enhance performance (Ghosh 2020). Although second-generation cells are now used in façade applications, silicon-based cells still account for 34% of applications (Pierluigi et al., 2015). Third-generation cells are rarely used. The main reason for the continued use of silicon-based cells is their high energy generation capacity and efficiency.

#### **2.4.1.3. Glazing Applications**

The integration of PV technology into windows increases the potential of fenestration systems. In today's technology, semi-transparent thin-film solar cells are implemented on windows. This newly emerged technology contributes to the energy generation capacity and improves daylight and thermal performance (Sun et al., 2020). BIPVs can be implemented on facades, and their optical properties may vary according to the energy demand of the building (Heinstein et al., 2017) (Figure 2.1.). A PV window's type, performance, and efficiency depend on its solar cell characteristics. With the newly emerged types, silicon-based and nonsilicon-based cells are available in

the industry. The silicon-based ones are monocrystalline, multi-crystalline, and amorphous silicon (a-Si). The non-silicon-based ones are cadmium sulphide (CdS), cadmium telluride (CdTe), copper indium selenide (CIS), and perovskite thin-film. Other non-silicon-based solar cells are still in the laboratory's experimental stage (Jelle et al., 2012).

According to the type of solar cell, there may be variations in the color and transmittance properties of the façade. Energy production efficiency may decrease for additional color and shading properties. Also, solar cells on the façade can be combined with double or triple glass panes, enhancing the system's thermal and acoustical insulation capacity (Cannavale et al., 2017).

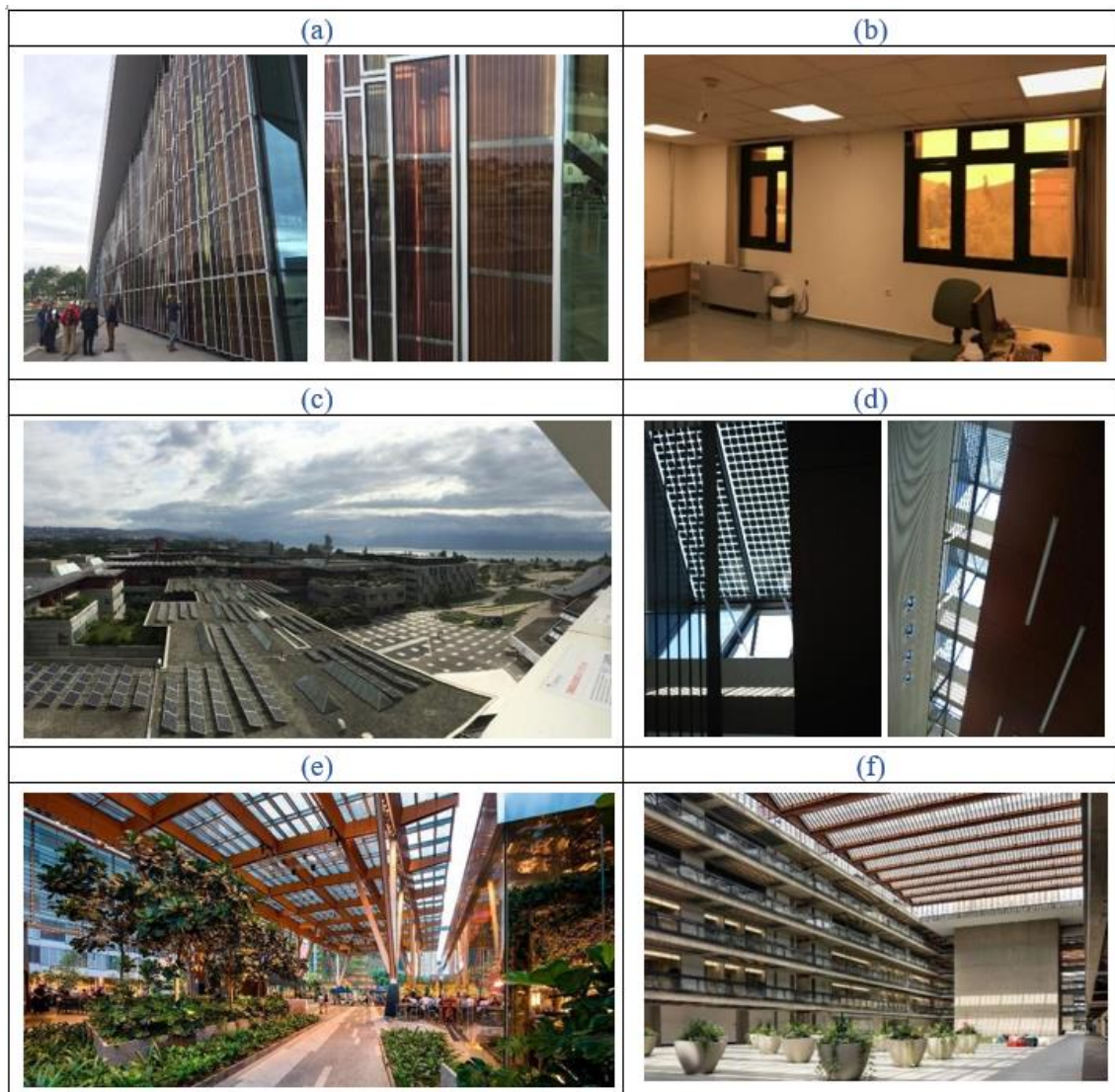


Figure 2.1. (a) PV glass implementation on the façade of SwissTech Convention Center in Lausanne, Switzerland (Photo by Dr. Berk Ekici) (b) PV window application on the south façade of an education building in IZTECH Campus in İzmir, Turkey (c) PV implementation on the roof

of EPFL building in Lausanne, Switzerland (Photo by Dr. Berk Ekici) (d) PV implementation on the roof of Schüco in Bielefeld, Germany (Photo by Dr. Onurcan Çakır) (e) PV canopy implementation on Tanjong Pagar Center by SOM Architects in Singapore by Solar Company OnyxSolar © (OnyxSolar 2022) (f) PV skylight implementation on Bell Works building in Holmdel, NJ (Solar Company: OnyxSolar ©) (OnyxSolar 2022)

BIPV windows can control daylight penetration through the building and solar gain due to the amount of daylight entering, reducing the heat flow between indoor and outdoor environments. Solar gain and daylight performance of the building are also related to the PV coverage area of glazing. Studies show that the PV coverage area is more effective in thermal and daylight performance than system efficiency. Efficiency and thickness directly affect power generation capacity; transmittance generally increases with thinner systems, but power generation decreases (Ghosh 2020).

#### **2.4.1.3. Shading System Applications**

As a capability of shading systems, these improve the daylight performance of an environment (Cesari et al., 2018). Also, they contribute the thermal performance by blocking excessive solar radiation (Jayathissa et al., 2017). Lately, PV systems have started to be implemented on shading elements due to their great potential. Studies show that PV-integrated shading elements effectively improve daylight uniformity while reducing the building's heating and cooling loads (Heangwoo et al., 2021a, 2021b). Some considerations must be studied during the design phase of PV-integrated shading systems since they affect their overall performance. The key ones are orientation, tilt angle, and a film type of shading element (Jayathissa et al., 2017). For instance, a study showed that the power performance of PV shading elements is better when placed horizontally, which results in more energy generation (Hwang et al., 2014). Also, one study shows that the optimum incline angle is different for a light shelf with and without PV implementation, and the uniform distribution of daylight decreases when the PV attachment area changes (Lee 2019). Therefore, it is important to investigate these variables to optimize performance. PV-integrated shading devices can be movable or fixed systems and can be designed in any size and shape. However, since these systems will obstruct the view and create shade, their daylight performance should be well investigated. BIPV systems can be implemented on a wide range of building

components. These components are the roof, wall, window, and shading elements. However, BIPV systems may also be implemented on even slabs and skylights with new developments. It is generally preferred in public buildings and open areas. According to the solar cell, the system can be opaque and semitransparent (Onyx Solar Energy S.L., 2021). The following variables for PV panels are significant for their overall energy performance: orientation, tilt angle, outdoor temperature, climate, geographical region, and cell type (Knera et al., 2015).

## **2.4.2. Production Technologies**

The cells in the PV module are between a weatherproof backing and a transparent cover to protect the system from outdoor exposure. The cells are laminated with tempered and low iron-content glass on the front face. Glass protects from water, moisture, and contaminant gases. On the back part, there is a thin polymer sheet or glass. To supply adhesion, there is also a layer called ethyl vinyl acetate (EVA) on each side of the cell. An aluminum frame strengthens the system (Petter Jelle et al., 2012). According to their production technologies, there are several types of solar cells. First-generation PV cells were first introduced in the industry and remained the best-known and most-used ones in the PV sector. Monocrystalline and multi-crystalline silicon solar cells are included in first-generation cells. With the development of technology, second-generation cells were introduced, generally known as thin-film solar cells. These have different materials and systems inside. A-Si, CdS, CdTe, and CIS solar cells are the most used. Other thin-film PV technologies, such as perovskite thin films, are still under development. Lastly, organic solar cells (OSC) are also being developed and introduced into the industry (Ghosh 2020). Figure 2.2. shows the scheme of production techniques of BIPV technology.

### **2.4.2.1. First-Generation PV Cells**

There are two main types of first-generation PV cells, called “first generation crystalline silicon PV cells,” monocrystalline and multicrystalline silicon PV cells. Both cells are durable and healthy, posing no risk to indoor air quality since they are not toxic (Battaglia et al., 2016).



They gained popularity between 2000 and 2008, resulting in higher prices and lower affordability. However, their costs decreased significantly in the last decade (Ran et al., 2015). Their energy payback time varies between three and four years (Luo et al., 2018). Monocrystalline silicon PV cells are produced using the Czochralski method, which is generated from single silicon crystals. Their manufacturing process is quite expensive since they require a specific processing period.

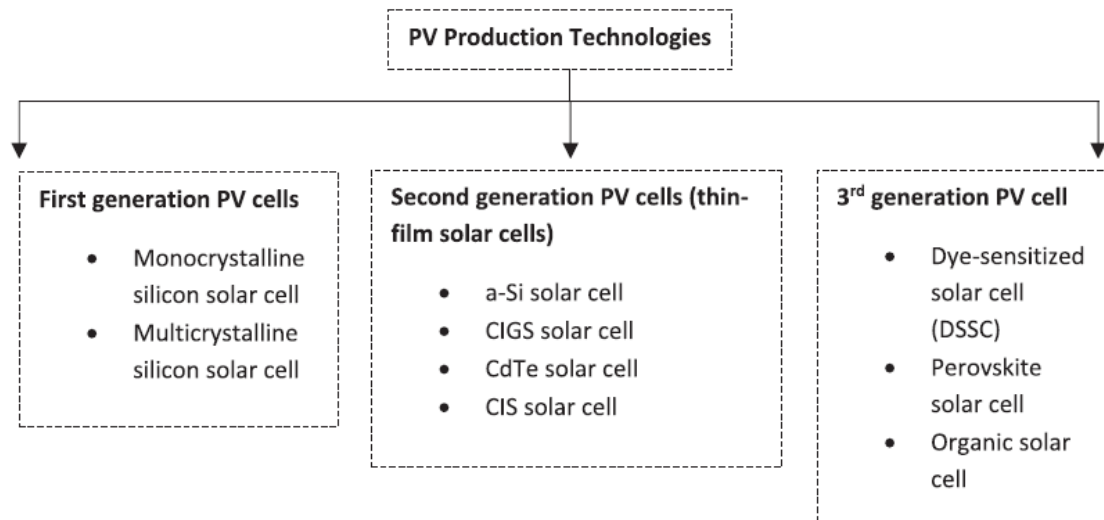


Figure 2.2. PV production technologies

Their energy pay-back time is around 3–4 years (Ghosh 2020). Their efficiency varies between 16% and 24%. They generally have dark colors, such as black and grey. Monocrystalline silicon cells' power per unit area varies between 75 and 155 Wp/m<sup>2</sup> (Petter Jelle et al., 2012). They have a more circular cell shape than multi-crystalline cells (Tripathy et al., 2016).

The solidification of molten silicon material produces polycrystalline silicon PV cells. These have a lower efficiency than monocrystalline ones but have a similar energy payback time (Ghosh 2020). Their efficiency varies between 14 and 18%. They are less expensive due to their relatively straightforward manufacturing process. They generally are a shiny blue color because of the tiny crystals. Monocrystalline silicon cells' power per unit area varies between 75 and 155 Wp/m<sup>2</sup> (Petter Jelle et al., 2012). They have a square cell shape and are similar in size to monocrystalline cells. Multicrystalline cells have many reflective facets, while monocrystalline cells are more uniform (Tripathy et al., 2016).

#### 2.4.2.2. 2<sup>nd</sup> Generation PV Cells (Thin-Film Solar Cells)

Thin-film solar cells mainly consist of thin layers of semiconductor materials implemented on an opaque backing material. According to the use of material, there are several thin-film solar cells: a-Si, CdS, CdTe, and CIS thin-film cells. First- and second-generation cells differ in materiality, but their structure and functioning are similar. Structurally, they consist of multiple, very thin layers. The arrangement of these layers is flexible (Tripathy et al., 2016). They can be combined with other smart window systems, such as Low-E coating.

“Second generation” was produced after first-generation silicon PV cells. In terms of cost, they are more affordable, but their efficiency is generally lower than silicon solar cells, and their performance may decrease after prolonged exposure to the outside environment. Despite such obstacles, thin-film solar cells are becoming popular. Radiation, incidence angle, outside temperature, and wind speed influence thin-film cells’ performance and efficiency. Conversely, thin-film PV cells capture the solar spectrum more efficiently than first-generation cells (Ghosh 2020). Thin-film solar cells have the advantage of a wide range of application areas and can be implemented on windows and vehicles (Tripathy et al., 2016).

A-Si solar cells’ efficiency is lower than silicon-based cells, generally between 4% and 10%. However, they perform better in higher and lower temperatures. The spectral changes of the ground radiation in summer and winter significantly affect the efficiency of a-Si solar cells (Ghosh 2020). Their thickness, size, and used areas may vary. a-Si solar cells have three advantages: Firstly, structurally, they are more flexible than conventional silicon-based cells; secondly, despite being less efficient, they are cheaper to produce (Tripathy et al., 2016); and finally, they can have different transparencies between fully opaque and transparent. Figure 2.3 shows that different colors can be produced according to the user’s preference, designer, etc. Their energy payback time varies between 2 and 3 years (Ghosh 2020).

It is understood from its name that copper indium gallium diselenide (CIGS) thin-film solar cells consist of copper, indium, gallium, and selenium materials (Liu and Chuang 2012). Their costs are less than silicon-based cells but more expensive than other thin-film cells. Compared with other technologies, their efficiency is moderate, between 12% and 15%. However, higher efficiency values are reached in a laboratory

environment (Buecheler et al., 2011). They can generally keep their initial power as an advantage even after 20 years. Their energy payback time varies between 1.2 and 2.4 years. Additionally, their operational lifetime is 20 years (Ghosh 2020).



Figure 2.3. (a) Colored (orange) PV glass application in Block E, IZTECH Campus  
(b) Colored (blue) PV glass application in Block E, IZTECH Campus  
\*Glazing is supplied by OnyxSolar Company © for a Doctoral Thesis supported by TUBITAK.

CdTe thin films are emerging technologies in the thin-film cell industry, being more cost-effective than other technologies. They are produced on a substrate glass with transparent conducting oxide (TCO). TCO is generally made from fluorinated tin oxide (FTO) material. Their color is reflective, primarily dark green or black. Their efficiency varies between 9.4% and 13.8% (Petter Jelle et al., 2012). They have a short energy payback time and 20 years of operational lifetime (Ghosh 2020).

CIS cells are the industry's most efficient types of thin-film cells. Generally, their efficiency varies between 11% and 18.7 %. Like CdTe thin-films, their color is usually dark gray or black (Buecheler et al., 2011).

### 2.4.2.3. Third Generation PV Cells

Although first- and second-generation PV cells are seen as technologically groundbreaking systems, their electricity generation capacity is limited. Not all solar energy can be transformed into electrical energy, as some energy turns into heat. The main advantage of third-generation PV cells is that they are highly efficient and can convert most of the collected solar energy into electrical energy. Additionally, they are low-cost (Dupr'e et al., 2015).

A type of these solar cells, dye-sensitized solar cells (DSSC), consist of three components: organic dye, electrolyte, and semiconductor layer sheets. Unlike conventional solar cells, these can be implemented on windows, terraces, facades, etc. Unlike the other cells mentioned above, natural elements can produce dye-sensitized solar cells, making them more affordable (Varga and Racz 2021). They are flexible in shape, color, transmittance, and size. Their efficiency reaches 11.9%, and they have a short energy payback time. Their operation time is similar to that of other cells, i.e., an average 20-year lifetime. (Ghosh 2020). They can work under overcast sky conditions (Gong et al., 2017). Their energy payback time varies between 2 and 2.63 years for different cell efficiencies (Greijer et al., 2001). Their performance is dependent mainly on the system's photo anode material properties. Generally,  $\text{TiO}_2$  is used for photo anodes since it has a large energy gap, chemical stability, is non-toxic, and is low cost (Nien et al., 2021).

Perovskite solar cells' power efficiency varies between 3% and 22% (Ghosh 2020). In terms of efficiency, it reaches higher values than other cells (Zardetto et al., 2014). Perovskite has a formula of  $\text{ABX}_3$ . A is the cation, and B is the anion. Generally, they use methyl-ammonium-lead-iodide ( $\text{MAPbI}_3/\text{CH}_3\text{NH}_3\text{PbI}_3$ ) in their system. PSCs are suitable for windows because they provide sufficient transparency and power efficiency (Cannavale et al., 2017). PSCs' optical properties differ from other cells, with a high absorption coefficient and low reflection (Hossain et al., 2020). In this sense, these are different than silicon-based solar cells. However, it is similar to DSSCs. Energy pay-back time is not well studied, but some studies suggest that it can vary between 0.2 and 5 years, depending on the material used (Espinosa et al., 2011; Gong et al., 2017).

Organic solar cells (OSC) are more efficient and cost-effective than conventional silicon-based solar cells. They can absorb light and produce electricity through conductive organic materials (Mime et al., 2021). Their efficiency is reportedly between 5% and 14% due to organic material's high absorption coefficient (Ameri et al., 2013). As a disadvantage, excitons diffusion length is smaller than inorganic cells, and they are not appropriate for areas lacking light since this affects photons' energy levels (Sajjad et al., 2020). Their thermal coefficient is low, and they do not resist outdoor exposure. Their energy pay-back time is relatively shorter than other cell types, although their efficiency is low. Pay-back time varies between 0.79 and 2.02 years

(Ghosh 2020). Their transparency varies between 16% and 41%, but increased transparency can be achieved at the cost of efficiency (Petter Jelle et al., 2012).

Figure 2.4. shows implementation examples of varied solar cells in different parts of the building facades. Table 2.1 shows that each solar cell has different properties, advantages, and disadvantages. Thus, their properties should be well understood, and their selection process is significant. Studies have shown that BIPV systems have developed considerably in the process. Industry developments have identified these systems' deficiencies and tried to eliminate them. The first-generation solar cells' opaque appearance turned transparent in the second and third generations. While higher-efficiency solar cells are being produced, BIPV systems have started integrating into different parts of buildings.






Building name	Visual	Location	Manufacturer	Field of application	Solar cell type
Bilbao Kukullaga Station	 (ONYX SOLAR ENERGY S.L., 2022)	Bilbao, Spain	ONYX SOLAR ENERGY S.L.	Skylight	a-Si
Corison Winery	 (ONYX SOLAR ENERGY S.L., 2022)	California, USA	ONYX SOLAR ENERGY S.L.	Roof	Crystalline silicon
Autonomous Office	 (ONYX SOLAR ENERGY S.L., 2022)	Asturias, Spain	ONYX SOLAR ENERGY S.L.	Façade	CIGS
Solstex, Solar facade system integrated with ACM and Granite for the reclad of the EllisDon offices	 (Elemex®, 2022)	London, ON	Elemex®	Façade	CdTe
College of Pierre Mendes	 (©Heliatek/LaRochelle, 2022)	La Rochelle, France	©Heliatek/LaRochelle	Roof	OSC

Figure 2.4. Varied solar cell implementation on buildings

Table 2.1. Comparison of different cell types regarding materials, efficiency, and appearance.

Solar cell type	Efficiency (%)	Material type	Transparency	Energy payback time (year)	Advantages	Disadvantages
Mono-crystalline silicon	16-24	single silicon crystals	opaque	3-4	High efficiency, high durability	High manufacturing process
Poly-crystalline silicon	14-18	molten silicon	opaque	3-4	Easy manufacturing process, high durability, high efficiency	Less expensive than monocrystalline silicon cells, more expensive than thin-films
a-Si	4-10	non-crystalline silicon	Varied transparency	2-3	More flexibility in size, shape, color, transparency, and implementation areas, cheaper, low-temperature processing, short energy payback time	Less efficiency
CIGS	12-15	copper, indium, gallium, and selenium	Varied transparency	1.2-2.4	Short energy payback time, long operational lifetime	More expensive than other thin-film cells
CdTe	9.4-13.8	cadmium and tellurium	Varied transparency	0.75-2	Cost-effective, short energy payback time	Low efficiency compared to other thin films has toxic effects on human health, complicated recycling, and disposal process
CIS	11-18.7	Copper, indium, and selenide	Varied transparency	-	Most efficient thin-film cell, short energy payback time	

(cont. on the next page)

Table 2.1 (cont.)

Dye-sensitized	Up to 11.9		Varied transparency	2-2.63	Affordable, flexible in terms of shape, color, transmittance, and size, short energy payback time, ability to work under overcast sky conditions, non-toxic	Low efficiency
Perovskite	3-22	methyl-ammonium-lead-iodide			High efficiency, long diffusion lengths, high mobility, tunable bandgaps, low cost,	require a large area for module fabrication, stable system device
OSC	5-14	carbon-based conductive organic molecules	Varied transparency	0.79-2.02	Low cost, short energy payback time	Small excitons diffusion length, not appropriate for areas which lack light, low thermal coefficient, low resistance to outdoor exposure

### 2.4.3. BIPV Types

#### 2.4.3.1. Solar Cell Glazing

Among the BIPV types, solar cell glazing has been developed recently. It has gained popularity due to the wide range of application areas such as façades, roofs, windows, skylights, and even slabs. Thin-film and third-generation solar cells are implemented on solar cell glazing products. Therefore, they are structurally flexible since they can be produced in different sizes, shapes, transmittance, and colors. Different than other product types, there is a gap between cells. This gap affects transmittance level and energy production efficiency and allows it to penetrate daylight through the system. Their transparency varies between 16-and 41%. However, higher transparency is achieved less efficiently (Petter Jelle et al., 2012).

### **2.4.3.2. BIPV Module**

BIPV modules have similar properties as PV modules. However, they may replace other roof types or be appropriate for a specific roof solution developed by the producers. They have an easy application process and a wide range of products in the industry. They may be building-attached or building-integrated. Both are available on the market. However, before buying the product, it should be well understood whether it is BAPV or BIPV because some products lack this information. Among the product brands, the fill factor is similar. However, their efficiency varies between 12.5-and 20%. Efficiency mainly depends on the solar cell type inside of it. These products use monocrystalline and multi-crystalline solar cells (Petter Jelle et al., 2012).

### **2.4.3.3. BIPV Tile**

Similar to foil types, tiles can be implemented on roofs. It can be a partial or full implementation. The appearance of the tiles is similar to typical roof tiles in size and dimensions. However, different shapes and sizes of tiles can be producible. Their high efficiency makes this technology more valuable. Sometimes the module may not be fully covered with PV cells. It is reducing its efficiency. Therefore, their efficiency is related to an active area of PV cells. In industry, there are C21e tiles that have a larger active PV area since monocrystalline silicon cells are fully applied to the module area.

### **2.4.3.4. BIPV Foil**

The main advantage of foil-type BIPVs is that they are lightweight and easy to implement on surfaces. Generally, they are applied on roofs. Since foil is a flexible material, thin-film cells are used in the system to maintain the flexibility and efficiency of the product. Thin-film cells' efficiency is low, and solar cell resistance is mainly due to the low fill factor of foil products (Petter Jelle et al., 2012).



#### **2.4.4. Opportunities in the Market and Feasibility**

BIPVs reduce CO<sub>2</sub> emissions in the atmosphere, generate solar energy, and reduce the buildings' environmental impacts. New regulations started to use their potential and benefit them more effectively. These new regulations help the BIPV market overgrow (Petter Jelle et al., 2012). National policies develop the BIPV market's influence at the national and international levels. For instance, Greece, Italy, Germany, Spain, France, and Austria have expanded their policies to enhance BIPV usage in their country (Petter Jelle et al., 2012). Also, the U.S. Department of Energy (DOE) strongly encourages those who want to build homes to participate in Zero Energy Homes (ZEH) and Energy Star. U.S. DOE reports that approximately 360,000 houses qualified with Energy Star were constructed between 1995 and 2004. (Henson 2005). Not every country has the same percentage share in the global BIPV industry. For instance, the European Commission mentioned that in 2020, Europe is expected to hold 44% of the World's BIPV market, followed by Asia-Pacific with 28% and the United States with 16%. Other regions like China and Japan have weaker investment returns but still, be attractive markets (European Commission as Project Deliverable D1.1. 2016).

The BIPV market has gained popularity not only due to the regulations of governments but also special agreements between significant companies and institutions. CA, USA-based company Open Energy and SunTech America, based in Wuxi, China, have signed an agreement regarding the BIPV products' manufacturing and marketing (2007).

BIPVs contribute to constructing a sustainable future for our cities. Developments in the BIPV industry help improve researchers who work in this field. With the overall developments, we can face ecological challenges in the future.

#### **2.5. Contributions from the Literature Review**

Studies are reviewed and analyzed, as indicated in Appendix A. Most studies can be divided into three categories based on their implementation areas: roof, façade, window, and shading device implementations of BIPV systems. Recently, BIPV systems have started to be implemented on different building elements, such as windows and shading devices.

Previously, these systems were more integrated with vertical facades and roofs. While reviewing the literature in online databases, the following keywords were used BIPV, PV, PV shading device, PV window, etc. The significant studies in the literature were reviewed and investigated in terms of publication years, locations, climate, building function, the field of application, cell type, performance criteria, aim, methodology, tools used in the study, analysis type, and results. The review result is analyzed in this section based on these criteria. Figure 2.5 shows that the studies were conducted from 2002 to 2022. 60% of the papers in the literature review were published in the last five years. There has been an increase in published articles related to BIPVs in recent years, and the graph suggests that this trend may continue soon. BIPV implementation depends on the following factors: country population, government policies, geographical location, and climatic characteristics (Figure 2.6.).

BIPV systems have begun to be implemented in some countries in Europe and China. The spread of its usage is due to its great potential. Figure 2.7 displays the 27 countries that implement BIPV technology. The most important countries are China, Korea, the UK, Brazil, and the USA, perhaps due to these countries' populations and government policies. For example, China and Brazil have seen dramatic increases in population in recent years. The increase in population also increases construction and energy consumption in cities. Therefore, due to the large population, BIPVs gained importance in saving energy in China and Brazil. Although the population is lower in Korea, the UK, and Germany, these countries' governments strongly support BIPV investments (Osseweijer et al., 2018).

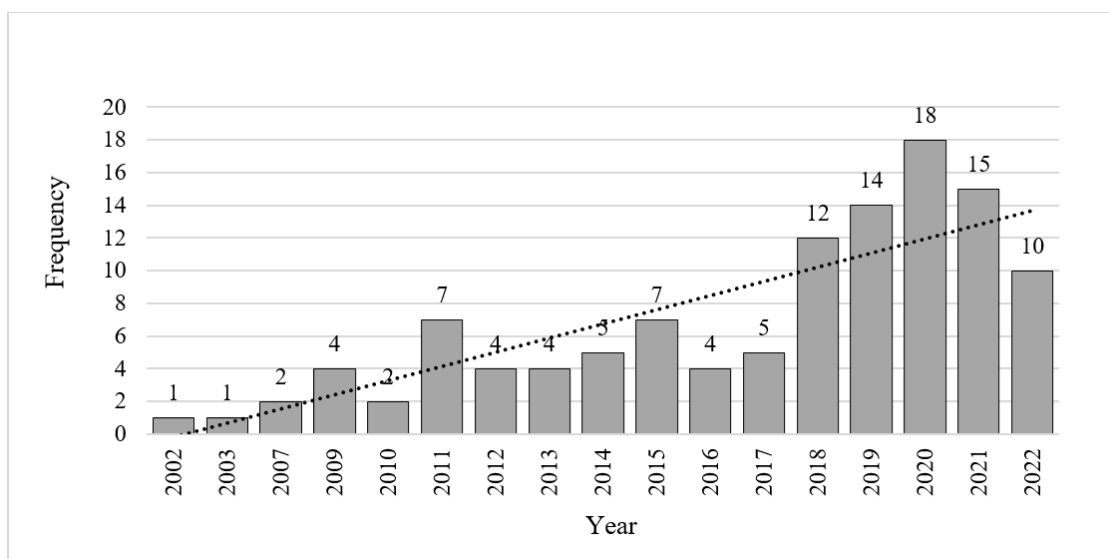


Figure 2.5. The number of annually published papers in 2002–2022 on BIPVs.

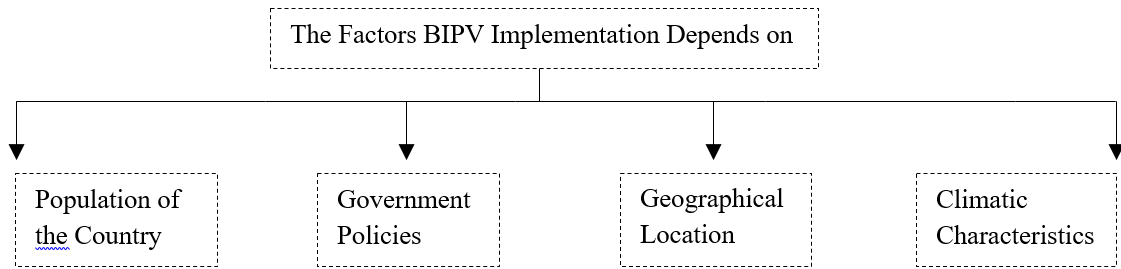


Figure 2.6. The factors BIPV implementation depends on

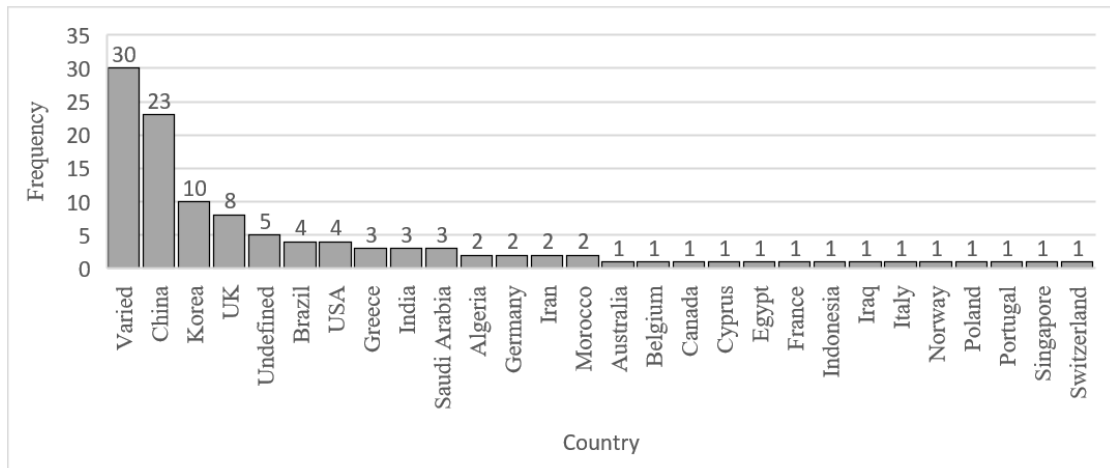


Figure 2.7. BIPV systems implemented in countries

Therefore, this may reflect the BIPV industry and literature. Additionally, BIPV implementation is related to the geographical conditions of countries.

BIPV systems are more beneficial in low-latitude regions with a more direct sun angle. Results show that BIPVs are more implemented in temperate, subtropical, cold, moderate, and Mediterranean climates. BIPV implementation is stronger in some countries with cold temperatures, despite relatively low solar gain due to government policies. However, it is seen in Figure 2.8. that with very high solar gain in hot countries, BIPVs are less popular in hot and hot desert climates compared to cold climate regions. It may be because BIPVs –mainly applied on vertical surfaces- may increase the temperature of the interior environment since they store all the heat and convert only some portion of it to energy.

One of the literature review’s most significant aspects is comparing selected cell types used in studies. Cell type selection is crucial because it affects a BIPV’s overall performance, cost, appearance, and payback time. In the literature review, seven different cell types are used. The most used cells are a-Si, monocrystalline, and multi-crystalline solar cells, with 25%, 23%, and 17% (Figure 2.8.). These are the industry’s

most popular, most efficient, flexible, and cheapest cells. Other cells used in studies are CdTe, CIGS, CID, and perovskite-based cells, but they are less common due to their recent emergence in the industry. Therefore, their performance is still being tested in labs.

The studies were conducted with different methods and materials. Some use experimental procedures, and others simulation methods. Each study and its method and tools used are described in Appendix A, and a summary is presented in Figure 2.9. There are many digital and manual tools for assessing a BIPV's performance. Some studies use mathematical formulas, monitoring, and real experiment methods, while others use only digital techniques, and others use both (Figure 2.10.). In terms of monitoring tools, many devices assess a building's energy, thermal, and daylight performance when applying a PV system to the building envelope.

The literature analysis of experimental studies shows that most of them implemented PV as a glazing or shading element. Thus, they mainly use a-Si and crystalline-based solar cells. Many of them used office type of buildings as references. It may be because office buildings are usually high rises and have larger surface areas to implement PV on their vertical surfaces. The climatic conditions of the studies are mostly subtropical and temperate climates. The performance criteria are primarily assessing the energy generation capacity of the PV system and the daylight performance of the selected room or building. Regarding digital methods, a wide range of software is used to assess a BIPV's energy performance.

They are as follows: Energy Plus, Open Studio, Design Builder, Skelion, etc. These are the most prominent ones in the studies in the literature, 43.4% of which investigate energy performance. DIVA, Radiance, DAYSIM, and Honeybee are generally used to evaluate the daylight performance of BIPVs (Food4Rhino, 2021; Radiance, 2021; DAYSIM, 2021). PW-WR, PV-DATA, PVSYST, SOLCEL, TRNSYS, MATLAB, etc., are generally used to evaluate a BIPV's electrical properties and energy generation ability. However, these are not very user-friendly and require expertise. Lastly, optimization studies are presented in Table 2.2.

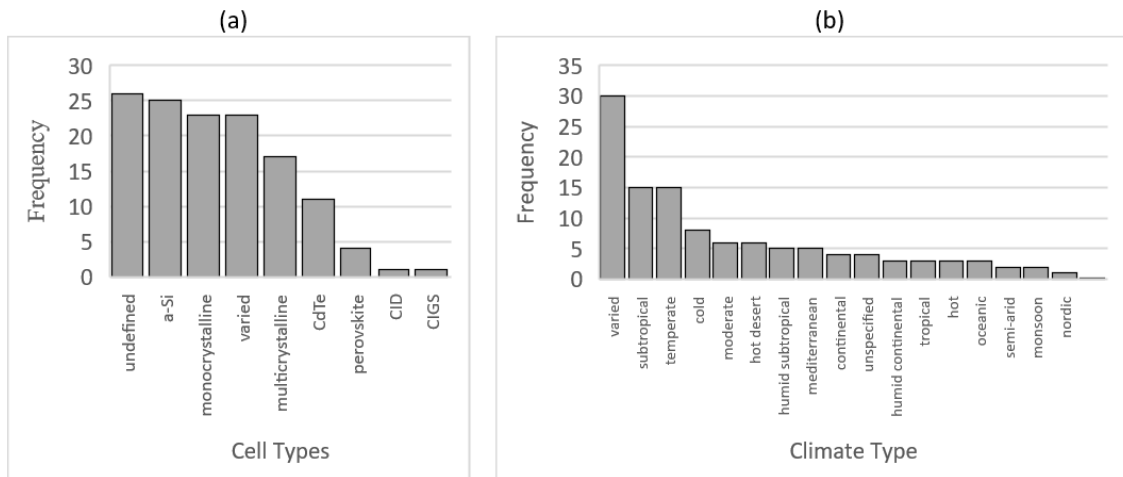


Figure 2.8. (a) Solar cell types used in studies (b) Climate types in studies.

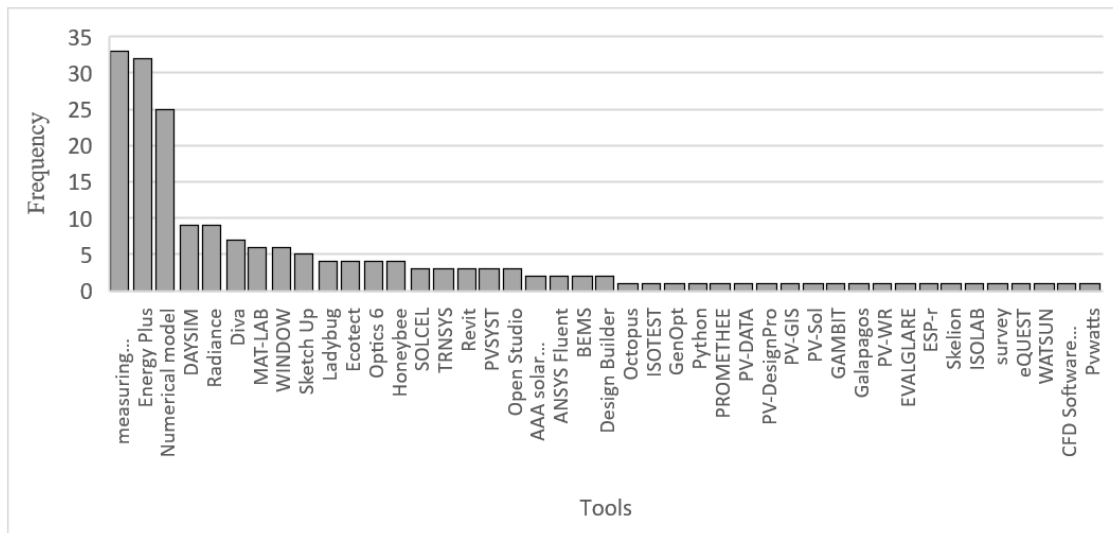


Figure 2.9. Tools used in the studies

Studies use different algorithms, variables, objectives, and tools. Galapagos and Octopus are Grasshopper plug-ins to conduct multi and single-objective optimization (Food4Rhino 2021). BIPV systems can be implemented on various building types. 44% of the studies focus on office buildings (Figure 2.11.).

Recently, extreme urbanization in cities resulted in the construction of high-rise buildings. Office buildings are defined as target buildings for energy reduction since these are the most prominent types in city centers, and most studies were conducted on office-type high-rise buildings. The application of BIPVs in residential buildings is significantly less, despite the more significant numbers of these buildings.

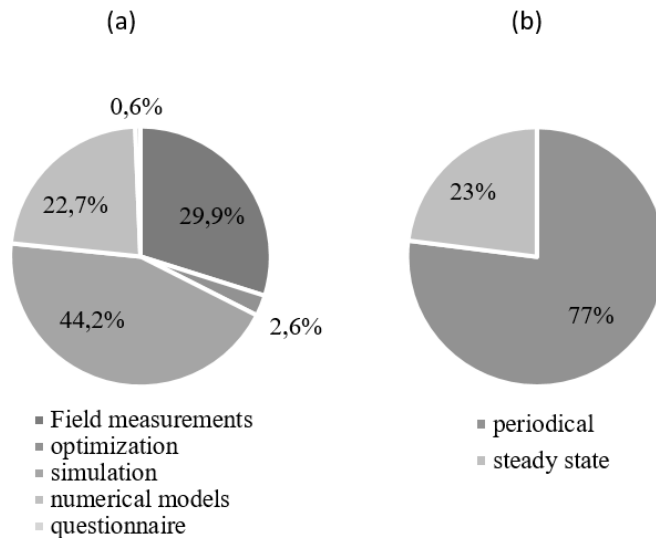


Figure 2.10. (a) Experimental conditions (b) Analysis type of the studies.

Table 2.2. Review of the optimization studies.

<i>Variables</i>	<i>Objectives</i>	<i>Tools</i>	<i>Algorithms and methods</i>
Solar cell-based variables (i.e., transparency, temperature, coefficient, etc.) Weather conditions BIPV geometry Daylight performance Building geometry	Energy conversion efficiency Power output Solar irradiation Life cycle cost	Octopus, Galapagos, GenOpt, Python, ANN- based tools	Genetic optimization, particle swarm, wind- driven, ANN, MOPSO, LINMAP, POF, MO, RVFL, JFSA, SCA, AEO, MRFO, NSGA II

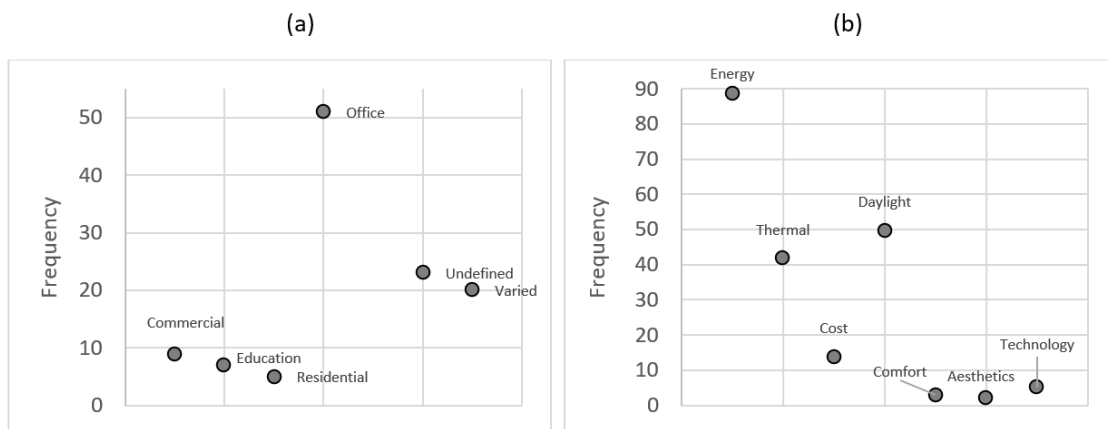


Figure 2.11. (a) Building types that BIPVs are implemented in studies (b) Evaluation criteria in studies

The main conclusions of this literature review, considering the results, may be listed as follows:

- PV systems emerged in the 1990s. In the 2000s, they gained popularity and a wide range of use. However, due to their high costs, they were gradually replaced by BIPV systems in the 2000s. BIPV systems have great potential for lower cost, easier manufacturing and implementation, greater structural flexibility, etc. Therefore, it is forecasted that there will be an important development in these systems.

- Previously, BIPV systems were more often integrated on walls and roofs. More recently, these tended to be implemented on different building components, such as windows and shading elements. New implementation areas of BIPVs bring both new opportunities and new technologies.

- The solar cell type changes as the integration area changes, leading to new solar cells (second and third generation). In previous studies, mono and multi-crystalline solar cells were the most common cells in the industry and literature. Still, recently a-Si, and other thin-film cells have appeared more frequently.

- BIPVs are generally evaluated in terms of their overall performance. It includes their thermal, daylight, and energy performance. However, the key aspect for assessment is their energetic properties, which consist of their energy production and energy-saving capacity. This capacity is primarily related to the solar cell included in PV panels.

- In studies, it is generally mentioned that certain parameters affect the overall performance of BIPV systems. These are building orientation, panel slope, solar cell type, ambient temperature, shadowing effect, and site geographical location. Most studies aimed to investigate the impact of these variables on the overall performance of BIPV systems. It is found that when a developed country is overpopulated, its government tends to give more importance to preserving energy due to the increase in the population of the cities. Even though the country is not overpopulated, the BIPV industry is pretty developed in some countries due to the government policy and support for this sector.

- Some of the study results indicate that BIPV performance significantly differs according to the climate and geographical region. It is found that their performance is directly related to how much the building exposes to the sun. BIPV systems are generally more effective in low latitude regions since the sun comes with a more direct angle and increases the solar gain of panels. However, due to different policies and considerations of governments, they are popularly applied in even cold

climatic regions such as Germany. In very hot climatic such areas as hot desert climates, BIPV applications are not very beneficial since they increase indoor air temperature more than usual. They are generally more helpful in moderate, temperate, and subtropical regions. Also, the system is more likely to generate electrical energy if the surrounding obstacles do not shade the building and PV-implemented area. In addition, building orientation is one variable that impacts energy generation performance. A BIPV system is mostly implemented on the south facade in the northern hemisphere. It is the north façade for the regions in the southern hemisphere. Similarly, the panel slope is a decisive factor in the system's efficiency. If the panel is installed at an incline, it can generate more energy than those installed vertically or horizontally.

- Also, solar cell type is one of the most prominent variables among these studies. Although recently emerged third-generation solar cells are promising, their application in the literature is rare. In industry, silicon-based cells are the most prominent ones. These are monocrystalline, polycrystalline, and a-Si solar cells. They have low cost, excellent efficiency, and easy implementation procedure. However, third-generation PV cells have recently gained importance in literature and the market. For instance, CdTe, CIGS, and perovskite-based ones are started to be implemented in several studies. Therefore, it is possible to see various studies on BIPVs in the future. The efficiency of a solar cell directly influences the system's energy generation capacity. If the aim is to generate more energy, then highly efficient solar cells (i.e., monocrystalline) are preferred. However, other solar cell types must be tested to evaluate the building's overall energy, thermal, and daylight performance.

- Studies have shown that BIPVs performed more efficiently on highrise buildings since the application area is the largest in these types of buildings.

- Among the variables examined so far, environmental-based ones (i.e., building orientation, panel slope, shadowing effect, and building location) are directly related to the success of a BIPV system. On the other hand, system-based variables (i.e., solar cell type, implementation area and location, and BIPV type) still influence the system's performance; however, they do not seem as the determinant and vital variables for a system's overall success.

- Tools used in studies are divided into two categories: digital and manual. Manual tools mainly include measurement instruments and scale models. Although these tools were common in early studies, digital tools gained popularity due to their



lower cost and effortless analysis procedure. Digital tools mainly consist of simulation software such as TRNSYS and Energy Plus. Simulation studies are generally conducted for energy performance assessment of BIPV systems.

## CHAPTER 3

### METHODOLOGY

#### 3.1. Study Design

Firstly, the architecture studio is monitored for one week. According to monitoring results, a calibration procedure is conducted on simulation models. Then, the study includes testing the base case model's daylight and energy performance through simulation software; analyzing three Low-E PV glass modules of OnyxSolar © (OnyxSolar 2021), in which the transmittance of solar cells is changed as 10%, 20%, and 30% respectively; calculating electrical energy of PVs and lighting energy load; then matching whether the PV glasses are advantageous in terms of balancing the lighting energy consumption monthly and yearly. The simulation engine calculates heating and cooling loads. Those are discussed together with occupant thermal comfort in the case room. The effect of PV glass on occupant visual comfort is also analyzed in the study.

The second phase implies the optimization process. The Octopus multi-objective optimization plug-in of Grasshopper optimizes the window-based variables of PV glass (i.e., window size and location and PV module transparency) to obtain minimum heating and cooling load and at least 50% of sDA. Octopus plug-in plots the results in a three-dimensional axis. The results are examined based on this axis. Output genomes with at least 50% of sDA and minimum total thermal loads are selected and defined as possible Pareto-front results. These are reviewed based on their energy generation, daylight, and energy performance. Then, the study continues with the selection of the possible Pareto-front results. Annual lighting loads are calculated for the best-performed Pareto-front genomes. This analysis is due to evaluating the overall performance of optimized models and seeing the performance potential of the architecture studio. Figure 3.1. shows the flowchart of the study.

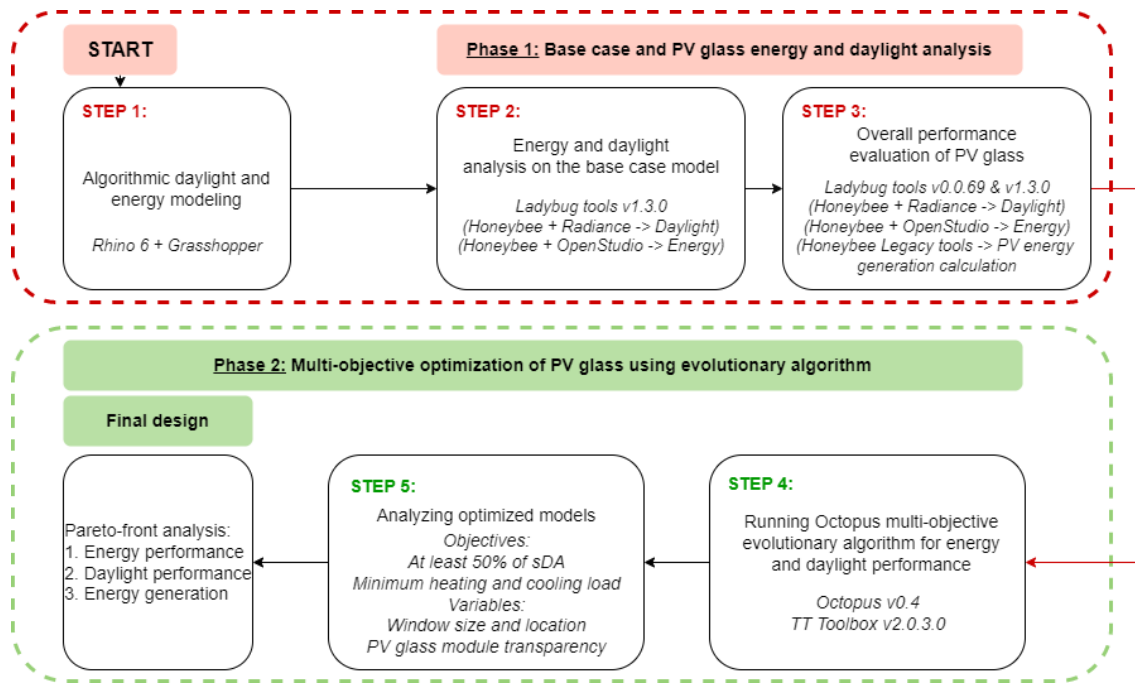


Figure 3.1. Method flowchart of the study

### 3.2. Case Building

The architecture studio is located in the three-story-high-faculty building in the Izmir Institute of Technology (IZTECH) Campus on the west side of Turkey, on the coast of the Aegean Sea. Its coordinates are 38.32 N and 26.63 E, and its sea elevation is 77m. The architecture studio (Figure 3.2.) is 4m in height, located on the first floor, facing south and east, with dimensions of 11.8x17.8m. The selected case room is a typical architecture studio.

The reference building is in the city of İzmir, Turkey, having a Mediterranean climate. Köppen-Geiger Climate Classification system defines İzmir’s climate as hot and dry in summer and rainy and warm in winter. This system is seen as one of the most valuable climates specification systems. Köppen classifies the climates into five groups (Figure 3.3.). These are labeled with letters A, B, C, D, and E. These correspond to tropical, dry, temperate, continental, and polar climates. İzmir is defined as Csa with a hot Mediterranean climate (Çetinkaya, Aydın, and Öztürk 2017).

The EnergyPlus weather data of İzmir is introduced to the daylight and energy simulation engine for climate-based proper calculations.



Figure 3.2. (a) Selected architecture faculty building (b) Interior of the architecture studio

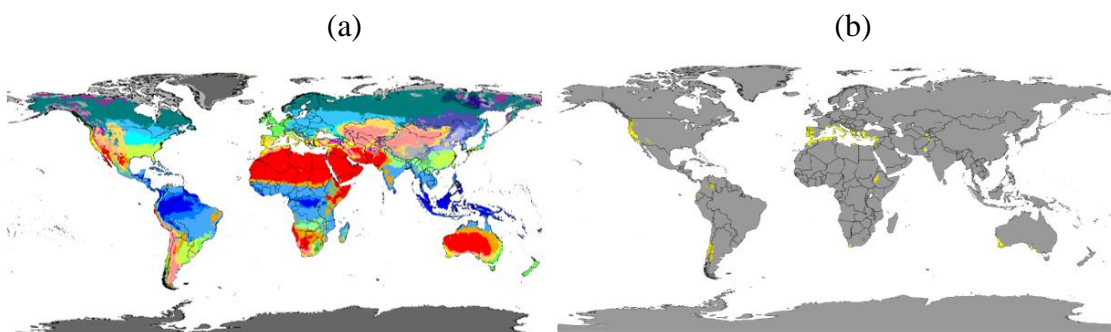


Figure 3.3. (a) Köppen-Geiger Climate Specification system in World (b) Mediterranean climate indication according to Köppen Climate Specification

The .epw file of the city represents the climate of the reference building provided by the EnergyPlus Weather Data website (EnergyPlus Weather Data 2022). The file was then introduced to Climate Consultant 6.0 software to generate radiation and illumination weather data and climate-based information presented in Table 3.1., Table 3.2., and Figure 3.4. below. Direct normal, global horizontal, and total surface radiations are the highest during summer compared to other seasons. In general, total surface radiation is higher than others. Also, global horizontal illumination is generally higher than direct normal radiation throughout the year. Figure 3.5. below indicates the sun path chart of the case building, with the aerial photo showing the surrounding rural context.

Table 3.1. The weather conditions and locations of the selected building.

City	Climate zone	Location	Altitude	Summer temperature	Winter temperature
İzmir	Hot summer and warm winter Köppen Climate Specification: Csa	38.31 N 26.63 E	42 m	Average: 27.4°C	Average: 9.5°C

Table 3.2. Annual radiation and illumination weather data of Izmir, Turkey.

File	Global horizontal radiation (Wh/m <sup>2</sup> )	Direct normal radiation (Wh/m <sup>2</sup> )	Global horizontal illumination (lux)
TUR_Izmir.172180_IWEC	399.1	493.5	21315

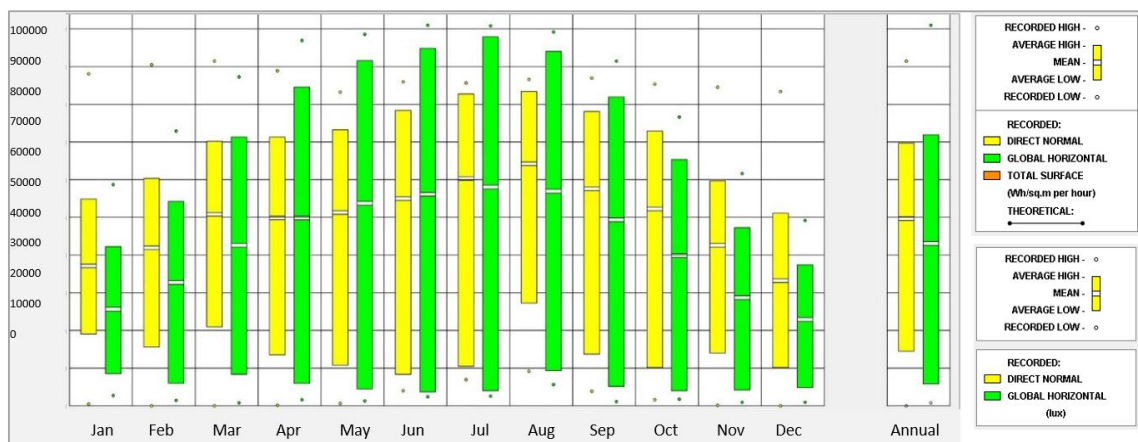


Figure 3.4. Hourly illumination of direct normal and global horizontal in lux

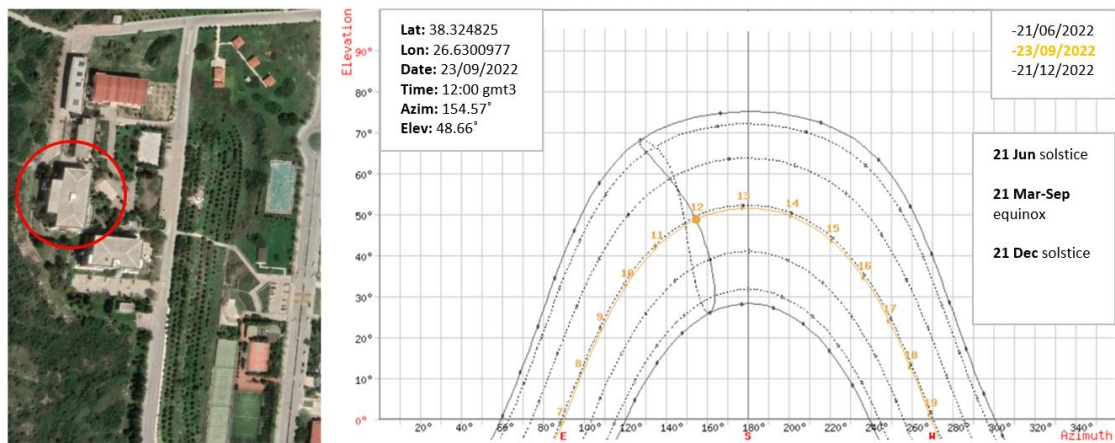


Figure 3.5. (a) Location of case building on the aerial view (b) Sun path diagram with the indication of the case building

### 3.3. Experimental Setting

Hobo data loggers conduct monitoring for one week. Dataloggers are attached to the interior and exterior surfaces of the studio. To monitor temperature, relative humidity, and illuminance, one data logger is placed on the wall of the outer window where direct sun and rain cannot reach it.

The datalogger is placed on the interior wall surface for the exact measurements in the indoor environment. (Figure 3.6.). The two data loggers are located near each other, attached to surfaces vertically, 1.5 m above from floor, and facing South. A shade from thick wooden is installed on the exterior datalogger for rain and sun protection. Approximately 25 people have occupied the case room for 8 hours a day. It is ventilated naturally. Students' computers are used in the case room throughout the daytime, which may be a potential heat gain source. There is a VRF HVAC system for the heating and cooling the whole building beside the toilets. No curtains are used in the building. LED linear lights are used in the studios, and LED panels are used in the corridors. Hobo data loggers are set to collect data for temperature, relative humidity, and illuminance levels every 10 minutes for indoor and outdoor environments.



Figure 3.6. Photos of inner and outer climate data loggers (1: indoor, 2: outdoor)

Measurements started on the 30<sup>th</sup> of November at 1:00 p.m. They ended on the 7<sup>th</sup> of January at 1:00 p.m. Data loggers have an accuracy of  $\pm 2.5\%$  for relative humidity between 10% and 90% and  $\pm 0.35$  °C for temperature between 0°C and 50°C. They can measure temperature between -20 °C and 70 °C and relative humidity between 5% and 95%.

For the light intensity, they measure between 1 and 3000 lumens/ft<sup>2</sup> (Onset 2020). After monitoring, monitored data is then exported to Excel for analysis. Figure 3.7. below is the location of the inner and outer dataloggers in the room.

## 3.4. Simulation Models

### 3.4.1. Daylight Simulation Model

Ladybug, a special plug-in of Grasshopper, runs the daylight simulations of this study. Ladybug has been considered as the parent plug-in. It has several children to conduct different types of simulations. Honeybee is one of the most widely used children for daylight, thermal, and energy simulations. It uses Radiance as the engine to compute the simulations (Goharian, Daneshjoo, and Yeganeh, 2022). The architecture studio is algorithmically and three-dimensionally modeled in Rhino/Grasshopper environment. Solid surface materials (i.e., floor, ceiling, and walls) and window properties are assigned to the simulation engine, as seen in Table 3.3. The engine uses the accurate weather file of Izmir for proper calculations.

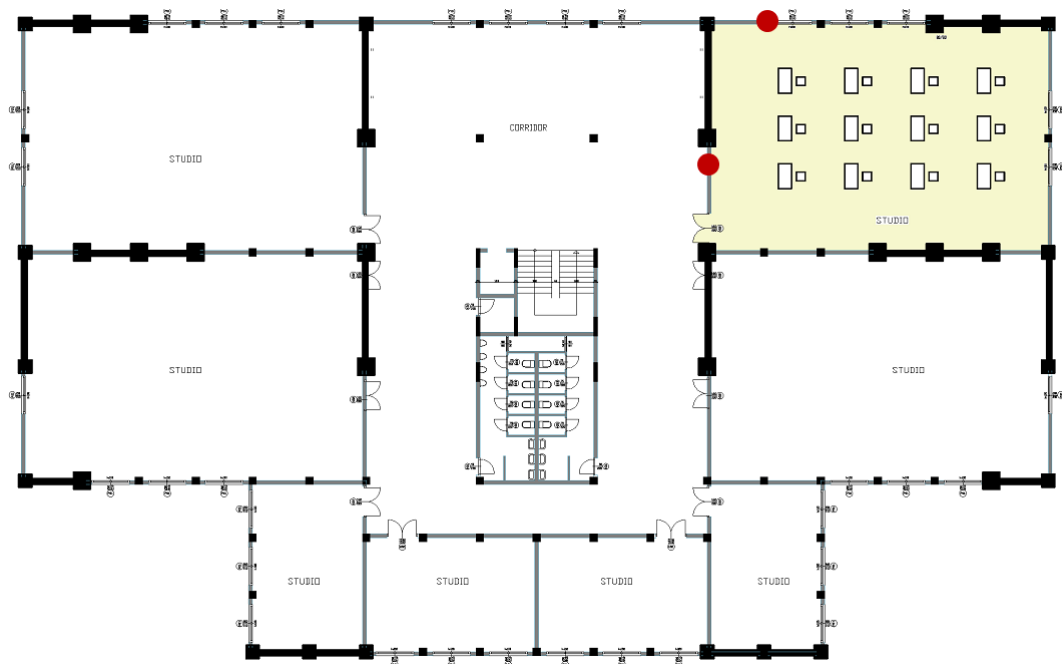


Figure 3.7. Location of inner and outer dataloggers with the red circle and an indication of the selected classroom in the yellow hatch

It runs the simulations annually, with an illuminance-based output, Spatial Daylight Autonomy (sDA). sDA defines the annual simulation area percentage exceeding the minimum illumination level for operating hours (IES 2012). Honeybee uses threshold values to conduct annual illuminance-based task simulations. These are -t for the daylight autonomy threshold, -lt for the lower threshold for useful daylight

illuminance, and -up for the upper threshold. These are specified as 500, 300, and 2000 lux, respectively. The measuring grid size for the simulation tests is 0.6 x 0.6m, and it is 0.75m above the ground surface of the studio.

Table 3.3. The surface material specifications for the daylight simulations.

Data	Building component			
	Wall	Floor	Ceiling	Window
Reflectance	0.6	0.8	0.65	Double-glazed window with 75% transparency
Specularity	0	0	0.1	
Roughness	0	0	0.02	

### 3.4.2. Energy Simulation Model

Monitoring and calibration procedures are applied to the energy simulation model to obtain a validated simulation model. One week of monitoring of indoor and outdoor temperature, relative humidity, and illuminance level is conducted for the studio (Taşer et al., 2022). Then, a calibration process is applied to the simulation models. MBEs and CV(RMSE), two different error ratios, are computed, and their range of acceptability is examined (Taşer et al., 2022). Similar to daylight, Honeybee computed the energy simulations. However, the simulations are conducted for the whole building instead of only the case room. Honeybee uses OpenStudio and EnergyPlus as engines to conduct the simulations. The algorithm uses accurate EnergyPlus weather data -the same as used for daylight simulations-, building envelope materials (i.e., wall, ceiling, roof, slab, and windows), building program, occupancy, lighting, electrical equipment, and natural ventilation schedules, HVAC system properties, and surrounding buildings and trees for the shading effect. Envelope material properties are presented in Table 3.4. Thirty-five architecture students use the studio during the weekdays of the year, between 9:00 am-06:00 pm. Their physical activity is seated in the studios and walking in the corridors. Computers in the studio become possible heat gain sources. All the doors in the building are kept closed. There are forty led panels in the studio with a 31-Watt for each. Natural ventilation is applied for the studios and corridors according to a temperature schedule. Maximum indoor and minimum outdoor temperatures are 21°C and 30°C, respectively. The infiltration level of the building is 0.0004 flow per exterior surface area. This value designates an average tightness. A VRF HVAC system heats the whole building besides corridors and toilets. It starts to



heat the building when the interior temperature is below 21°C and cools when it exceeds 24°C. All these setpoint values are based on ASHRAE Standards (ASHRAE Guideline-14 2002). The simulation engine calculates the shadow effect of surrounding buildings and trees based on their height, width, and material properties. The Grasshopper script definition is presented in Figure 3.8. Honeybee computed annual heating and cooling loads in kWh for the whole building. Honeybee and its engine EnergyPlus computed the energy generation calculations from PV. All the specifications are introduced to Honeybee as in Table 4.2. and Table 4.3. Annual lighting loads are calculated manually based on simple energy equations. (Bayram & Kazanasmaz 2020). Although manually calculated lighting loads give a rough estimation, the study does not aim to understand the numerical value of the lighting loads. It aims to understand the change in the results due to variables. The logic is the same in computing the energy simulations. The heat gain from the lighting system is neglected for this study because it is purposed to estimate the change in thermal loads due to the implementations.

Table 3.4. Building material specifications

Building component	Type	Position	Layer name	Conductivity (W/mK)	Specific heat (j/kgK)	Density (kg/m <sup>3</sup> )	Thickness (m)	U-value (W/m <sup>2</sup> K)
<b>External/ Ground Floor</b>	Typical RF Floor	Outermost	Painted metal	45	410	7690	0.0015	
			Ceiling air gap	0.556	1000	1.28	0.1	
			Insulation	0.03	1210	43	0.05	
		Innermost	Concrete	0.53	840	1280	0.1	
<b>Exterior Wall</b>	Generic Exterior Wall	Outermost	Brick	0.9	790	1920	0.1	
			LW concrete	0.53	840	1280	0.1	
			Insulation	0.03	1210	43	0.05	
			Wall air gap	0.667	1000	1.28	0.1	
		Innermost	Gypsum board	0.16	1090	800	0.0127	
<b>Internal Floor</b>	Typical Interior Floor	Outermost	Acoustic tile	0.06	590	368	0.02	
			Ceiling air gap	0.556	1000	1.28	0.1	
		Innermost	LW concrete	0.53	840	1280	0.1	

(cont. on the next page)

Table 3.4. (cont.)

								<b>1.155</b>
<b>Ceiling</b>	Typical Ceiling	Outermost	LW concrete	0.53	840	1280	0.1	
			Ceiling air gap	0.556	1000	1.28	0.1	
			Acoustic tile	0.06	590	368	0.02	
<b>Internal Wall</b>		Outermost	Gypsum board	0.16	1090	800	0.0127	
			Wall air gap	0.667	1000	1.28	0.1	
			Gypsum board	0.16	1090	800	0.0127	
<b>Roof</b>	Typical Roof	Outermost	Roof membrane	0.16	1210	1120	0.01	
			Insulation	0.03	1210	43	0.05	
			LW concrete	0.53	840	1280	0.1	
			Ceiling air gap	0.556	1000	1.28	0.1	
		Innermost	Acoustic tile	0.06	590	368	0.02	
<b>Glazing</b>	Double glazing	U-factor (W/m <sup>2</sup> K)	SHGC (g-value)	Transmittance (%)				
		<b>3.1</b>	0.67	75				

Table 3.5. Data input details and schedules for energy simulation model

	<b>Building Area</b>				
<b>Base Program</b>		<i>Large class</i>	<i>Small class</i>	<i>Corridor</i>	<i>WC</i>
<b>People</b>	People/area	0.17	0.17	0.17	0.18
	Occupancy	Mon-Fri 9:00-18:00	Mon-Fri 9:00-18:00	Mon-Fri 9:00-18:00	Mon-Fri 9:00-18:00
<b>Elect. Equip.</b>	Watts/area	1.42	1.42	-	-
	Schedule	Mon-Fri 9:00-18:00	Mon-Fri 9:00-18:00	-	-
<b>Doors</b>	Schedule	Closed	Closed	Closed	Closed
<b>Natural Vent.</b>	Min. indoor temperature (°C)	21	21	21	21
	Max. indoor temperature (°C)	30	30	30	30
<b>Infiltration</b>	Flow/ exterior surface area	0.0004	0.0004	0.0004	0.0004
<b>Condition</b>	HVAC	VRF	VRF	VRF	-
<b>Heating/ Cooling Setpoint</b>	Degree (°C)	21/24	21/24	21/24	-

### 3.5. Calibration

Calibration must be evaluated to understand whether the simulation model and actual conditions correlate. ASHRAE Guideline 14-2002 is used for this procedure. This study conducted calibration according to indoor simulated and monitored data temperature values. “Typically, models are declared to be calibrated if they produce MBEs within  $\pm 10\%$  and CV(RMSE)s within  $\pm 30\%$  when using hourly data” is given as a guideline (ASHRAE Guideline 14 2002). Two different error ratios are calculated as MBEs and CV(RMSE)s and analyzed if they are in the acceptable range.

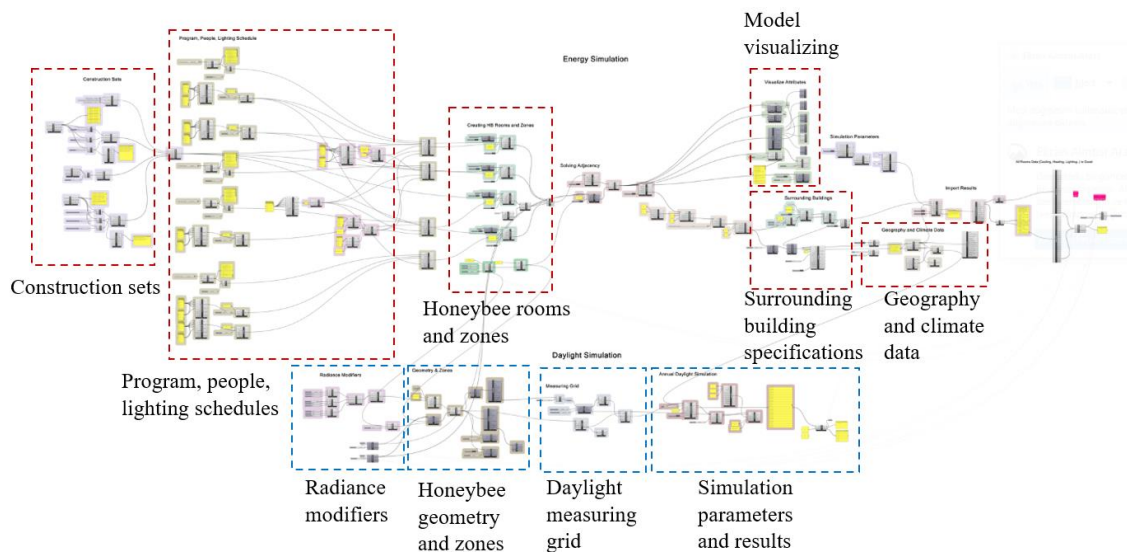


Figure 3.8. Grasshopper component script for the thermal and daylight simulations

### 3.6. Multi-Objective Genetic Optimization

A genetic optimization algorithm Octopus, a plug-in of Grasshopper, runs the optimization process. Octopus uses SPEA-2 and HypE algorithms (Zimmel 2018). It computed the optimization based on the PV glass implemented model. Table 3.5 shows some of the optimization specifications in the Octopus interface. Algorithm settings and specifications are necessary because they influence the optimization process and results. First, the optimization type is defined in the navigation part. Pareto-front is selected; however, elite and history solutions are also visible in the three-dimensional axis. Pareto-front solutions are necessary for multi-objective optimization studies because they are the dominant solutions meaning that the algorithm computes and optimizes all objectives with the same priority level.

Table 3.6. Optimization specifications for the Octopus multi-objective optimization algorithm.

<b>Octopus specification</b>	<b>Value</b>
Elitism	0.5
Mutation probability	0.2
Mutation rate	0.9
Crossover rate	0.8
Population size	100
Maximum generations	0

There are some specifications in the Octopus interface related to genetic algorithm logic (Figure 3.9.). The first one of these is Elitism. Instead of the whole pool, Elitism indicates the ratio of new solutions bred from the elite. More local optimization is obtained when it is assigned to a high value. The Octopus defines this as 0.5 (i.e., 50%) as the default level. There is also the mutation rate that estimates the possibility of every variable or gene being mutated. A low mutation rate indicates minor changes in input variables, while a high rate indicates significant changes. Mutation probability and rate are defined as 0.2 and 0.9 in Octopus. The possibility of two sequentially generated solutions exchanging parameter values is known as the crossover rate. It is set at 0.8 for the study. One influential variable is the population size of an optimization study. Population size is known as the solution number of each generation. There are two variables defined in this optimization study. These are the window-to-wall ratio and glazing transmittance. For two variables, three number strings are defined in the Grasshopper interface. Two number strings are for the window size on the east and south façade, and one string is for the window transmittance value. The algorithm selects ten samples for each variable to increase the model feasibility and reduce the complexity of optimization duration, making the population size 30 for only one generation, and the elite size is estimated accordingly. Maximum generation in Octopus is set to 0 as default. It means that there is no end to the research. The Octopus algorithm continued to run until the objectives were at the desired level and a sufficient number of populations had formed. The algorithm ran for a week and then stopped. Then, it generated the results three-dimensionally. Many inputs were entered into the energy and daylight simulation models, increasing one simulation's duration. For this reason, the optimization algorithm had to be run for a week to reach a sufficient number of results.

The optimization balances the window-to-wall ratio (i.e., window size and location) and PV glass' transmittance value (Table 6). Octopus algorithm kept the PV glass transmittance between 20-40%. Also, window height is not changed throughout the optimization process, but the width is increased from the center to the wall corners (Figure 6). There is only one window in each façade. The window does not change its location. Only its width increases from the center to the edges. The objectives are minimum heating and cooling loads and a maximum sDA value. IES defines sDA as “the percent of an analysis area that meets a minimum daylight illuminance level for a specified fraction of the operating hours per year” (IES 2012). According to IES standards, a space requires at least 50% sDA as an acceptable sDA level. Also, it needs at least 500 lux illumination as the threshold illuminance (CIBSE 2002). This optimization study defines threshold sDA value as  $sDA_{500,50\%} \geq 50\%$ . It means sDA provides 500 lux illumination for half of the year in at least 50% of the analysis area. The complexity of this optimization problem comes from the objectives of the study. Two objectives (i.e., sDA and thermal loads) conflict with each other during the optimization. It means that while the optimization algorithm increases one of the objectives, the other tends to decrease. It is challenging to keep both at an optimum level. Thus, Pareto solutions are significant for achieving satisfactory results.

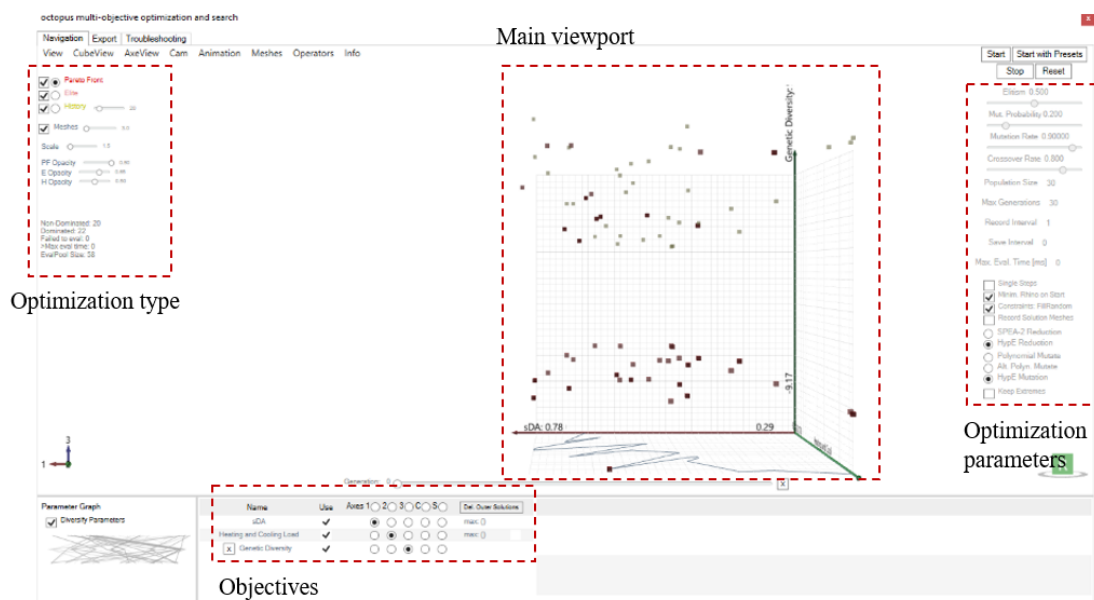


Figure 3.9. Octopus interface

Table 3.7. Optimization specifications for the Octopus multi-objective optimization algorithm.

Variable	Range
PV glass transmittance (%)	20-40
Window size and location	same height width increases from the center to the wall corners

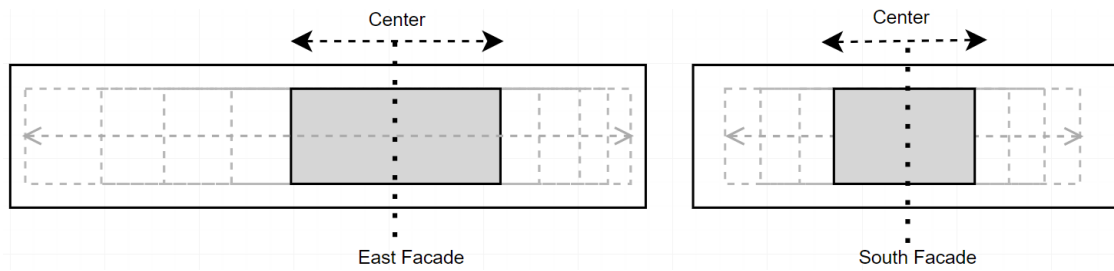


Figure 3.10. Illustration of window size change during the optimization process

# CHAPTER 4

## RESULTS

### 4.1. Measurement Results

According to the monitoring results, a calibration procedure is conducted based on the simulation models. The monitoring process is conducted between the 30<sup>th</sup> of November at 1:00 p.m. and the 7<sup>th</sup> of December at 1:00 p.m. Hobo data loggers are set to collect data for temperature, relative humidity, and illuminance level every 10 minutes for indoor-outdoor environments. According to Table 4.1. below, the average outdoor temperature is calculated as 15.2°C. It is recorded as 19.6 °C as the highest and 8.8 °C as the lowest value. Average relative humidity (RH) is defined as 68.5%. The maximum and minimum relative humidities are 88.12% and 40.5%, respectively.

Table 4.1. Monitored data on highest/lowest temperature and relative humidity

<b>Monitored Data</b>					
<b>Environment</b>	<i>Data</i>	<i>Date</i>	<i>Temperature (°C)</i>	<i>RH (%)</i>	<i>Illuminance (lux)</i>
<b>Outdoor</b>	Hottest hour	6.12.21, 3:30 p.m.	19.6	67.6	2400
	Coldest hour	2.12.21, 1:00 a.m.	8.8	64	3.9
	Highest RH	6.12.21, 7:00 p.m.	16.1	88.1	3.9
	Lowest RH	30.11.21 1:00 p.m.	18	40.5	32.280
	Average	-	15.2	68.5	3832
<b>Indoor</b>	Hottest hour	06.12.21 9:10 a.m.	24.9	51.7	350
	Coldest hour	02.12.21 9:00 a.m.	22	42.7	240.5
	Highest RH	06.12.21 8:30 p.m.	23.2	58.4	303.5
	Lowest RH (%)	01.12.21 6:30 a.m.	22.1	38.6	145.8
	Average	-	23.4	50.5	212.9

The average outdoor illuminance level is measured as 3832 lux. Maximum and minimum values are calculated as 32.280 lux and 3.9 lux, respectively. The minimum value refers to night-time. The hottest monitored data was obtained on the 6<sup>th</sup> of December at 3:30 p.m. at 19.6°C. RH is monitored as 67.65% when this is received, and the illuminance level is calculated as 2400 lux. The coldest observed data was obtained on the 2<sup>nd</sup> of December at 1:00 a.m. At this time, RH is calculated as 64%, and the

illuminance level is noted as 3.9 lux because of the lack of daylight during night-time. In the highest observed RH, the outdoor temperature is monitored as 16.1°C, and the illuminance level is defined as 3.9 lux similarly. In the lowest observed RH, the temperature is obtained as 18°C, and the illuminance level is monitored as 32.280, the highest observed value during monitoring. Besides night-time, the average illuminance level is calculated as 3832 lux. Maximum and minimum values are monitored as 32.280 and 3.9 lux. While defining the daytime, 8:10 a.m.-06:00 p.m. are taken as the interval.

According to these, relative humidity is increased when the temperature drops and the illuminance value is decreased. Due to temperature decrease, the sky may be covered with more clouds, and the sun may become more invisible. Thus, there occurred a decrease in illuminance values when the temperature dropped. Also, due to night-time, illuminance levels and temperatures drop.

For the indoor environment, the average indoor temperature is calculated as 23.4°C. It is recorded as 24.9°C as the highest and 22°C as the lowest value. The average relative humidity is calculated as 50.5%. Maximum and minimum relative humidity is 58.4% and 38.6%, respectively. The average indoor illuminance level is 167.64 lux, including the nighttime illuminance levels. Maximum and minimum values are calculated as 1028 lux and 3.9 lux, respectively.

The hottest monitored data was obtained on the 6<sup>th</sup> of December at 9:10 a.m. at 24.9°C. When this is obtained, RH is monitored as 51.7%. Also, the illuminance level is calculated as 350 lux. The coldest monitored data was obtained on the 2<sup>nd</sup> of December at 9:00 a.m. At this time, RH is calculated as 42.7%, one of the lowest values (Figure 4.1.).

It is observed that when the temperature drops at this hour, RH also drops. In the highest observed RH, the indoor temperature is monitored as 23.2°C. In the lowest observed RH, the temperature is obtained as 22.1°C.

Since the building is continuously heated, there is no considerable temperature fluctuation. However, there are still received changes in relative humidity values. Therefore, temperature and RH are not as correlated as in outdoor monitoring.



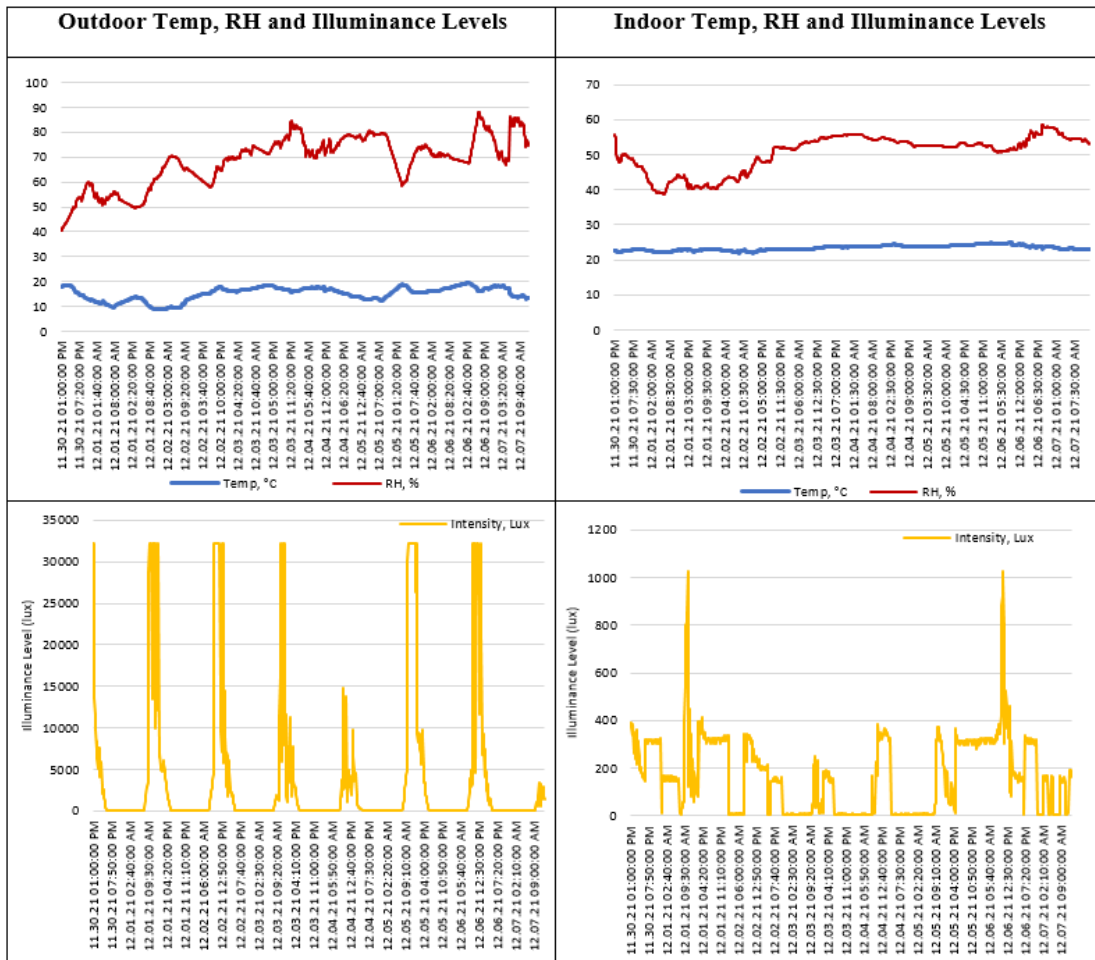


Figure 4.1. Indoor and outdoor monitored data of temperature, relative humidity

Besides night-time, the average illuminance level is calculated as 212.9 lux. Maximum and minimum values are monitored as 1028 lux and 3.9 lux. While defining the daytime, 8:10 a.m.-06:00 p.m. are taken as the interval.

## 4.2. Calibration Results

According to the results, average simulated and monitored indoor air temperatures are calculated as 21.6°C and 23.4°C. The difference between the two is noted as 1.78. The average outdoor air temperature for this period is monitored as 15.2°C. The minimum and maximum temperature differences between simulated and monitored indoor air temperature are calculated as 3.27°C and 0.39°C, respectively. The maximum difference is observed on the 4<sup>th</sup> of December between 11:00 a.m. and 2:00 p.m. when the average outdoor air temperature is monitored as 17°C.

Two types of error ratios are calculated and evaluated for calibration. These are MBEs and CV(RMSE)s. RMSE is calculated by multiplying  $(\sqrt{(1/N * \sum (T_{\text{simulated}} - T_{\text{monitored}})^2)})$  with  $100/T_{\text{monitored}}$ . MBE is calculated as  $(100/T_{\text{monitored}}) \times (\sum (T_{\text{simulated}} - T_{\text{monitored}}) \text{ hours})$ . According to the results, RMSE and MBE are calculated as 8.57% and -7.6%, respectively. They are both calculated in the acceptable range. There could be no observation of high fluctuations in indoor simulated and monitored temperature (Figure 4.2.). It may be due to the classroom being continuously heated during the monitoring period. The natural ventilation and HVAC schedule are changed in the second calibration model. Natural ventilation's minimum and maximum indoor air temperatures are adjusted to 22°C and 26°C, respectively. The HVAC system's heating set point is increased to 23°C. The results show that the average simulated indoor air temperature is 22,5°C. The difference between the average monitored and simulated temperature is decreased by 0,9°C. The minimum and maximum temperature differences between simulated and observed indoor temperatures are calculated as 0 and 2,92°C. RMSE and MBE are calculated as 6,3 and -3,78, respectively. These are calculated lower than the previous results. When the results are compared with the first model, indoor simulated and monitored temperatures are calculated closer. On the fourth day, indoor observed temperature increases, although indoor simulated and outdoor monitored temperatures decrease. This difference may be due to insufficient natural ventilation and high occupancy.

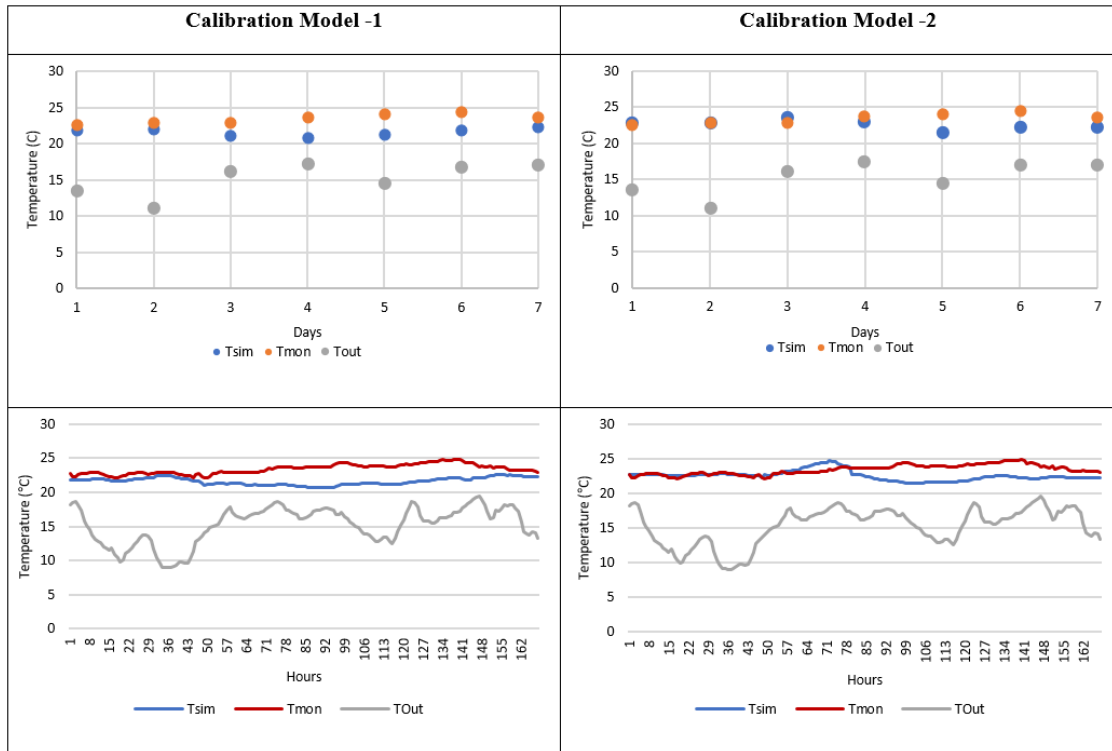


Figure 4.2. Daily average temperatures per two calibration models: simulated/monitored indoor temperatures and outdoor temperatures

### 4.3. Base Case Results

Daylight performance is evaluated based on Spatial Daylight Autonomy (sDA). sDA is a climate-based method that calculates daylight performance with a time-varying sky. The sDA is a tool for estimating daylight availability that indicates how much of a given space's floor area meets and exceeds the necessary illumination throughout the specific analysis time. In classrooms, 500 lux and above illumination is required. Below 300 lux illumination is defined as unacceptable. In this study, the threshold sDA value is defined as  $sDA_{500,50\%} \geq 75\%$ , which means that in 50% of the total period in 75% of the analysis zone, sDA offers a 500-lux daylight illumination.  $sDA_{500,50\%} \geq 55\%$  is also defined as nominally acceptable.  $sDA_{500,50\%} \leq 55\%$  is insufficient. This performance criterion is defined according to the studies in the literature. According to the results, in 50% of the total analysis period, sDA offers a 500-lux daylight illumination in 59.1% of the analysis zone. Although it is considered nominally acceptable, it is not at the desired level. In the studio, there are very bright and very dark areas. So, the homogenous distribution of daylight is not achieved. A threshold of 2000 lux is defined to evaluate the glaring risk of the studio. It is seen that, in 50% of the total analysis period, a

minimum of 2000 lux illumination is available in 13.6% of the analysis zone (Figure 4.3.). The aim is to decrease glare risks and increase the illuminance of poor daylight areas.

Heating, cooling, and lighting loads are calculated annually for energy calculations. Honeybee calculates heating and cooling loads with EnergyPlus and OpenStudio for the whole building. Lighting load is calculated manually for only the case room according to some equations (Bayram and Kazanasmaz 2019):

(1) Daily Energy Consumption = luminaire power x luminaire number x operating hours

(2) Seasonal Energy Consumption = Daily Energy Consumption x 60 (days)

(3) Annual Energy Consumption = Season<sub>1</sub> + Season<sub>2</sub> + Season<sub>3</sub> + Season<sub>4</sub>

According to this calculation method, two different annual lighting loads are calculated. One is operated for the clear sky with the sun, while the other is for the overcast sky.

Point-in-time grid-based simulations are conducted for two different sky components on the 21<sup>st</sup> of March, June, December, and 23<sup>rd</sup> of September. Simulations are performed for various periods, such as 8:00 a.m., 10:00 a.m., 12:00 p.m., 3:00 p.m., 6:00 p.m., and 8:00 p.m. Studio, which students use, including nightshift on spring and winter seasons. It is used between 9 a.m. and 6 p.m. in summer and fall. Areas not meeting 300 lux thresholds are defined, and artificial lights are applied there.

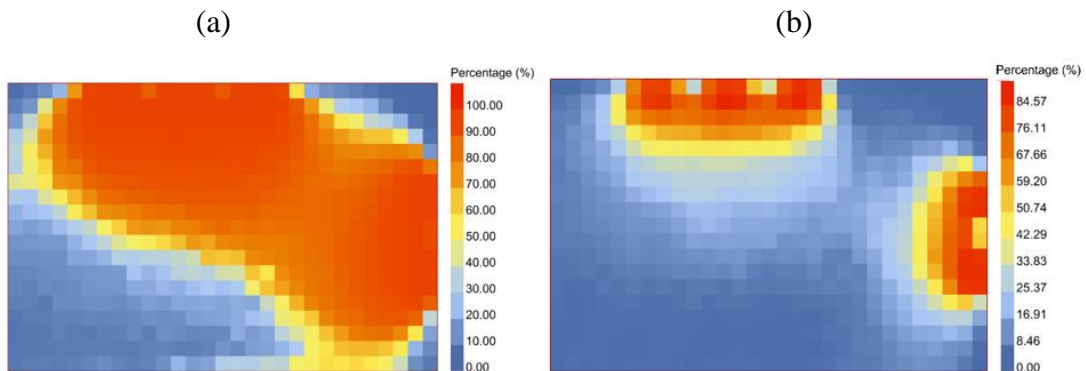


Figure 4.3. (a) Annual daylight autonomy results according to 500 lux threshold  
(b) Annual daylight autonomy results according to 2000 lux threshold

According to the results, annual lighting loads are calculated as 2453 and 3730 kWh in clear sky with sun and overcast sky conditions, respectively (Figure 4.4.). A VRF system is used to heat and cool spaces beside toilets in the entire building.

According to the results, the building's annual heating and cooling loads are calculated as 7.909.507 kWh and 1.114.731 kWh, respectively (Figure 4.5.).

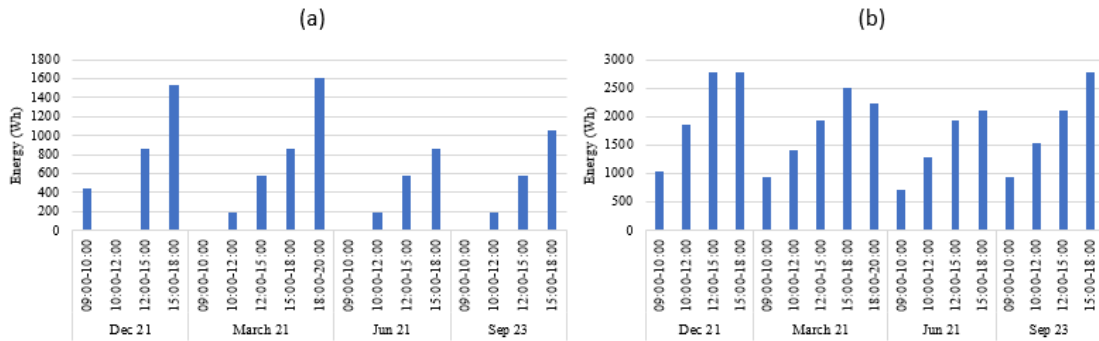


Figure 4.4. (a) Daily energy consumption for lighting during day-time on the clear sky with sun (b) Daily energy consumption for lighting during day-time on overcast sky

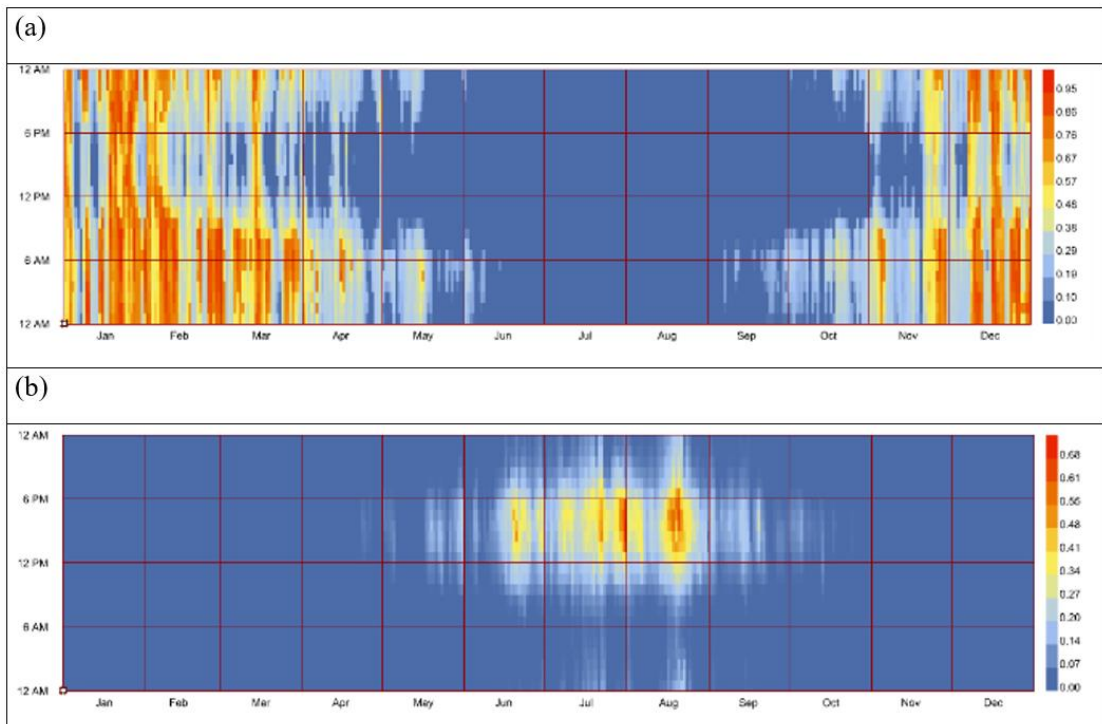


Figure 4.5. (a) Hourly energy consumption for heating of whole building (b) Hourly energy consumption for cooling the whole building.

For the case room, time not comfortable according to simple ASHRAE 55-2004 Standards with winter clothes, summer clothes, and winter or summer clothes is calculated as 877, 1278.5, and 94.75 hours respectively. The case room had its peak outdoor temperature on the 21<sup>st</sup> of June at 3:00 p.m. at 39.9°C. At this time, the indoor air temperature is calculated as 24°C. The outdoor lowest temperature is calculated as 6.3°C on the 21<sup>st</sup> of January at 00:00 a.m., while the indoor air temperature is calculated

as 22.97°C. The time set point not met during heating is calculated as 2060.5 hours for this room. Annual building sensible heat gain components are also calculated for the case room. According to this, heat gain from HVAC zone equipment sensible heating, people, electricity equipment, windows, and infiltration are calculated as 1.494.734, 5388, 608, 11.472, and 329.363 kWh, respectively. Heat loss from HVAC zone equipment sensible cooling, windows, infiltration, opaque surface conduction, and other heat removal is calculated as 335.808, 2750, 1.501.512, and 3.972.254 kWh, respectively.

The peak value of heat gain through the case room is noted on the 3<sup>rd</sup> of February at 2:58 a.m. as 129 kW. At this hour, the heat is gained through the HVAC heating system, and most of the heat is lost due to opaque surface conduction, windows, and infiltration.

#### **4.4. PV Glass Scenario Results**

In this section, the study evaluates the daylight, thermal, and energy performance of a-Si thin film solar cells implemented on Low-E PV glass of OnyxSolar © through simulation software (OnyxSolar). Three different modules are tested in terms of the studio's daylight, thermal, and energy performance. These are differed according to their transmittance. 10, 20, and 30% transmittance thin-film modules are installed individually. The study estimates the annual and seasonal electricity generation of PV glass and the annual lighting load of the case room to evaluate the room's overall performance for accurate analysis. The software calculates the building's annual heating and cooling loads, which are evaluated along with the thermal and visual comfort of the occupants. This part of the study aims to understand the performance capacity of PV glass when its properties are not optimized and introduced to the software as manufactured. Tables 4.2. and 4.3. present selected PV glass' optical and electrical properties. All these specifications are introduced to Honeybee for PV electrical energy generation calculations. Honeybee uses EnergyPlus as the engine for this type of calculation.

Table 4.2. Photovoltaic glass specifications (Source: Onyx 2021)

Glass Properties								
Thickness configuration	G-value (%)	U-value (W/m <sup>2</sup> K)	External light reflection (%)	Transmittance (%)	Peak power (Wp/m <sup>2</sup> )	Nominal peak power (W <sub>p</sub> )	Length, width, thickness (mm)	Surface area (m <sup>2</sup> )
6T+3.2+6T/12Air/6T low-e	17	1.6	7.3	30	28	20	1200,600,8.1	0.72
	12			20	34	24	0 (EVA)	
	9			10	40	29	8.72 (PVB)	

Table 4.3. Photovoltaic system electrical specifications (Source: Onyx 2021)

Electrical Properties									
Thickness conf.	Open circuit voltage (V)	Short-circuit current (A)	Voltage at nominal power (V)	Current at nominal power (A)	Power tolerance not to exceed (%)	Temp. coefficient of P <sub>mpp</sub> (%/°C)	Temp. coefficient of V <sub>oc</sub> (%/°C)	Temp. coefficient of I <sub>sc</sub> (%/°C)	Transparency (%)
6T+3.2+6T/12Air/6T low-e	47	0.74	32	0.63	+-5	-0.19	-0.28	0.09	30
		0.93		0.76					20
		1.11		0.90					10

According to the results, in 50% of the total analysis period, 500 lux illumination was found available in 28.8%, 17.6%, and 7% of the analysis zone for 30%, 20%, and 10% transmittance PV glass, respectively (Figure 4.6.). None of these results meet the minimum daylighting requirements of the studio. However, the 30% transmittance PV module represents the best result.

Three different a-Si thin-film modules are applied to the case model. The results can be seen in the table below. Energy generation is calculated on Honeybee with EnergyPlus, OpenStudio, and the Onyx Solar Company website (OnyxSolar 2021). The results of Grasshopper and OnyxSolar are compared, and it is found that they calculated the results almost the same. So, the results of Honeybee are validated. According to its results, the lowest transmittance (10%) module produced the highest amount of electricity, while the highest transmittance module (30%) generated the lowest electrical energy. The case room has three windows on the east façade and two on the south. Windows on the same façade have equal energy production results. For 30% transmittance modules, total AC power for a year is calculated as 108 kWh and 148.5 kWh per window on the east and south, respectively (Figure 4.7.). The CO<sub>2</sub> emission rate is 291.5 kWh and 212.2 kWh per window on the east and south. Annual energy

production is noted as 620.9 kWh. For 20% transparency modules, total AC power for a year is calculated as 130.2 kWh and 178.9 kWh per window on the east and south, respectively. The CO<sub>2</sub> emission rate is 241.9 gCO<sub>2</sub>/kWh and 176 gCO<sub>2</sub>/kWh per window on the east and south, respectively. Annual energy production is noted as 748.4 kWh. For 10% transmittance modules, total AC power for a year is calculated as 154 kWh and 211.5 kWh per window on the east and south, respectively. The CO<sub>2</sub> emission rate is 204.6 gCO<sub>2</sub>/kWh and 148.9 gCO<sub>2</sub>/kWh per window on the east and south, respectively. Annual energy production is noted as 884.9 kWh.

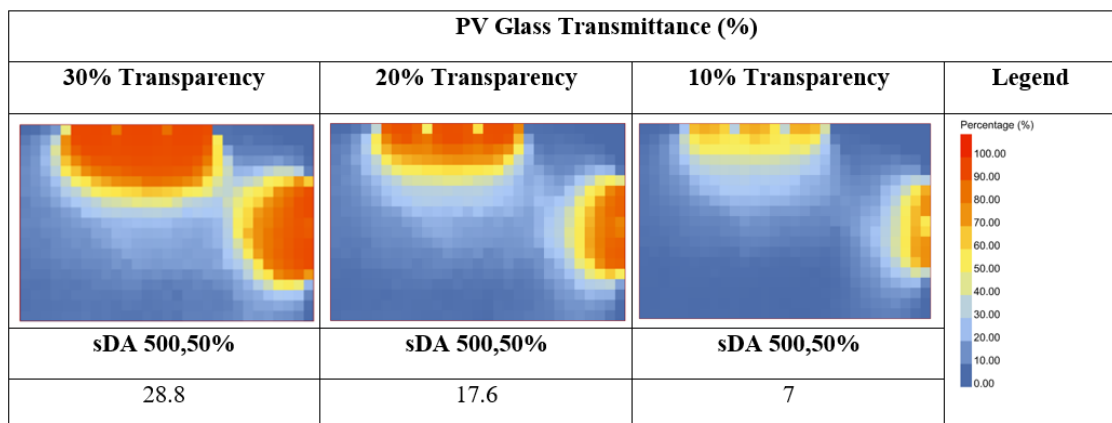


Figure 4.6. The studio's annual daylight autonomy results in different transmittance a-Si thin-film photovoltaic modules

Since PV modules created a difference in illuminance level, the studio's lighting load also changed. The lighting load range, as minimum and maximum, is calculated as 3509-4106 kWh, 3997-4210 kWh, and 4354-4417 kWh for 30%, 20%, and 10% transmittance PV modules, respectively (Table 4.4.). Therefore, the lighting load of the studios is significantly increased.

New PV glass' U-value, transparency, and SHGC (g-value) are lower. A low U-value can decrease the heating and cooling load. However, low transparency and SHGC may increase the heating load and reduce the cooling load (Table 4.5.).



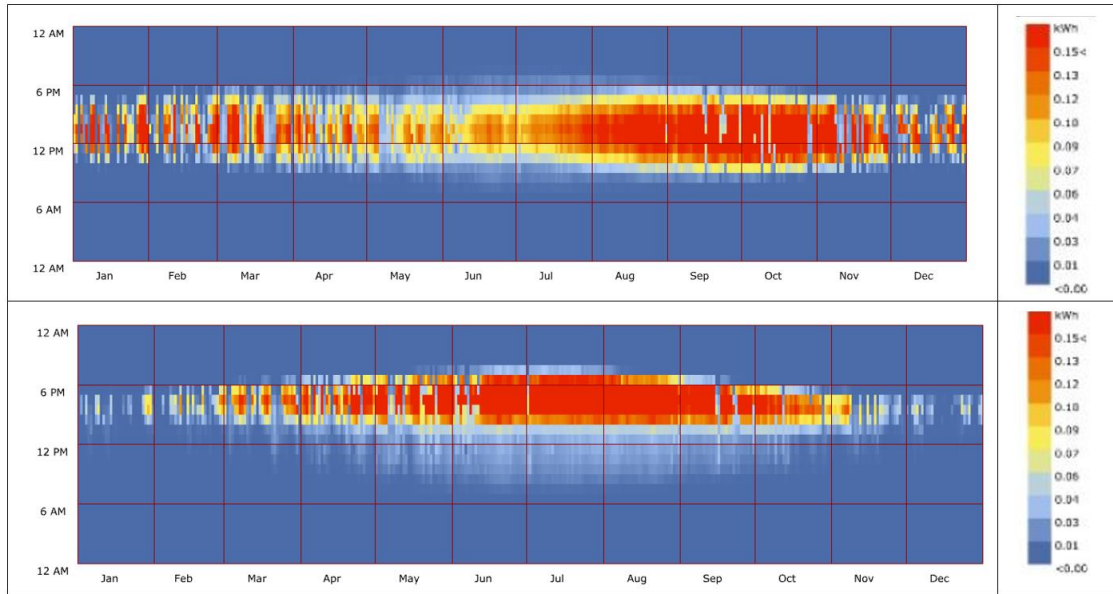


Figure 4.7. Hourly energy production results of 10% transmittance PV glass for South and East façades, respectively

Table 4.4. Seasonal lighting load and PV energy generation comparison

Season	Data Input			
	Total lowest and highest lighting load (kWh)	Electrical energy generation from PV (kWh)		
		30% Transmittance	20% Transmittance	10% Transmittance
Winter	1178-1514	54	65	76.9
Spring	1067-1413	140.8	169.7	200.7
Summer	97-360	241.3	290.8	343.8
Fall	109-441	182	219.4	259.4

Table 4.5 Overall energy and daylighting data

Energy Data	Case model	Transmittance (%)		
		30	20	10
Whole building heating end use (kWh)	7909507	7910341	7911702	7912563
Whole building cooling end-use (kWh)	1114731	1097786	1094508	1092536
Case room annual lighting load range (kWh)	2453-3730	3509-4106	3997-4210	4354-4417
Time not comfortable for winter, summer and both clothes (hour)	877 1278.5 94.7	465.7 1411.5 96.3	410.2, 1456.5 98	386.7 1494.7 102
Time setpoint not met during heating (hour)	2060	2075	2079	2081
HVAC zone equipment sensible air heating (kWh)	1494734	1496123	1496400	1496678
Heat gain from people (kWh)	5388	5416	5416	5416
Heat gain from electricity equipment (kWh)	608	608	608	608
Heat gain from windows (kWh)	11472	2944	2047	1511
Heat gain from infiltration (kWh)	329363	329391	329391	329391

Table 4.5. (cont.)

HVAC zone equipment sensible air cooling (kWh)	335808	332752	332447	332280
Windows heat removal (kWh)	2750	1555	1608	1647
Infiltration heat removal (kWh)	1501512	1499317	1499039	1499095
Opaque surface conduction heat removal (kWh)	3972254	3166692	3055580	2958079
Peak Heating Sensible Heat Gain Components: HVAC zone sensible air heating (kW)	February, 3 <sup>rd</sup> , 1299	February 3 <sup>rd</sup> , 1299	February 3 <sup>rd</sup> , 1299	February 3 <sup>rd</sup> , 1299
PV energy generation (kWh)	-	620.9	748.4	884.9
Power output per window (kWh)	-	East: 108	East: 130.2	East: 153.9
		South: 148.5	South: 178.9	South: 211.5
sDA500,50%	59.1	28.8	17.6	7

According to the results, PV glass modules increased the building’s lighting and heating load while they decreased the cooling load (Figure 4.8.). It is because windows absorb less heat compared to the base case model. Less heat gain from windows resulted in higher heating and lowered cooling load. Since they transmit less daylight through the interior, they also increase the lighting load. The HVAC system and natural ventilation were off in the last analysis. It aims to understand how windows will be critical to indoor temperatures. According to the results, the annual average indoor temperature is calculated as 22.57°C, 22.8 °C, and 22.3 °C for 10%, 20%, and 30% transparent PV glass. It is calculated as 26.6°C for the base case model.

## 4.5. PV Glass Optimization Results

### 4.5.1. Pareto-front Analysis: Optimum Design Variables and Objectives

The Octopus multi-objective optimization algorithm runs with the Grasshopper interface for one week. After computing, the algorithm stopped working, and the results were

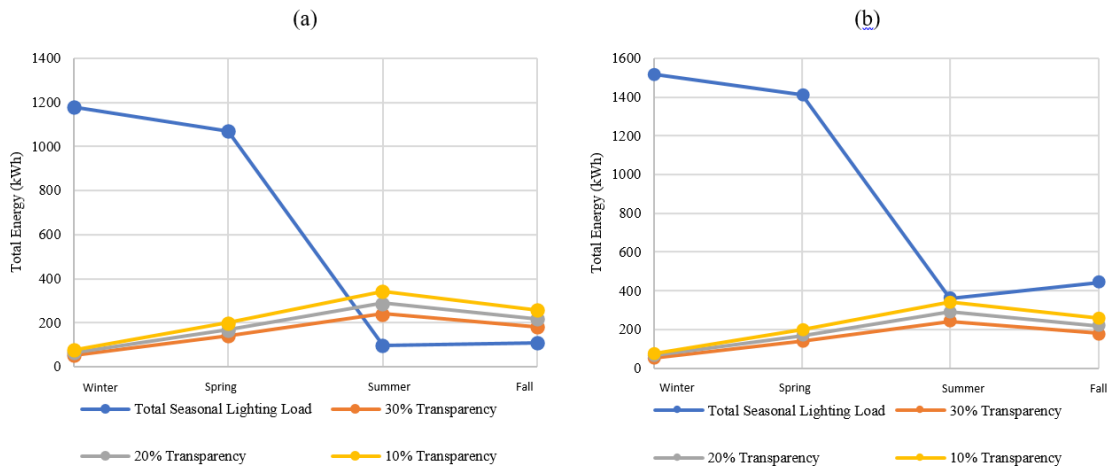


Figure 4.8. a) Seasonal lighting load under a clear sky with sun condition and PV energy generation comparison (b) Seasonal lighting load under overcast sky condition and PV energy generation comparison

obtained on the three-dimensional axis. While evaluating the results, the optimum Pareto-front results with the highest sDA and the lowest thermal loads were selected. Pareto-front aims to improve both objectives in the optimization process. However, these objectives influence each other, meaning that as one of the objectives increases, the other may decrease due to the influence of one on another.

Thus, a multi-objective evolutionary algorithm is significant in this sense. The optimization aims to increase sDA, reduce the total thermal loads of the building, and increase the energy-saving potential of the studio. The optimum Pareto solutions are selected according to the possible highest sDA and the lowest total heating and cooling load. Figure 4.9. below is the multi-axe view of the evolutionary algorithm and selection of the Pareto-front genomes. The solutions with at least 50% of sDA are indicated with a red line on the figure. The lowest total thermal load above this line corresponds to the Pareto-front genomes for this optimization study.

Table 4.6. below shows the results in detail. The three best-performed solutions were selected as indicated with a grey color on the table. In one solution [i.e., Pareto-front genome (1)], sDA reached 58.24% without falling below the threshold level with 40% transmittance of the PV glass modules. In addition, the total thermal load of the studio increased by 2.91% compared with the base case model. The simulation engine calculates total heating and cooling loads as 8.151.201 kWh and 1.136.220 kWh, respectively. In this genome, the glass surface area is optimized as 14.7 m<sup>2</sup> for the

South façade and 18.28 m<sup>2</sup> for the East façade. In total, the algorithm obtains 32.98 m<sup>2</sup> of glass surface area. It is increased by 49.1% compared to the existing model.

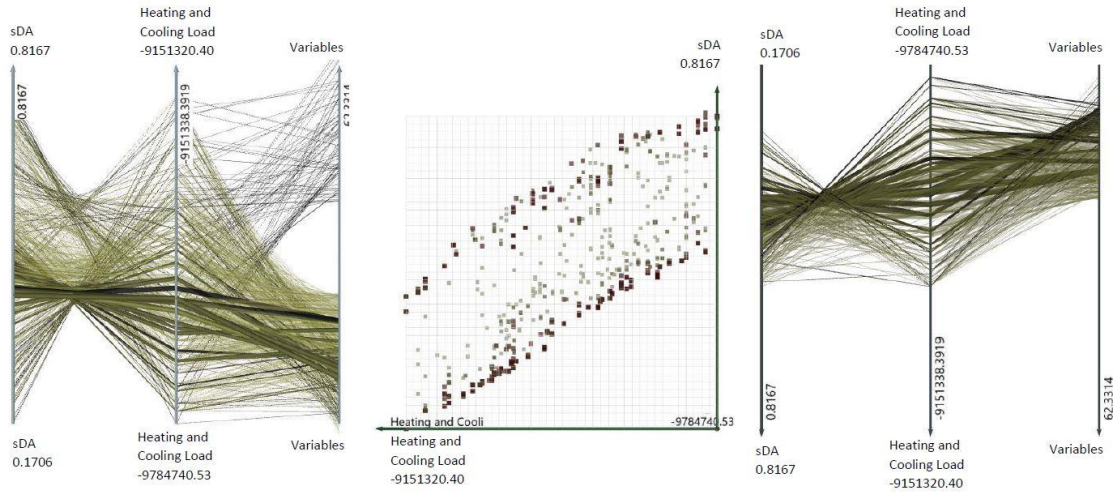



Figure 4.9. Pareto-front results of evolutionary algorithm

Table 4.6. Pareto-front optimization genomes show each objective and variable in detail.

Variables			Objectives							
Window surface (m <sup>2</sup> )	Transmittance (%)	sDA (%)	Heating load (kWh)	Cooling load (kWh)	Total thermal load (kWh)	(%) <sup>1</sup>	(%) <sup>2</sup>	(%) <sup>3</sup>	(%) <sup>4</sup>	
										East/South
<b>Base Case</b>										
12.6/8.4	21	75	59.9	--	--	7909507	1114731	9024238	--	--
<b>30% transmittance PV glass</b>										
17.28/11.52	28.8	30	28.8	-31.1	--	7910341	1097786	9008127	0.17	--
<b>Pareto-front genome (1)</b>										
16.62/14.7	31.32	40	55.37	-4.53	26.6	8117258	1131037	9248295	-2.48	-2.66
<b>Pareto-front genome (2)</b>										
18.28/14.7	32.98	40	58.24	-1.66	29.4	8151201	1136220	9287421	-2.91	-3.10
<b>Pareto-front genome (3)</b>										
19.94/10.5	30.44	39	50	-9.9	21.2	8101755	1127855	9229610	-2.27	-2.45
<b>Other Pareto solutions</b>										
21.61/11.55	33.16	39	56	-3.9	27.2	8156232	1136444	9292676	-2.97	-3.15
23.27/10.5	33.77	37	54.43	-5.47	25.6	8168928	1138303	9307231	-3.13	-3.32
16.62/19.95	36.57	38	62.21	2.31	33.4	8220917	1148080	9368997	-3.82	-4.00
19.94/16.8	36.74	39	64	4.1	35.2	8226570	1148257	9374827	-3.88	-4.07

(cont. on the next page)

Table 4.6. (cont.)

18.28/19.95	38.23	38	64.97	<b>5.07</b>	<b>36.2</b>	8254787	1153322	9408109	- <b>4.25</b>	<b>-4.44</b>
23.27/10.5	33.77	34	50.82	<b>-9.08</b>	<b>22</b>	8168928	1138303	9307231	- <b>3.13</b>	<b>-3.32</b>
23.27/12.6	35.87	38	59.5	<b>-0.4</b>	<b>30.7</b>	8210905	1145113	9356018	- <b>3.67</b>	<b>-3.86</b>
18.28/21	39.28	38	66.2	<b>6.3</b>	<b>37.4</b>	8275581	1156706	9432288	- <b>4.52</b>	<b>-4.70</b>
16.62/14.7	31.32	38	50.62	<b>-9.28</b>	<b>21.8</b>	8152827	1112472	9265299	- <b>2.67</b>	<b>-2.85</b>
16.62/16.8	33.42	34	50	<b>-9.9</b>	<b>21.2</b>	8158731	1137836	9296567	- <b>3.01</b>	<b>-3.20</b>
18.28/19.95	38.23	37	63.5	<b>3.6</b>	<b>34.7</b>	8254787	1153322	9408109	- <b>4.25</b>	<b>-4.44</b>
16.62/16.8	33.42	37	55.32	<b>-4.58</b>	<b>26.5</b>	8213723	1142837	9356560	- <b>3.68</b>	<b>-3.86</b>
26.59/10.5	37.09	40	63.35	<b>3.45</b>	<b>34.6</b>	8236553	1148734	9385287	- <b>4.00</b>	<b>-4.18</b>
16.62/19.95	36.57	38	62.7	<b>22.82</b>	<b>33.9</b>	8220917	1148080	9368997	- <b>3.82</b>	<b>-4.00</b>
21/18.28	39.28	37	65.15	<b>5.25</b>	<b>36.4</b>	8275581	1156706	9432287	- <b>4.52</b>	<b>-4.70</b>
16.62/19.95	36.57	34	57.7	<b>-2.2</b>	<b>28.9</b>	8220917	1148080	9368997	- <b>3.82</b>	<b>-4.00</b>
23.27/12.6	35.87	40	62.4	<b>2.5</b>	<b>33.6</b>	8210905	1145113	9356018	- <b>3.67</b>	<b>-3.86</b>
(%)1: sDA difference between the base case and the Pareto-front gene										
(%)2: sDA difference between the 30% transmittance PV glass and the Pareto-front gene										
(%)3: Total heating and cooling load difference between the base case and the Pareto-front gene										
(%)4: Total heating and cooling load difference between the 30% transmittance PV glass and the Pareto-front gene										
 Pareto-front genomes										

Regarding the glaring risk of the studio, sDA is calculated as 58.24%, 55.37%, and 50% for the three best-performed genomes, respectively. These are increased by 29.44%, 26.57%, and 21.2% compared with the 30% transmittance PV glass. sDA values are calculated very close to the base case situation, with less glare risk and more visual comfort for the occupants (Figure 4.10.). At least 2000 lux of illumination was found usable in 12.1%, 9.9%, and 11.25% of the analysis area in half of the year for the three genomes.

Annual and seasonal lighting load and PV electrical energy generation of the selected Pareto-front genome are calculated to evaluate the energy performance of the optimized model. According to the results, the seasonal lighting energy consumption of optimized PV glass is calculated as 1153-1495 kWh, 1119-1440 kWh, 192-426 kWh, and 107-453 kWh for winter, spring, summer, and autumn periods for the two sky types respectively: clear sky with sun and overcast sky (Table 4.7.). Table 4.8. shows the overall energy and daylighting data of the studio. Total power generation for a year is

375.15 kWh and 432.2 kWh for the south and east facades, respectively. Energy generation is 807.35 kWh annually (Figure 4.11.)

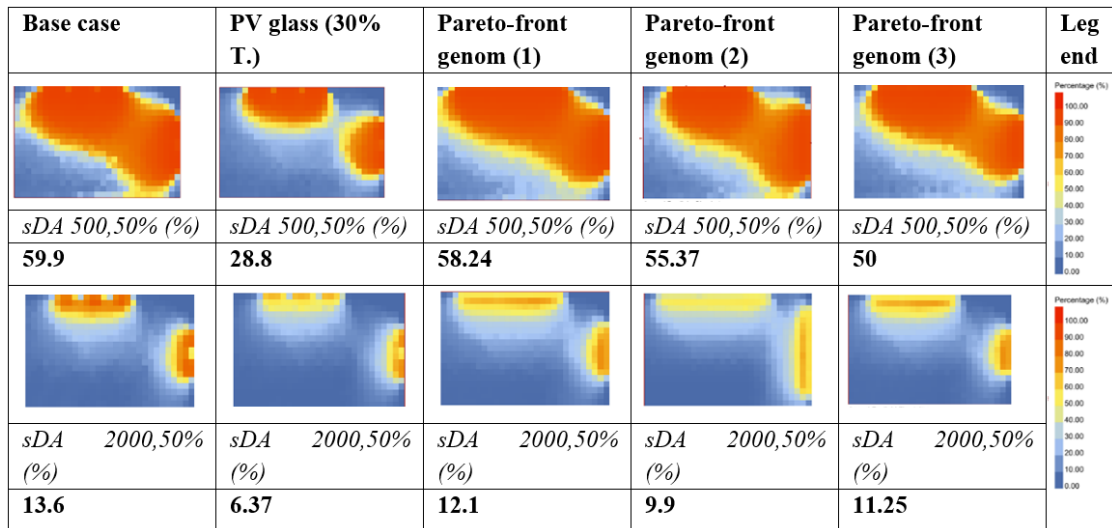


Figure 4.10. The base case, 30% transmittance PV glass, and three best-performed Pareto-front genomes' daylight autonomy results according to the 500 lux and 2000 lux thresholds

Table 4.7. Seasonal lighting load of the studio and PV glass electrical energy generation comparison.

Season	Data Input					
	Lighting load range (kWh)			PV electricity generation (kWh)		
	<i>Base case</i>	<i>30% transmittance PV glass</i>	<i>Pareto-front genome (1)</i>	<i>Base case</i>	<i>30% transmittance PV glass</i>	<i>Pareto-front genome (1)</i>
<b>Winter</b>	1178-1514	1392-1549	1153-1495	-	54	74.7
<b>Spring</b>	1067-1413	1322-1532	1119-1440	-	140.8	172.1
<b>Summer</b>	97-360	428-501	192-426	-	241.3	320.4
<b>Fall</b>	109-441	366-524	107-453	-	182	240.2
<b>Total</b>	2453-3730	3509-4106	2572-3815	-	620.9	807.35

Table 4.8. Overall energy and daylighting data.

Energy Data	Data Input		
	Case model	30% Transmittance PV glass	Pareto-front genome (1)
Annual energy consumption to heat the whole building (kWh/m <sup>2</sup> )	12554	12556	12884
Annual Energy consumption to cool the whole building (kWh/m <sup>2</sup> )	1769	1742	1795
Heat gain from windows (kWh/m <sup>2</sup> )	18233	4677	7052
Infiltration heat gain (kWh/m <sup>2</sup> )	522	522	780
Heat removal from windows (kWh/m <sup>2</sup> )	4375	2492	3701
Heat removal from infiltration (kWh/m <sup>2</sup> )	2383	2379	3544
Range of annual lighting load for the case room (kWh)	2453-3730	3509-4106	2572-3815
Annual PV energy generation (kWh)	-	620.9	807.35
The power output of facades (kWh)	-	East: 324	East: 432.2
		South: 297	South: 375.15
sDA500,50 (%)	59.1	28.8	55.37

#### 4.5.2. Optimum Daylight Performance Model: Highest sDA Solutions

The optimization goal is to achieve an sDA of at least and preferably higher than 50%. The base-case results have shown that sDA was considerably reduced in low-transparency PV glasses due to the low transmittance of daylight to the studio. However, as the window size changed with the optimization, the highest sDA was achieved at 82%, with a 40% transmittance of the PV glass (Table 4.9.). In this genome, sDA increased by 22.1% compared to the base case results and reached 82%. Heating and cooling loads were increased by 8.23% and 7.68% compared to the base case, respectively, which was undesirable for the studio. Lastly, the window size has been expanded by 153.3% and increased to 53.2 m<sup>2</sup>. During the optimization process, the largest window size is 54.25 m<sup>2</sup>, in which the sDA is calculated as 81.6%, and total thermal loads are estimated as 9.784.740 kWh.

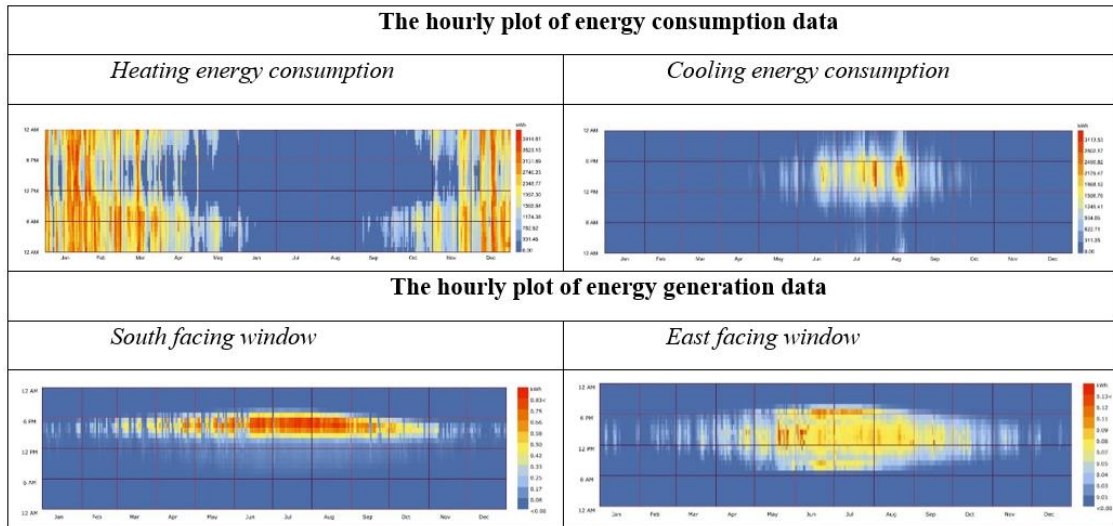


Figure 4.11. The hourly plot of heating and cooling energy consumption data and PV electrical energy generation data of the Pareto-front (1) solution

Table 4.9. Optimization genomes for highest sDA showing each objective and variable.

Variables				Objectives						
Window surface (m2)	Transmittance (%)	sDA (%)	sDA <sub>1</sub> (%)	sDA <sub>2</sub> (%)	Heating load (kWh)	Cooling load (kWh)	Total thermal load (kWh)	sDA <sub>3</sub> (%)	sDA <sub>4</sub> (%)	
										East/South
<b>Base Case</b>										
12.6/8.4	21	75	59.9	-	-	7909507	1114731	9024238	-	-
<b>30% transmittance PV glass</b>										
17.28/11.52	28.8	30	28.8	31.1	-	7910341	1097786	9008127	0.17	-
<b>Other Pareto solutions</b>										
33.24/20	53.2	40	82	22.1	53.2	8560372	1200359	9760731	8.16	8.35
33.25/21	54.25	39	81.6	21.7	52.8	8580953	1203787	9784740	8.42	8.62
33.24/19.95	53.19	40	81.6	21.7	52.8	8560372	1200359	9760731	8.16	8.35
33.24/19.95	53.19	40	81.1	21.2	52.3	8560372	1200359	9760731	8.16	8.35
31.58/21	52.58	39	80.5	20.6	51.7	8547007	1198539	9745546	7.99	8.18
31.58/21	52.58	39	79.8	19.9	51	8547007	1198539	9745546	7.99	8.18
29.9/21	50.92	39	79.1	19.2	50.3	8513096	1193343	9706439	7.5	7.7



									5	5
28.25/18.9	47.1 5	40	78. 2	<b>18.</b> <b>3</b>	<b>49,</b> <b>4</b>	843760 7	118124 8	961885 5	- <b>6.5</b> <b>8</b>	- <b>6,7</b> <b>7</b>
31.58/21	52.5 8	37	78. 9	<b>19</b>	<b>50,</b> <b>1</b>	853700 7	119853 9	973554 6	- <b>7.8</b> <b>8</b>	- <b>8,0</b> <b>7</b>
29.9/21	50.9 2	37	77. 6	<b>17.</b> <b>7</b>	<b>48,</b> <b>8</b>	851309 6	119334 3	970643 9	- <b>7.5</b> <b>5</b>	- <b>7,7</b> <b>5</b>

### 4.5.3. Optimum Energy Performance Model: Lowest Thermal Load Solutions

As a result of the optimization process, the lowest total thermal load has been achieved at 9.151.337 kWh, with a 39% transmittance of PV glass and 27.12 m<sup>2</sup> surface area (Table 4.10.). The annual total thermal load is increased by 1.58% compared to the base case situation. The sDA is 44.4% for this genome which is below the acceptable level. The simulation engine calculates annual heating and cooling loads as 8.033.983 kWh and 1.117.354 kWh, respectively. Both thermal loads are calculated as higher than the base case condition. Total thermal loads, heating, and cooling loads are increased by 1.40%, 1.57%, and 0.24%, respectively, compared to the base case model. This genome optimized the glass surface area as 16.62 m<sup>2</sup> for the South façade and 10.5 m<sup>2</sup> for the East façade. The window size has been enlarged by 22.5% and increased to 27.12 m<sup>2</sup>. It is noted that the optimization algorithm tends to enlarge the window size to increase annual daylight autonomy, but this causes an increase in the total energy consumed to heat and cool the building. During the optimization process, the narrowest window size is noted for this genome, in which the total thermal load is estimated as the lowest.

Table 4.10. Optimization genomes for the lowest total thermal loads show each objective and variable in detail.

Variables					Objectives					
Window surface (m <sup>2</sup> )		Transmittance (%)	sDA (%)	(%) <sub>1</sub>	(%) <sub>2</sub>	Heating load (kWh)	Cooling load (kWh)	Total thermal load (kWh)	(%) <sub>3</sub>	(%) <sub>4</sub>
East/South	Total									
<b>Base Case</b>										
12.6/8.4	21	75	<b>59.9</b>	-	-	790950 7	111473 1	902423 8	-	-

<b>30% transmittance PV glass</b>										
17.28/11.5 2	28.8	30	28.8	- 31. 1	-	791034 1	109778 6	900812 7	0.1 7	-
<b>Other Pareto solutions</b>										
16.62/10.5	27.1 2	39	44.4	- 15. 5	15, 6	803398 3	111735 4	915133 7	- 1.4 0	- 1,7 8
16.62/11.5 5	28.1 7	24	23.5 9	- 36. 3	- 5,2 1	805473 5	112074 4	917547 9	- 1.6 7	- 2,0 9
16.62/11.5 5	28.1 7	30	32.8	- 27. 1	4	805475 8	112078 2	917554 0	- 1.6 7	- 2,0 9

(cont. on the next page)

Table 4.10. (con.t)

16.62/11.5 5	28.1 7	38	46.2 2	- 13. 7	17, 4	805483 5	112074 4	917557 9	- 1.6 7	- 2,0 9
16.62/10.5	27.1 2	37	41.3 6	- 18. 5	12, 6	807382 7	110384 2	917766 9	- 1.7 0	- 0,5 5
18.28/10.5	28.7 8	33	40.6 4	- 19. 3	11, 8	806784 5	112258 1	919042 6	- 1.8 4	- 2,2 5
18.28/11.5 5	29.8 3	27	31.7	- 28. 2	2,9	808875 9	112601 2	921477 1	- 2.1 1	- 2,5 7
19.94/10.5	30.4 4	22	24.3	- 35. 6	-4,5	810175 5	112785 5	922961 0	- 2.2 7	- 2,7 3
18.28/12.6	30.8 8	22	24.9	- 35	-3,9	809928 3	112995 8	922924 1	- 2.2 7	- 2,9 3
18.28/12.6	30.8 8	21	23.5	- 36. 4	-5,3	810971 0	112941 3	923912 3	- 2.3 8	- 2,8 8

Table 4.11. Optimization solutions range for each objective and variable.

<b>Variables and Objectives</b>	<b>Range (min-max)</b>
Window size (m2)	27-53
Window transparency (%)	20-40
sDA (%)	44-82
Heating load	8033983-8560372
Cooling load	1117354-1200359
Total thermal load	9151337-9760731

## CHAPTER 5

### DISCUSSION AND CONCLUSION

The study first analyzes three a-Si thin-film solar cells due to their transmittance. Solar PV glasses are modeled 90° vertically to the South and east facades and tested in energy, thermal, and daylight performance. Then, the study applies a multi-objective evolutionary optimization algorithm for a-Si PV modules' transmittance and window size to enhance the building's energy performance, the case room's daylight performance, and the PV's energy generation capacity.

The following is a list of the key findings:

- Regarding energy generation, less transparent solar cells provide more electricity generation. The 10% transmittance PV glass produced the highest, while the 30% one produced the lowest energy. Less transparent Low-E PV glass is better to prefer to obtain higher energy production. When the annual energy production is analyzed, all the tested PV glasses generate higher energy on the south-facing façade than on the other facades. Orientation becomes the key consideration in installing these systems.

- Regarding daylight performance, less transparent PV glasses worsened the room's daylight performance and increased lighting loads. They block most of the amount of daylight entering the space. Their application in north-oriented areas may cause problems since no direct sunlight reaches the surface of the PV glass. The case studio showed us that the possible largest windows could benefit daylight performance when less transparent PV glasses are used. In this study, the total window area is 28.8 m<sup>2</sup> which is relatively narrow and unable to transmit daylight to the back parts of the room. Thus, PV glasses did not perform at the desired level. On the other hand, another benefit is their potential to mainly eliminate glare risks and provide visual comfort.

- The annual energy generated by PV glasses covered the room's annual lighting loads between 15.1-and 20.3%. Although the lighting load increases with less transmittance, electrical energy increases relatively. It may make less transparent glasses preferable in this sense. In summer, the energy generation of PV glass is the highest. It covers at least 67% of the seasonal lighting loads of the case room. Under a clear sky with sun conditions, PV glasses cover all seasonal lighting loads. In the fall

season, electrical energy generation is lower than in summer but higher than in other seasons. Under overcast sky conditions, it covers at least 41.2% of the seasonal lighting load. It covers all the lighting load under the clear sky with sun conditions. In the spring season, the lighting load increases significantly. Still, PV glass covers at least 10% of the seasonal lighting load. Under a clear sky with sun conditions, PV glasses can cover 18.7% of the seasonal lighting load. The lowest energy generation is provided in the winter season. PV glasses provide only 3.5% of the seasonal lighting load. Under a clear sky with sun conditions, they can cover up to 6.5%.

- Selected Low-E PV glass has a lower u-value, g-value, and transmittance. A lower u-value means better insulation, decreasing the heating loads in mostly heated buildings. A lower g-value absorbs less heat. Heat gain through windows decreased significantly in PV scenarios. It increases the building's heating load and lowers the cooling load. The selected Low-E PV glasses can be preferred in hot climate areas with high solar radiation to reduce the cooling loads of buildings. Applying them on the South, east, and west-oriented facades can generate more electrical energy and decrease the cooling load. During the winter and spring seasons, the electrical energy generation of PV glass is the lowest, and energy consumption for heating is the highest. Most of the consumed energy belongs to these seasons. In summer and fall, heating energy consumption is the lowest. The building is cooled mainly, but the energy used to cool it is relatively lower than that used to heat it. In these seasons, the energy generation of PV glass is highest. The lowest generation and highest savings are achieved.

- After PV glasses implementation, indoor air temperatures are decreased. Besides, annual thermally uncomfortable hours are reduced by 12.3%, 12.6%, and 11.9% for 30%, 20%, and 10% transmittance. The simulation engine calculates this according to ASHRAE standards using indoor air temperatures. Since Low-E PV glasses decrease indoor air temperatures, they benefit cooling-dominated regions better.

- The seasons that generate the closest electrical energy are summer and fall. Sun has a more direct angle in summer. Therefore, it may not be able to hit the window surface for some hours. Still, more energy is generated in that season. During the hours when the sun hits the window surface, the solar cells heat more, resulting in more energy generation. All PV glasses generate more energy than those used for lighting load in the summer and fall seasons under a clear sky with sun conditions. It is

worth mentioning that energy generation increases in the spring, summer, and fall. In these seasons, the lighting load is also significantly decreased.

- A small scale of PV glass is applied on a low-rise building, but when PV glass applications in larger-scale buildings are examined, payback times vary between 3.7-16 years, and an internal rate of return between 5-29.3% is noted (OnyxSolar 2022). They may be seen as profitable in high-rise buildings.

- The computational algorithm improved the studio's sDA rather than the building's thermal loads. The final sDA is significantly enhanced compared to the base case model and 30% transmittance PV glass model. It is crucial to achieving such an increase in sDA in a scenario where the transparency is very low and close to the transmittance of a PV glass. In this respect, the sDA results exceeded the target value and were satisfactory. The key reason for achieving such high sDA may be optimizing only window-based parameters. It may also lead to low improvements in the thermal loads of the building because it depends on many variables instead of only window-based ones.

- Although the sDA of the optimized model and the base case model is quite close, the optimized model has improved daylight distribution and reduced glare risk. It shows the PV glass's capacity to improve daylight's homogenous distribution.

- The transmittance range of the glass during the optimization process is kept very close to the transmittance of the actual PV glass. This way, it aims to test the PV glass's sDA potential. During the optimization, enlarged windows were obtained to achieve high sDA. It has been observed that during the optimization, the window sizes are narrower in the Pareto-front results and the narrowest at low thermal loads. The optimization algorithm narrows the window sizes to reduce heat losses and infiltration. It reduces the heating load of the building in this way. The largest window size is 158.3% more than the existing windows and 88.3% more than the window sizes with PV glass applied.

- Although the optimization algorithm increased the studio's potential in terms of sDA, the expected results could not be obtained for the thermal loads of the building. The optimization genome with the lowest thermal loads received a slight increase in total thermal loads compared to the current situation. It is because the sDA and thermal loads are inversely proportional. While the optimization algorithm increases the sDA, it also aims to reduce the thermal loads. However, the numerical

limitations in the variables were insufficient to reduce the thermal loads. Total energy consumption is slightly increased compared to the case where 30% transmittance PV glass was implemented in the studio. This study does not aim to retrofit an existing building. Instead, it aims to understand the capacity of PV glazing using window-based variables. Thus, less improvement in energy performance has shown us the insufficient contribution and potential of PV glass in such a building.

- Since the optimization algorithm aims to increase sDA, it tends to expand the window sizes. Thus, seasonal and annual lighting loads are considerably reduced compared to the 30% transmittance PV glass-integrated model before the optimization. The lighting loads are calculated very closely compared with the base case model. Window transmittance was 75% in the base case model and 40% in the optimized PV glass model. Although the transparency is considerably reduced, the lighting loads are almost identical. It is due to the expanding window sizes by the multi-objective evolutionary optimization algorithm.

- It is seen that the optimized PV glass generates 23.2% more annual electrical energy than the non-optimized PV glass. The importance of window sizes and transparency was seen in this respect. Annual electricity generation on the East and South facades increased by 25% and 20.8%, respectively.

- The number of hours the user is uncomfortable during the year increased by 17% and decreased by 36% when the optimized PV glass is compared to non-optimized PV glass and the base case model.

- Infiltration heat removal increased by 32.8% compared to the base case model and non-optimized PV glass due to the enlarged window sizes. High infiltration heat removal may be one reason for not reducing heating loads during the optimization.

The items listed below may be important to guide researchers working in the field of performance and optimization of PV glass:

- Window-based parameters (i.e., window-to-wall ratio and window transmittance) are extremely effective in improving the daylight performance of a PV glass. Using these variables in optimization studies can improve the daylight performance of these buildings in such climates.

- In such a building and climate, it is necessary to increase the number of optimization variables to improve the energy performance of buildings where PV glass is implemented. Building envelope parameters (i.e., thermal transmittance of the wall,

roof, floor, use of shading elements, natural ventilation, etc.) should also be included as the optimization variables because it is seen that window-based variables are not sufficient to reduce energy consumption from heating and cooling.

- In a Mediterranean climate, PV glass optimization is beneficial to reduce glare risks and enhance occupant visual comfort. Optimizing this technology in low-latitude regions with high solar radiation can improve the daylight performance of buildings as well as the comfort of the users. In addition, since Low-E PV glass can reduce building cooling loads, it is strongly recommended to use it in regions with high solar exposure.

- This thesis proves that PV glass implementation is feasible, and this technology can be applied to different types of buildings in different climate regions. In a socially responsible manner, the study supports using this technology and enhances building performance with the comfort of occupants.

This study demonstrates the significant potential of PV glass to enhance daylight performance and reduce glare risks while improving occupant visual comfort. Running a multi-objective optimization algorithm reveals its potential in terms of daylight performance, lighting energy consumption, and energy generation potential.

## REFERENCES

- Ammar H. Elsheikh, Mohamed E. Zayed, S. Senthilraja, Mohamed Abd Elaziz, Songfeng Lu, and Reham R. Mostafa. 2021. "A New Random Vector Functional Link Integrated with Mayfly Optimization Algorithm for Performance Prediction of Solar Photovoltaic Thermal Collector Combined with Electrolytic Hydrogen Production System." *Applied Thermal Engineering* 193 (July): 117055.
- Abdelhakim Mesloub, Ghazy Abdullah Albaqawy, and Mohd Zin Kandar. 2020. "The Optimum Performance of Building Integrated Photovoltaic (BIPV) Windows Under a Semi-Arid Climate in Algerian Office Buildings." *Sustainability*, no. 4: 1.
- Ahmad, Asim, Om Prakash, Anil Kumar, S.M. Mozammil Hasnain, Puneet Verma, Ali Zare, Gaurav Dwivedi, and Anukul Pandey. 2022. "Dynamic Analysis of Daylight Factor, Thermal Comfort and Energy Performance under Clear Sky Conditions for Building: An Experimental Validation." *Materials Science for Energy Technologies* 5 (January): 52–65. doi:10.1016/j.mset.2021.11.003.
- Khaled Alhagla, Alaa Mansour, and Rana Elbassuoni. 2019. "Optimizing Windows for Enhancing Daylighting Performance and Energy Saving." *Alexandria Engineering Journal* 58 (1): 283–90. doi:10.1016/j.aej.2019.01.004.
- Ali Goharian, Khosro Daneshjoo, and Mansour Yeganeh. 2022. "Standardization of Methodology for Optimizing the Well Aperture as Device (Reflector) for Light-Wells; A Novel Approach Using Honeybee & Ladybug Plugins." *Energy Reports* 8, pp. 3096–3114. doi:10.1016/j.egyr.2022.01.176.
- Alrashidi, Hameed, Walid Issa, Nazmi Sellami, Aritra Ghosh, Tapas K. Mallick, and Senthilarasu Sundaram. 2020. "Performance Assessment of Cadmium Telluride-Based Semi-Transparent Glazing for Power Saving in Façade Buildings." *Energy Build* 215: N.PAG-N.PAG.
- Ning Li, Tayebbeh Ameri, and Christoph J. Brabec. 2013. "Highly Efficient Organic Tandem Solar Cells: A Follow up Review." *Energy & Environmental Science* vol. 6 (January): 2390.



- Zong Woo Geem, and Somayeh Asadi. 2014. "Sustainable Building Design: A Review on Recent Metaheuristic Methods," *Recent Advances in Swarm Intelligence and Evolutionary Computation*, pp. 203–223.
- Augenbroe, Godfried. 2002. "Trends in Building Simulation," *Building and Environment*, 37(8), 891-902.
- Azami, Ahadollah and Sevinç, Harun. 2021. "The Energy Performance of Building Integrated Photovoltaics (BIPV) by Determination of Optimal Building Envelope." *Building and Environment* 199 (July). doi:10.1016/j.buildenv.2021.107856.
- Berk Ekici, Okan F. S. F. Turkcan, Michela Turrin, Ikbal Sevil Sariyildiz, and Mehmet Fatih Tasgetiren. 2022. "Optimising High-Rise Buildings for Self-Sufficiency in Energy Consumption and Food Production Using Artificial Intelligence: Case of Europoint Complex in Rotterdam." *Energies* 15 (660): 660. doi:10.3390/en15020660.
- Stefaan De Wolf, Corsin Battaglia, and Andres Cuevas. 2023. "High-Efficiency Crystalline Silicon Solar Cells: Status and Perspectives." *Energy and Environment Sci.* 9 (5), 1552–1576.
- Bayram, Göze, and Tuğçe Kazanasmaz. 2016. "Simulation-Based Retrofitting of an Educational Building in Terms of Optimum Shading Device and Energy Efficient Artificial Lighting Criteria." *Light & Engineering* 24 (2): 45–55.
- BIPV market and stakeholder analysis and needs, European Commission as Project Deliverable D1.1 in October 2016, Members of the PVSITES Consortium.
- Biyik, Emrah, Mustafa Araz, Arif Hepbasli, Mehdi Shahrestani, Runming Yao, Li Shao, Emmanuel Essah, et al. 2017. "A Key Review of Building Integrated Photovoltaic (BIPV) Systems." *Engineering Science and Technology, an International Journal* 20 (3): 833–58. doi:10.1016/j.jestch.2017.01.009.
- Daniel Chemisana, Chiara Lodi, Jordi Cipriano, and J.J. Bloem. 2012. "An Outdoor Test Reference Environment for Double Skin Applications of Building Integrated PhotoVoltaic Systems." *Energy and Buildings* 50 (July): 63–73.

- Pierluigi Bonomo, Anatoli Chatzipanagi, and Francesco Frontini. 2015. "Overview and Analysis of Current BIPV Products: New Criteria for Supporting the Technological Transfer in the Building Sector." *Vitruvio: International Journal of Architectural Technology and Sustainability*, no. 1 (December): 67–85. doi:10.4995/vitruvio-ijats.2015.4476.
- Roberto Lamberts, EH Edward Borgstein, and Jlm Jan Hensen. 2016. "Evaluating Energy Performance in Non-Domestic Buildings: A Review." *Energy and Buildings* 128 (September): 734–55.
- Brembilla, E., N.C. Drosou, and J. Mardaljevic. 2022. "Assessing Daylight Performance in Use: A Comparison between Long-Term Daylight Measurements and Simulations." *Energy & Buildings* 262.
- Xiang, Changying, and Barbara Szybinska Matusiak. 2022. "Façade Integrated Photovoltaics Design for High-Rise Buildings with Balconies, Balancing Daylight, Aesthetic and Energy Productivity Performance." *Journal of Building Engineering* 57 (October). doi:10.1016/j.jobe.2022.104950.
- Reinhart, Christoph. 2001. "Daylight Availability and Manual Lighting Control in Office Buildings: Simulation Studies and Analysis of Measurement." (Ph.D. thesis), University of Karlsruhe, Germany.
- Cannavale, Alessandro, Maximilian Hörantner, Giles E. Eperon, Henry J. Snaith, Francesco Fiorito, Ubaldo Ayr, and Francesco Martellotta. 2017. "Building Integration of Semitransparent Perovskite-Based Solar Cells: Energy Performance and Visual Comfort Assessment." *Applied Energy* 194 (May): 94–107. doi:10.1016/j.apenergy.2017.03.011.
- Junjie Liu, Xilei Dai, and Xiaodong Cao. 2016. "Building Energy-Consumption Status Worldwide and the State-of-the-Art Technologies for Zero-Energy Buildings during the Past Decade." *Energy and Buildings* 128 (September): 198–213.
- Cemre Cubukcuoglu, Berk Ekici, Mehmet Fatih Tasgetiren, and Sevil Sariyildiz. 2019. "OPTIMUS: Self-Adaptive Differential Evolution with Ensemble of Mutation Strategies for Grasshopper Algorithmic Modeling." *Algorithms* 12 (7): 141.

- Cesari, Silvia, Paolo Valdiserri, Maddalena Coccagna, and Sante Mazzacane. 2018. "Energy Savings in Hospital Patient Rooms: The Role of Windows Size and Glazing Properties." *Energy Procedia* 148 (August): 1151–58. doi:10.1016/j.egypro.2018.08.027.
- Çetinkaya, Gülden, Selman Aydin, Muhammed Zeynel Öztürk. 2017 "Climate Types of Turkey According to Köppen-Geiger Climate Classification." *Journal of Geography* 35: 17-27.
- Chae, Young Tae, Jeehwan Kim, Hongsik Park, and Byungha Shin. 2014. "Building Energy Performance Evaluation of Building Integrated Photovoltaic (Bipv) Window with Semi-Transparent Solar Cells." *Applied Energy* 129: 217–27.
- Chatzipanagi, Anatoli, Francesco Frontini, and Alessandro Virtuani. 2016. "BIPV-Temp: A Demonstrative Building Integrated Photovoltaic Installation." *Applied Energy* 173 (July): 1–12. doi:10.1016/j.apenergy.2016.03.097.
- Chen, Mo, Wei Zhang, Lingzhi Xie, Zhichun Ni, Qingzhu Wei, Wei Wang, and Hao Tian. 2019. "Experimental and Numerical Evaluation of the Crystalline Silicon PV Window under the Climatic Conditions in Southwest China." *Energy* 183 (September): 584–98.
- Adara, Mojisola. 2019. "Comparative Analysis of Glazing Alternatives - a Case Study of Temperature Differentials." M.S., The University of North Carolina at Charlotte.
- Y.Joe Huang, Drury B. Crawley, Jason Glazer, Richard Karl Strand, R.J. Liesen, Walter F. Buhl, C.O. Pedersen, et al. 2001. "EnergyPlus: Creating a New-Generation Building Energy Simulation Program." *Energy and Buildings* 33 (April): 319–31.
- Day, Julia K., Benjamin Futrell, Robert Cox, Shelby N. Ruiz, Armin Amirazar, Amir Hosseinzadeh Zarrabi, and Mona Azarbayjani. 2019. "Blinded by the Light: Occupant Perceptions and Visual Comfort Assessments of Three Dynamic Daylight Control Systems and Shading Strategies." *Building and Environment* 154 (May): 107–21. doi:10.1016/j.buildenv.2019.02.037.

- Defaix, P. R., W. G. J. H. M. van Sark, E. Worrell, E. de Visser. 2012. "Technical Potential for Photovoltaics on Buildings in the Eu-27." *Solar Energy* 86, no. 9, 2644-53.
- Rodolphe Vaillon, Olivier Dupré, and Martin A. Green. 2015. "Physics of the Temperature Coefficients of Solar Cells." *Solar Energy Materials and Solar Cells* 140 (September): 92–100.
- Ekici, Berk, Cemre Cubukcuoglu, Michela Turrin, and I. Sevil Sariyildiz. 2019. "Performative Computational Architecture Using Swarm and Evolutionary Optimisation: A Review." *Building and Environment* 147 (January): 356–71.
- Ekici, Berk, Z. Tuğçe Kazanasmaz, Michela Turrin, M. Fatih Taşgetiren, and I. Sevil Sariyildiz. 2021. "Multi-Zone Optimisation of High-Rise Buildings Using Artificial Intelligence for Sustainable Metropolises. Part 1: Background, Methodology, Setup, and Machine Learning Results." *Solar Energy* 224 (August): 373–89.
- Electricity Generation in Singapore by Multicrystalline Silicon Technologies. *Solar Energy Mater. Solar Cells* 174, 157–162.
- M. Abd Elaziz, and Ammar H. Elsheikh. 2018. "Review on Applications of Particle Swarm Optimization in Solar Energy Systems." *International Journal of Environmental Science and Technology* 16 (August): 1159–70.
- Mohamed E. Mostafa, Ammar H. Elsheikh, Mohamed Kamal Ahmed Ali, Fadl A. Essa, and Swellam W. Sharshir. 2018. "Applications of Nanofluids in Solar Energy: A Review of Recent Advances." *Renewable and Sustainable Energy Reviews* 82 (February): 3483–3502.
- EPA. 2016. "The difference between source and site energy." Retrieved from: <https://www.energystar.gov/buildings/facility-owners-and-managers/existing-buildings/use-portfolio-manager/understand-metrics/difference>.
- Espinosa, Nieves, Rafael García-Valverde, Antonio Urbina, and Frederik C. Krebs. 2011. "A Life Cycle Analysis of Polymer Solar Cell Modules Prepared Using Roll-

- to-Roll Methods under Ambient Conditions.” *Solar Energy Materials and Solar Cells* 95 (5): 1293–1302. doi:10.1016/j.solmat.2010.08.020.
- Martellotta, Francesco, Alessandro Cannavale, and Ubaldo Ayr. 2017. “Comparing Energy Performance of Different Semi-Transparent, Building-Integrated Photovoltaic Cells Applied to ‘Reference’ Buildings.” *Energy Procedia* 126 (September): 219–26. doi:10.1016/j.egypro.2017.08.143.
- Fatiha Outgouga and Hicham Jamouli. 2022. “Improving the Passive Energy Efficiency of an Office Building in Agadir Morocco Using Dynamic Thermal Simulations in DesignBuilder,” *International Conference on Decision Aid Science and Application (DASA)*. doi: 10.1109/DASA54658.2022.9765148
- Fang, Yuan. "Optimization of Daylighting and Energy Performance Using Parametric Design, Simulation Modeling, and Genetic Algorithms." PhD diss., North Carolina State University, 2017.
- food4Rhino, n.d., accessed June 2021, <https://www.food4rhino.com/en>.
- Freitas, Sara, Brito M.C. 2015. “Maximizing the Solar Photovoltaic Yield in Different Building Facade Layouts,” January. doi:10.4229/eupvsec20152015-6av.5.6.
- Frontczak, Monika, and Pawel Wargocki. 2011. “Literature Survey on How Different Factors Influence Human Comfort in Indoor Environments.” *Building and Environment* 46, no. 4 (2011): 922–37.
- Nicoletti, Giovanni, Natale Arcuri, Gerardo Nicoletti, and Roberto Bruno. 2015. “A Technical and Environmental Comparison between Hydrogen and Some Fossil Fuels.” *Energy Conversion and Management* 89 (January): 205–13. doi:10.1016/j.enconman.2014.09.057.
- Yu, Guoqing, Hongxing Yang, Daina Luo, Xu Cheng, and Mark Kyeredey Ansah. 2021. “A Review on Developments and Researches of Building Integrated Photovoltaic (BIPV) Windows and Shading Blinds.” *Renewable and Sustainable Energy Reviews* 149 (October). doi:10.1016/j.rser.2021.111355.

- Galal, Kareem S. 2019. "The Impact of Classroom Orientation on Daylight and Heat-Gain Performance in the Lebanese Coastal Zone." *Alexandria Engineering Journal* 58 (3): 827–39. doi:10.1016/j.aej.2019.07.003.
- Thomas Back. 1996. *Evolutionary Algorithms in Theory and Practice : Evolution Strategies, Evolutionary Programming, Genetic Algorithms*. New York: Oxford University Press.
- Gholami, Hassan, and Nils Røstvik Harald. 2021. "The Effect of Climate on the Solar Radiation Components on Building Skins and Building Integrated Photovoltaics (Bipv)." *Energies* 14: 1847-1947.
- Ghosh, Aritra. 2020. "Potential of Building Integrated and Attached/Applied Photovoltaic (BIPV/BAPV) for Adaptive Less Energy-Hungry Building's Skin: A Comprehensive Review." *Journal of Cleaner Production* 276 (December). doi:10.1016/j.jclepro.2020.123343.
- Giouri, Evangelia Despoina, Tenpierik, Martin, Turrin, Michela. 2020. "Zero Energy Potential of a High-Rise Office Building in a Mediterranean Climate: Using Multi-Objective Optimization to Understand the Impact of Design Decisions Towards Zero-Energy High-Rise Buildings." *Energy and Buildings* 209.
- Gong, Jiawei, Sumathy, K., Qiao, Qiquan, Zhou, Zhengping. 2017. "Review on Dye-Sensitized Solar Cells (DSSCs): Advanced Techniques and Research Trends." *Renewable and Sustainable Energy Reviews* 68, part 1 (January): 234–246.
- Sten-Eric Lindquist, Lennart Karlson, Anders Hagfeldt, and Helena Greijer. 2023. "Environmental Aspects of Electricity Generation from a Nanocrystalline Dye Sensitized Solar Cell System," *Renewable Energy* 23 (1): 27–39.
- Mostafa Refat Ismail, Hanan Sabry, Mohamed Ayman Ashour, and Hussein Hamza. 2020. "Identifying the Influence of Design Variations on the Performance of PV Systems for Net-Plus Energy Residential Buildings in Egypt." *International Journal of Engineering Research and Technology* 13 (3): 528–539.
- Heangwoo Lee, Xiaolong Zhao, and Janghoo Seo. 2021. "A Study of Optimal Specifications for Light Shelves with Photovoltaic Modules to Improve Indoor

- Comfort and Save Building Energy.” *International Journal of Environmental Research and Public Health* 18: 2574. doi:10.3390/ijerph18052574.
- Hee, W.J., M.A. Alghoul, B. Bakhtyar, OmKalthum Elayeb, M.A. Shameri, M.S. Alrubaih, and K. Sopian. 2015. “The Role of Window Glazing on Daylighting and Energy Saving in Buildings.” *Renewable and Sustainable Energy Reviews* 42 (February): 323–43. doi:10.1016/j.rser.2014.09.020.
- Heinstein, Patrick, Ballif, Christophe, Perret-Aebi, Laure-Emmanuelle, 2017. *Building Integrated Photovoltaics (BIPV): Review. Potentials, Barriers and Myths.*
- Henson, Jesse. 2005. “Integrating BIPV: How the Market for Building Integrated Photovoltaics Is Being Created in the USA.” *Refocus* 6, no. 3 (2005).
- Safayet Ahmed, Dietmar Knipp, Mohammad Ismail Hossain, Yuen Hong Tsang, Ahmed Mortuza Saleque, Wayesh Qarony, Jahid Anowar, and Md. Abdur Rahman. 2020. “Optics of Perovskite-Based Highly Efficient Tandem Solar Cells.” 2020 IEEE Region 10 Symposium (TENSymp).
- Huang, Junchao, Xi Chen, Jinqing Peng, and Hongxing Yang. 2021. “Modelling Analyses of the Thermal Property and Heat Transfer Performance of a Novel Compositive PV Vacuum Glazing.” *Renewable Energy* 163 (January): 1238–52. doi:10.1016/j.renene.2020.09.027.
- Yugun Chung, Taeyon Hwang, and Jeong Tai Kim. 2014. “Power Performance of Photovoltaic-Integrated Lightshelf Systems.” *Indoor and Built Environment* 23 (February): 180–88.
- I. Sevil Sariyildiz, M. Fatih Tasgetiren, Michela Turrin, Berk Ekici, and Z. Tuğçe Kazanasmaz. 2021. “Multi-Zone Optimisation of High-Rise Buildings Using Artificial Intelligence for Sustainable Metropolises. Part 2: Optimisation Problems, Algorithms, Results, and Method Validation.” *Solar Energy* 224 (August): 309–26.
- International Energy Agency. "World Energy Outlook Special Report: Energy and Air Pollution." Accessed August 1, 2022. <https://www.iea.org/reports/energy-and-air-pollution>.

- Jahanara, Alireza. 2013. "Strategy towards Solar Architecture by Photovoltaic for Building Integration," Eastern Mediterranean University (EMU), Famagusta, Turkey Ph.D. Thesis.
- Nebojsa Jakica, Mikkel K. Kragh, Rebecca J. Yang, W.M.Pabasara, U.Wijeratne, Eric Too, Ron Wakefield, et al. 2019. "BIPV Design and Performance Modelling: Tools and Methods," January. doi:10.13140/rg.2.2.26359.16806.
- Johannes Hofer, Prageeth Jayathissa, Jeremias Schmidli, Zoltan Nagy, Mauro Luzzatto, and Arno Schlueter. 2017. "Optimising Building Net Energy Demand with Dynamic BIPV Shading." *Applied Energy* 202 (September): 726–35.
- Petter Jelle, Bjørn, Christer Breivik, and Hilde Drolsum Røkenes. 2012. "Building Integrated Photovoltaic Products: A State-of-the-Art Review and Future Research Opportunities." *Solar Energy Materials and Solar Cells* 100 (May): 69–96. doi:10.1016/j.solmat.2011.12.016.
- Jiang, Ying, Nianping Li, A Yongga, and Wenyun Yan. 2022. "Short-Term Effects of Natural View and Daylight from Windows on Thermal Perception, Health, and Energy-Saving Potential." *Building and Environment* 208 (January). doi:10.1016/j.buildenv.2021.108575.
- Mardaljevic, John. 1999. "Daylight Simulation : Validation, Sky Models and Daylight Coefficients," Ph.D. thesis, De Montfort University, Leicester, UK.
- Kirimtat, Ayca, M. Fatih Tasgetiren, Peter Brida, and Ondrej Krejcar. 2022. "Control of PV Integrated Shading Devices in Buildings: A Review." *Building and Environment* 214 (April). doi:10.1016/j.buildenv.2022.108961.
- Kirimtat, Ayca, Ondrej Krejcar, Berk Ekici, and M. Fatih Tasgetiren. 2019. "Multi-Objective Energy and Daylight Optimization of Amorphous Shading Devices in Buildings." *Solar Energy* 185 (June): 100–111. doi:10.1016/j.solener.2019.04.048.
- Knera, Dominika, Szczepanska-Rosiak, Eliza, Dariusz, Heim. 2015. "Potential of Pv Façade for Supplementary Lighting in Winter." Article. *Energy Procedia* 78: 2651–2656.



- L. Dzunova, M. Rusko, and Ruzena Kralikova. 2019. "Impact of Natural Daylight for Human Comfort and Health," International Council on Technologies of Environmental Protection (ICTEP), Technologies of Environmental Protection (ICTEP), 2019 International Council On, 160–163.
- Kryszak, Marek, and Lai Wang Wang. 2020. "The Value of Aesthetics in the BIPV Roof Products Segment: A Multiperspective Study under European Market Conditions." *Energy Sources, Part A: Recovery, Utilization, and Environmental Effects*, August, 1–22.
- Leccese, Francesco, Giacomo Salvadori, Giuseppe Tambellini, and Zehra Tugce Kazanasmaz. 2020. "Application of Climate-Based Daylight Simulation to Assess Lighting Conditions of Space and Artworks in Historical Buildings: The Case Study of Cetacean Gallery of the Monumental Charterhouse of Calci." *Journal of Cultural Heritage* 46 (November): 193–206.
- Lee, Heangwoo. 2019. "Performance Evaluation of a Light Shelf with a Solar Module Based on the Solar Module Attachment Area." *Building and Environment* 159 (July).
- Li, Danny H.W., Tony N.T. Lam, Wilco W.H. Chan, and Ada H.L. Mak. 2009. "Energy and Cost Analysis of Semi-Transparent Photovoltaic in Office Buildings." *Applied Energy* 86 (5): 722–29. doi:10.1016/j.apenergy.2008.08.009.
- Liu, Chung Ping, and Chuan Lung Chuang. 2012. "Fabrication of Copper–indium–gallium–diselenide Absorber Layer by Quaternary-Alloy Nanoparticles for Solar Cell Applications." *Solar Energy* 86 (9): 2795–2801. doi:10.1016/j.solener.2012.06.018.
- Liu, Gang, Guanhua Qu, Lei Ren, Yuanyuan Zhang, Xingyu Zang, and Rui Dang. 2022. "The Influence Mechanism of Daylight Visual Evaluation in College Classrooms under Visual Field Physiological Characteristics of Student Group: Case Study." *Building and Environment* 209 (February). doi:10.1016/j.buildenv.2021.108655.
- Liu, Zhijian, Yulong Zhang, Xitao Yuan, Yuanwei Liu, Jinliang Xu, Shicong Zhang, and Bao-jie He. 2021. "A Comprehensive Study of Feasibility and Applicability of Building Integrated Photovoltaic (BIPV) Systems in Regions with High Solar

- Irradiance.” *Journal of Cleaner Production* 307 (July).  
doi:10.1016/j.jclepro.2021.127240.
- Choudhary, Kailash, Sanjeev Jakhar, Nikhil Gakkhar, and Kuldip Singh Sangwan. 2022. “Comparative Life Cycle Assessments of Photovoltaic Thermal Systems with Earth Water Heat Exchanger Cooling.” *Procedia CIRP* 105 (January): 255–60. doi:10.1016/j.procir.2022.02.042.
- Mangkuto, Rizki A., Fathurrahman Feradi, Rialdi Eka Putra, R. Triyogo Atmodipoero, and Federico Favero. 2018. “Optimisation of Daylight Admission Based on Modifications of Light Shelf Design Parameters.” *Journal of Building Engineering* 18 (July): 195–209.
- Marins, Daniela PA, Cristina E Alvarez, Beatriz Piderit, and Marcelo Segatto. 2019. “Below Useful Daylight Illuminance (BUDI): A New Useful Range Measurement Parameter.” Paper presented at the 2019 SBFoton International Optics and Photonics Conference (SBFoton IOPC), Photonics Conference (SBFoton IOPC), October 1-5.
- Martín-Chivelet, Nuria, Konstantinos Kapsis, Helen Rose Wilson, Veronique Delisle, Rebecca Yang, Lorenzo Olivieri, Jesús Polo, et al. 2022. “Building-Integrated Photovoltaic (BIPV) Products and Systems: A Review of Energy-Related Behavior.” *Energy & Buildings* 262 (May). doi:10.1016/j.enbuild.2022.111998.
- MathWorks. 2016. "Genetic algorithm." Accessed April 26, 2023.  
<https://www.mathworks.com/discovery/genetic-algorithm.html>.
- Megahed, Tamer F., and Ali Radwan. 2020. “Performance Investigation of Zero-Building Integrated Photovoltaic Roof System: A Case Study in Egypt.” *Alexandria Engineering Journal* 59 (6): 5053–67.
- Mesloub, Abdelhakim, and Aritra Ghosh. 2020. “Daylighting Performance of Light Shelf Photovoltaics (LSPV) for Office Buildings in Hot Desert-Like Regions.” *Applied Sciences* 10 (7959): 1–17.
- Farha Islam Mime, Md. Rafiqul Islam, Eklas Hossain, Ibrahim M. Mehedi, and Md. Tanvir Hasan. 2021. “Design and Performance Analysis of Tandem Organic Solar

- Cells: Effect of Cell Parameter.” IEEE Access 9 (January): 40665–80.  
doi:10.1109/ACCESS.2021.3063810.
- Skandalos, Nikolaos, and Dimitris Karamanis. 2021. “An Optimization Approach to Photovoltaic Building Integration towards Low Energy Buildings in Different Climate Zones.” Applied Energy 295 (August).  
doi:10.1016/j.apenergy.2021.117017.
- Kevin Van Den Wymelenberg, and Amir Nezamdoost. 2017. “A Daylighting Field Study Using Human Feedback and Simulations to Test and Improve Recently Adopted Annual Daylight Performance Metrics.” Journal of Building Performance Simulation 10 (June): 471–83.
- Nguyen, Anh-Tuan, Sigrid Reiter, and Philippe Rigo. 2014. “A Review on Simulation-Based Optimization Methods Applied to Building Performance Analysis.” Applied Energy 113 (January): 1043–58. doi:10.1016/j.apenergy.2013.08.061.
- Geng-Ming Hu, Chih-Hsien Lai, Huang-Hua Chen, Jung-Chuan Chou, Zhen-Rong Yong, Yu-Hsun Nien, Jun-Xiang Chang, et al. 2021. “The Characterization of Dye-Sensitized Solar Cell Modified by Reduced Graphene Oxide- and ZrO<sub>2</sub>-Doped TiO<sub>2</sub> Nanofibers at Low Light Intensities.” IEEE Transactions on Electron Devices 68 (March): 1155–61.
- Nundy, Srijita, and Aritra Ghosh. 2020. “Thermal and Visual Comfort Analysis of Adaptive Vacuum Integrated Switchable Suspended Particle Device Window for Temperate Climate.” Renewable Energy 156 (August): 1361–72.  
doi:10.1016/j.renene.2019.12.004.
- Diego Oliva, Mohamed Abd Elaziz, Ammar H. Elsheikh, and Ahmed A. Ewees. 2019. “A Review on Meta-Heuristics Methods for Estimating Parameters of Solar Cells.” Journal of Power Sources 435 (September): 126683.
- OnyxSolar. n.d. Accessed June 2021. <https://www.onyxSolar.com/>.
- Ricardo R  ther, Priscila Braun, Martin Ordenes, and Deivis Luis Marinoski. 2007. “The Impact of Building-Integrated Photovoltaics on the Energy Demand of Multi-Family Dwellings in Brazil.” Energy and Buildings 39 (June): 629–42.

- Osseweijer, Floor J.W., Linda B.P. van den Hurk, Erik J.H.M. Teunissen, and Wilfried G.J.H.M. van Sark. 2018. "A Comparative Review of Building Integrated Photovoltaics Ecosystems in Selected European Countries." *Renewable and Sustainable Energy Reviews* 90 (July): 1027–40. doi:10.1016/j.rser.2018.03.001.
- Ying Huang, Zhishen Wu, and Changhai Peng. 2011. "Building-Integrated Photovoltaics (BIPV) in Architectural Design in China." *Energy and Buildings* 43 (December): 3592–98.
- Peng, Jinqing, Dragan C. Curcija, Lin Lu, Stephen E. Selkowitz, Hongxing Yang, and Weilong Zhang. 2016. "Numerical Investigation of the Energy Saving Potential of a Semi-Transparent Photovoltaic Double-Skin Facade in a Cool-Summer Mediterranean Climate." *Applied Energy* 165 (March): 345–56. doi:10.1016/j.apenergy.2015.12.074.
- Qiu, Changyu, and Hongxing Yang. 2020. "Daylighting and Overall Energy Performance of a Novel Semi-Transparent Photovoltaic Vacuum Glazing in Different Climate Zones." *Applied Energy* 276.
- Rababah, Haitham Esam, Azhar Ghazali, and Mohd Hafizal Mohd Isa. 2021. "Building Integrated Photovoltaic (BIPV) in Southeast Asian Countries. Review of Effects and Challenges." *Sustainability* 13 (23): 12952.
- Ravi Kumar, Amit Sharma, Sathans Suhag, Dharmendra Singh, and C.S. Rajoria. 2021. "Development of Flat-Plate Building Integrated Photovoltaic/Thermal (BIPV/T) System: A Review." *Materials Today: Proceedings* 46 (January): 5342–52.
- Ran Fu, T.L. James, and M. Woodhouse. 2015. "Economic Measurements of Polysilicon for the Photovoltaic Industry: Market Competition and Manufacturing Competitiveness." *IEEE Journal of Photovoltaics, Photovoltaics, IEEE Journal of, IEEE J. Photovoltaics* 5 (2): 515–24. doi:10.1109/JPHOTOV.2014.2388076.
- Refat, Khalid H., and Redwan N. Sajjad. 2020. "Prospect of Achieving Net-Zero Energy Building with Semi-Transparent Photovoltaics: A Device to System Level Perspective." *Applied Energy* 279 (December). doi:10.1016/j.apenergy.2020.115790.

- RESNET (Residential Energy Services Network, Inc.) and the International Code Council. "ANSI/RESNET/ICC Standard 301-2014 Standard for the Calculation and Labeling of the Energy Performance of Low-Rise Residential Buildings using an Energy Rating Index." January 15, 2016.
- Røstvik, Harald N., Müller-Eie, Daniela, Gholami, Hassan. 2019. "Holistic Economic Analysis of Building Integrated Photovoltaics (BIPV) System: Case Studies Evaluation." *Energy Build* 203.
- Lamela, Sonia. 2020. "Effect of Group Tutoring on Promoting Students Independent Learning in Architecture Studio." 2020 Sixth International Conference on E-Learning, December, 92–97. doi:10.1109/econf51404.2020.9385449.
- Sajjad, Muhammad T., Arvydas Ruseckas, and Ifor D.W. Samuel. 2020. "Enhancing Exciton Diffusion Length Provides New Opportunities for Organic Photovoltaics." *Matter* 3 (2): 341–54. doi:10.1016/j.matt.2020.06.028.
- Samiou, A.I., L.T. Doulos, and S. Zerefos. 2022. "Daylighting and Artificial Lighting Criteria That Promote Performance and Optical Comfort in Preschool Classrooms." *Energy & Buildings* 258 (March). doi:10.1016/j.enbuild.2021.111819.
- Saretta, Erika, Paola Caputo, and Francesco Frontini. 2019. "A Review Study about Energy Renovation of Building Facades with BIPV in Urban Environment." *Sustainable Cities and Society* 44 (January): 343–55. doi:10.1016/j.scs.2018.10.002.
- Saretta, Erika, Paola Caputo, and Francesco Frontini. 2019. "A Review Study about Energy Renovation of Building Facades with BIPV in Urban Environment." *Sustainable Cities and Society* 44 (January): 343–55. doi:10.1016/j.scs.2018.10.002.
- Simon, Dan. 2013. "Evolutionary Optimization Algorithms" *Biologically-Inspired and Population-Based Approaches to Computer Intelligence*. John Wiley & Sons Inc.

- Singh, Baljinder, Shikha Sharma, and S. K. Singal. 2019. "Modeling of Solar Energy Systems Using Artificial Neural Network: A Comprehensive Review." *Solar Energy* 180: 622–639.
- Singh, Digvijay, and Rubina Chaudhary. 2022. "Performance Evaluation of Thermally Insulated Building Integrated Photovoltaic Roof." *Materials Today: Proceedings* 52 (Part 3): 888–92. doi:10.1016/j.matpr.2021.10.294.
- Singh, Digvijay, Ajay Kumar Gautam, and Rubina Chaudhary. 2021. "Application of Phase Change Material in Building Integrated Photovoltaics: A Review." *Materials Today: Proceedings* 45 (Part 6): 4624–28. doi:10.1016/j.matpr.2021.01.021.
- Sun, Liangliang. 2011. "Simulation and Experimental Investigation on Optimum Applications of the Shading-Type Bipv and Bipvt Systems on Vertical Building Facades." Ph.D. diss., Hong Kong Polytechnic University, Hong Kong.
- Sun, Yanyi, Dingming Liu, Jan-Frederik Flor, Katie Shank, Hasan Baig, Robin Wilson, Hao Liu, Senthilarasu Sundaram, Tapas K. Mallick, and Yupeng Wu. 2020. "Analysis of the Daylight Performance of Window Integrated Photovoltaics Systems." *Renewable Energy* 145 (January): 153–63. doi:10.1016/j.renene.2019.05.061.
- Sun, Yanyi, Katie Shanks, Hasan Baig, Wei Zhang, Xia Hao, Yongxue Li, Bo He, et al. 2018. "Integrated Semi-Transparent Cadmium Telluride Photovoltaic Glazing into Windows: Energy and Daylight Performance for Different Architecture Designs." *Applied Energy* 231 (December): 972–84. doi:10.1016/j.apenergy.2018.09.133.
- Syafaruddin, Yunita Arum Sari, and Sri Mawar Said. 2021. "Review of Building Integrated Photovoltaic-Thermal (BIPV/T) Systems: Current and Potential Technology Development." *Journal of Engineering Science & Technology Review* 14 (4): 197–206.
- Hwang, Taeyon, Seokyoung Kang, and Jeong Tai Kim. 2012. "Optimization of the Building Integrated Photovoltaic System in Office Buildings - Focus on the Orientation, Inclined Angle and Installed Area." *Energy & Buildings* 46 (March): 92.

- Taveres-Cachat, Ellika, Gabriele Lobaccaro, Francesco Goia, and Gaurav Chaudhary. 2019. "A Methodology to Improve the Performance of PV Integrated Shading Devices Using Multi-Objective Optimization." *Applied Energy* 247 (August): 731–44. doi:10.1016/j.apenergy.2019.04.033.
- Tonui, Patrick, Saheed O. Oseni, Gaurav Sharma, Qingfenq Yan, and Genene Tessema Mola. 2018. "Perovskites Photovoltaic Solar Cells: An Overview of Current Status." *Renewable & Sustainable Energy Reviews* 91 (August): 1025–44. doi:10.1016/j.rser.2018.04.069.
- Sarat Kumar Panda, Pradip Kumar Sadhu, and M. Tripathy. 2016. "A Critical Review on Building Integrated Photovoltaic Products and Their Applications." *Renewable and Sustainable Energy Reviews* 61 (August): 451–65.
- van Bommel, Wout J.M. 2006. "Non-Visual Biological Effect of Lighting and the Practical Meaning for Lighting for Work." *Applied Ergonomics* 37 (4): 461–66. doi:10.1016/j.apergo.2006.04.009.
- Vanhoutteghem, Lies, Gunnlaug Cecilie Jensen Skarning, Christian Anker Hviid, and Svend Svendsen. "Impact of Façade Window Design on Energy, Daylighting and Thermal Comfort in Nearly Zero-Energy Houses." *Energy & Buildings* 102 (2015): 149-56.
- Varga, Zoltan, Ervin Racz. 2021. "Influence of the Cell Temperature on the Performance of a Dye Sensitized Solar Cell." In 2021 IEEE 19th World Symposium on Applied Machine Intelligence and Informatics (SAMI), Applied Machine Intelligence and Informatics (SAMI), 2021 IEEE 19th World Symposium On, January, 175-180.
- Veitch, Jennifer, Guy Newsham, Peter Robert Boyce, and CC Jones. 2008. "Lighting Appraisal, Well-being, and Performance in Open-plan Offices: A linked Mechanisms Approach." *Lighting Research and Technology* 40, no.2: 133-151.
- Wijeratne, W.M. Pabasara Upalakshi, Tharushi Imalka Samarasinghalage, Rebecca Jing Yang, and Ron Wakefield. 2022. "Multi-Objective Optimisation for Building Integrated Photovoltaics (BIPV) Roof Projects in Early Design Phase." *Applied Energy* 309 (March). doi:10.1016/j.apenergy.2021.118476.

- W. Zhang, L. Lu, J. Peng, and A. Song, 2016. "Comparison of the overall energy performance of semi-transparent photovoltaic windows and common energy-efficient windows in Hong Kong," *Energy and Buildings* vol. 128, pp. 511-18.
- Wang, Chuyao, Jie Ji, Md Muin Uddin, Bendong Yu, and Zhiying Song. 2021. "The Study of a Double-Skin Ventilated Window Integrated with CdTe Cells in a Rural Building." *Energy* 215 (Part A). doi:10.1016/j.energy.2020.119043.
- Wang, Jun, Minchen Wei, and Xiukai Ruan. 2021. "Comparison of Daylight Simulation Methods for Reflected Sunlight from Curtain Walls." *Building Simulation: An International Journal* 14 (3): 549–64.
- Wijeratne, W.M.P.U., T.I. Samarasinghalage, R.J. Yang, and R. Wakefield. 2022. "Multi-Objective Optimisation for Building Integrated Photovoltaics (BIPV) Roof Projects in Early Design Phase." *Applied Energy* 309 (March). doi:10.1016/j.apenergy.2021.118476.
- X. Liu and Y. Wu, 2022. "Numerical evaluation of an optically switchable photovoltaic glazing system for passive daylighting control and energy-efficient building design," *Building and Environment*, vol. 219.
- Zayed, Mohamed E., Jun Zhao, Ammar H. Elsheikh, Wenjia Li, and Mohamed Abd Elaziz. 2020. "Optimal Design Parameters and Performance Optimization of Thermodynamically Balanced Dish/Stirling Concentrated Solar Power System Using Multi-Objective Particle Swarm Optimization." *Applied Thermal Engineering* 178 (September). doi:10.1016/j.applthermaleng.2020.115539.
- Zhang, Tiantian, Wang, Meng, Hongxing, Yang, 2018. "A Review of the Energy Performance and Life-Cycle Assessment of Building-Integrated Photovoltaic (BIPV) Systems," *Energies* 11 (11), 31–57.
- Zhang, Xin, Du, Jiangtao, 2015. "Lighting Performance in Office Buildings with BIPV Facades: Visual and Non-Visual Effects." *Solar World Congress, 2015. Conference.*



# APPENDICES

## APPENDIX A. COMPARATIVE ANALYSIS OF LITERATURE REVIEW

Table A.1. Comparative analysis of literature review.

Reference	Location	Climate	Building function	Field of Application	Cell type	Performance Criteria	Aim	Methodology	Tools	Analysis Type	Results
Yoo et al., 2002	Gyeonggi-Do, Korea	Cold	Commercial	PV Shading	monocrystalline and polycrystalline solar cell	Energy	Performance analysis of a PV shading by considering weather conditions, aesthetic, cost, etc.	Reference building, field measurements, monitoring	PV-WR 1800=1500 PV-DATA, measuring instruments	Periodical analysis	Depending on the weather, climate, and shading effects, the efficiency of the modules significantly varies.
Omer et al., 2003	Nottingham, UK	Cold	Education	BIPV	a-Si and monocrystalline silicon solar cell	Energy and cost	To compare two different PV systems in terms of design, installation, performance, and economics	Reference building, 3D modeling, simulation	PVSYST simulation model	Periodical analysis	Results compare amorphous silicon and crystalline PV in terms of design, installation, performance, and economics.
Fung et al., 2008	Hong Kong, China	Subtropical	-	PV Window	Polycrystalline silicon semi-transparent and opaque solar cells	thermal	To develop a one-dimensional heat transfer model for PV glazing to forecast heat gain under different variables	Reference building, numerical model, field tests, simulation	Calorimeter box, an adjustable solar simulator, mathematical formulas	Steady-state	It is proved that the solar cell's area in a PV module affects heat gain.
Ordenes et al., 2007	Natal, Brasília and Florianópolis, Brazil	Moderate	Residential	BIPV	a-Si, monocrystalline, polycrystalline silicon, CdTe, CID	Energy	To evaluate the energy performance of six different PV systems in 3 other cities of Brazil	Reference building, 3D modeling, simulation	Energy Plus	-	Results show that the energy-saving potential is directly associated with the climatic region of the city.
Li et al., 2009	Hong Kong, China	Subtropical	Office building	PV Window	a-Si solar cell	Daylight, thermal, energy and cost	To explore the capacity of a PV glazing for thermal, daylight, and energy performance	Reference building, field measurements	Measurement tools	Steady-state	PV glazing and shading devices can reduce lighting loads and electricity consumption.
Rüther et al., 2009	Florianópolis, Brazil	Moderate	Airport	BIPV	a-Si solar cell	Energy	To see the potential of a-Si PV modules on energy demand reduction	Reference building, simulation	Simulation model	Periodical analysis	Full coverage of PV on the façade can supply the whole electricity energy demand of the airport.

(cont. on the next page)

Appendix A. (cont.)

Cheng et al., 2009	20 cities	Varied	-	BIPV	monocrystalline and polycrystalline silicon solar cell	Energy	To investigate the relation between the incline angle of BIPV system on roof and latitude of a region	Mathematical model, simulation	Mathematical equations, PVSYST	Periodical analysis	Latitude angle needs to be used as tilt angle to provide a better thermal performance and comfort.
James et al., 2009	Southampton, UK	Oceanic	Education building	PV Shading	monocrystalline solar cell	Energy, thermal, daylight, cost	To assess different shading solutions for electricity generation, daylight, and thermal performance	Reference building, questionnaire, numerical model	Mathematical equations, survey	Periodical analysis	PV system has a significant effect on not only the overall performance of a building but also its cost and carbon footprint.
Han et al., 2010	Unspecified	Unspecified	-	PV Window	a-Si solar cell with Low-E coating	Thermal	To understand the convective heat transfer rate of double-pane window integrated with a-Si PV cells with Low-E coatings	Numerical method	Mathematical equations	Steady-state	Results proved that the Low-E coatings could help to reduce heat transfer via radiation.
Sun et al., 2010	Hong Kong, China	Subtropical	-	PV Shading	Monocrystalline solar cell	Energy and thermal	To understand the effect of tilt angles of shading devices on the energy performance of the system	Numerical model	Mathematical equations	Periodical analysis	The proper tilt angle of the shading device is determined for better energy performance.
He et al., 2011	Hefei, China	Humid subtropical	Office building	PV Window	a-Si solar cell	Thermal and energy	To assess thermal and energy performance of thin-film a-Si PV window	Reference building, numerical model, field tests, simulation	Measuring tools CFD software tool FLUENT, GAMBIT	Periodical analysis	Results show that the numerical model performed parallel to field experimental data.
Yoon et al., 2011	Gyeonggi-Do, Korea	Cold	Office building	PV Window	a-Si solar cell	Energy	To compare the energy performance of a-Si PV glazing by monitoring and estimation	Reference building, field measurements	Monitoring	Periodical analysis	Estimated and actual energy production results of the PV window were found unrelated.

(cont. on the next page)

Appendix A. (cont.)

Yoo et al., 2011	Suwon-si, Korea	Moderate	Office building	PV shading	monocrystalline silicon	Thermal, daylight, and energy	To evaluate the performance of the BISTS system in terms of daylight, thermal, and energy performance	Reference building, 3D model and simulation, field measurement	SOLCEL	Steady-state	Outdoor air temperature increases when a remodeled system reaches higher flows. It results in reduced power generation and an increasing energy generation effect.
LiangLiang et al., 2011	Hong Kong, China	Subtropical	Undefined	PV shading	Mono and polycrystalline silicon	Energy	To evaluate the use of PV more effectively vertically on high rise building	Reference building, numerical model, 3D model, and simulation	Solar simulation lab of the Department of the Building Services Engineering, TRANSYS	Steady-state	Compared with traditional PV implementations, PV shadings provide more energy savings.
Yoo 2011	Suwon, Korea	Humid continental	Commercial building	PV shading	monocrystalline	Energy, thermal comfort, and daylight	To develop a numerical, experimental, and simulation model of a BIPV shading device	Reference building, 3D model and simulation, numerical model	SOLCEL, mathematical equations and measuring instruments	Periodical analysis	SOLCEL may be applicable to develop a multi-functional BIPV shading device to improve overall building performance.
Peng et al., 2011	China	Varied	Varied	BIPV review	Varied	Function, cost, technology, aesthetics, maintenance, and replacement	To discuss the issues of BIPV on several criteria	Literature review	Undefined	-	BIPV-associated problems in China may occur due to a lack of maintenance and replacement structures.
Urbanetz et al., 2011	Florianópolis, Brazil	Warm humid subtropical	Education building and car park	Façade and roof	a-Si	Energy	To test the hypothesis of whether there is a satisfactory compromise between form and function	Reference building, 3D model, and simulation	Ecotect	Periodical analysis	The energy generation of the curve PV module is 12% lower than the other one. However, in summer, it performed better.
Mandalaki et al., 2012	Athens, Chania, Greece	Mediterranean and temperate	Office building	PV shading	Undefined	Thermal, daylight, and energy	Thermal and daylight performance of 13 different configurations of BIPV shading devices	A reference building, 3D model, and simulation	Energy Plus, Autodesk Ecotect, Desktop Radiance	Steady-state	The authors develop 13 different energy and daylighting models for two other Greece cities.

(cont. on the next page)

Appendix A. (cont.)

Cronemberger et al., 2012	Brazil	Hot	-	BIPV	Undefined	Energy	To understand the relationship between solar irradiation, tilt angle, and orientation	Numerical model	Mathematical formulas	Periodical analysis	The optimal tilt angle is always above the latitude angle value or 9°C.
Hwang et al., 2012	Gyeonggi-Do, Korea	Cold	Office building	BIPV	polycrystalline silicon	Energy	To propose an energy model to compare the base case and PV-integrated models.	Experimental measurements, reference building, 3D model, and simulation	PV-DesignPro, eQUEST, BEMS	Periodical analysis	BIPV can supply the electricity demand between 1-and 5% when some variables are optimized.
Sun et al., 2012	Hong Kong, China	Subtropical	Undefined	BIPV	monocrystalline and polycrystalline silicon	Energy	To test the effect of BIPV shading systems' façade orientation and incline angle on building energy performance	Numerical model, reference building, 3D model, and simulation	Undefined	Periodical analysis	An optimum design for the BIPV shading system is proposed for different orientations.
Lu et al., 2013	Hong Kong, China	Subtropical	Office building	PV window	Undefined	Thermal, daylight, and energy	To assess the PV window's daylight, thermal, and energy performance	Reference building, simulation	Undefined	Periodical analysis	The PV window system provided electricity and lighting, saving between 900 and 1300 kWh.
Leite Didoné et al., 2013	Fortaleza and Florianopolis, Brazil, Frankfurt, Germany	Subtropical/continental	Office building	PV window	a-Si	Thermal, daylight, and energy	To create an energy and daylight model for an a-Si PV glass in various climate zones	Reference building, 3D model, and simulation	DAYSIM, Radiance, Energy Plus, Optics 6	Periodical analysis	PV glass can decrease the cooling and lighting loads of the building.
Ng et al., 2013	Singapore	Tropical	Office building	PV window	a-Si and micro-morph silicon PV modules	Thermal, daylight, and energy	Different PV windows are tested for energy and daylight performance.	Reference building, 3D model, and simulation	Energy Plus	Periodical analysis	Daylight and energy performance are affected by building orientation, solar cell choice, and window-to-wall ratio.
Bigot et al., 2013	Reunion Island, France	Subtropical	Undefined	BIPV	polycrystalline silicon	Energy	To present an optimization and validation model between simulation and field experiments	Experimental measurements, reference building, 3D model and simulation, numerical model	ISOLAB, GenOpt, MATLAB, ISOTEST	Steady-state	Results propose that PV application on roof can significantly reduce heat flux via roof.

(cont. on the next page)

Appendix A. (cont.)

Hwang et al., 2014	Chungbuk, Korea	Moderate	Office building	PV shading	Undefined	Energy	To assess the power generation capacity of PV light shelf	Reference building, scale model, field tests	The Solarlink photovoltaic monitoring system	Periodical analysis	The energy performance of PV shading elements is better when they are placed horizontally.
Kim et al., 2014	Korea	Undefined	Office building	Facade	a-Si and monocrystalline	Energy	To develop a PV blind system together with daylight responsive dimming system for better energy performance	Experimental measurements, reference building	Power meter, illuminance meter, several measuring instruments, etc.	Periodical analysis	PV blind incline angle and artificial light fixture affect the overall performance of a PV system.
Lee et al., 2014	Incheon-si, Korea	Continental	Research center	Façade, roof, and window	Monocrystalline and a-Si	Energy	To evaluate the zero-energy potential of a building with various BIPV systems	Reference building, field experiments, numerical model	pyrheliometer, thermometer, hygrometer, etc., mathematical formulas	Periodical analysis	The building is classified as a zero-energy building with the contribution of a BIPV façade.
Chae et al., 2014	Varied	Varied (6 different zones)	Commercial building	PV window	a-Si solar cell	Energy	To develop a model for a BIPV window to assess its energy and daylight performance	Reference building, 3D model and simulation, field measurements, numerical model	Energy Plus, mathematical formulas,	Periodical analysis	It is suggested that window optical characteristics should be optimized according to climate.
Mandalaki et al., 2014	Chania, Athens/Greece	Warm and temperate/Mediterranean	Office building	PV shading	Monocrystalline and polycrystalline	Energy	To compare the results of 3 different methods of PV energy performance calculation	Reference building, 3D model and simulation and field measurements	Energy Plus, Sketch Up, Open Studio	Periodical and steady-state	Simple and more complex energy models present similar results, and field measurement of PV systems provides more accurate results.
Jinqing et al., 2015	Hong Kong, China	Subtropical	Office building	PV window	a-Si	Thermal, daylight and energy	To evaluate capacity of a-Si based PV double-skin façade on energy and daylighting performance	Reference building, 3D model and simulation, field measurements	Energy Plus, spectrometer, OPTICS software, WINDOW	Periodical analysis/ steady-state	A simulation model that can predict the overall energy and daylight performance is presented for further design developments.

(cont. on the next page)

Appendix A. (cont.)

Kapsis et al., 2015	Toronto, Canada	semi-continental	Office building	PV window	a-Si	Daylight	To investigate the daylight performance potential of 3 different PV windows	Reference building, 3D model, and simulation	DAYSIM, Energy Plus	Periodical analysis	BIPV windows can provide optimum daylight performance and maximize daylight and outdoor view.
Li 2015	Los Angeles, USA	Moderate	Office building	PV shading	Undefined	Energy and daylight	To evaluate the performance of BISTS on energy and daylight performance	Reference building, 3D model and simulation, mathematical equations	Energy Plus, DAYSIM, TRNSYS	Periodical analysis	BISTS improves daylight performance and is efficient for hot water, space heating and cooling strategies.
Freitas et al., 2015	Geneva, Switzerland, Lisbon, Portugal	Continental, mild subtropical	Undefined	PV shading	Undefined	Energy	To analyze different BIPV shading system configurations to maximize solar irradiation	Reference building, 3D model and simulation, optimization	Rhino, Grasshopper, Diva, Galapagos, MatLab	Periodical analysis	A tilted louvre can produce 20-40% more electric energy than a typical flat and vertical shading system.
Knera et al., 2015	Lodz, Poland	Moderate	Office building	BIPV	Undefined	Energy	To assess the capacity of BIPV to supply electricity demand and daylight	Reference building, 3D model and simulation, numerical model	ESP-r, WATSUN, DAYSIM	Periodical analysis	Energy generated from BIPV cover most of the lighting loads for the south façade.
Du et al., 2015	Beijing, China and London, UK	Warm and temperate	Office building	Facade	Undefined	Daylight	To evaluate the daylight performance of a BIPV through a simulation model	Reference building, 3D model, and simulation	DAYSIM, EVALGLARE	Steady-state	Configuration of BIPV has a significant effect on daylight performance.

(cont. on the next page)

Appendix A. (cont.)

Zhang et al., 2016	Hong Kong, China	Subtropical	Office building	PV window	a-Si	Thermal, daylight and energy	To evaluate energy, daylighting, and thermal performance of PV window	Experimental measurements, Reference building, 3D model, and simulation	Energy Plus	Periodical analysis	When it is compared with single and double-pane glazing, a-Si PV window can reduce the heating and cooling loads differently on varying facades.
Göksu, et al., 2016	Stuttgart, Germany	Temperate	Office building	PV shading	Undefined	Energy	To BIPV shading device's energy performance	Reference building, 3D model, and simulation	Ecotect, Energy Plus	Periodical analysis	Vertical multiple shading elements on the south façade provide the best thermal performance.
Stamatakis et al., 2016	Crete, Greece	Mediterranean	Office building	PV shading	Monocrystalline	Energy, Thermal, and Daylight performance	To analyze PV integration in buildings in a multipurpose way	Reference building, 3D model, and simulation	PROMETHEE	Periodical analysis	Brise soleil full facade performed best while canopy inclined double or louvers horizontal inwards inclined present worse.
Tripathy et al., 2016	Varied	Varied	Varied	BIPV review	Varied	Life cycle assessment	To conduct an analysis on BIPV for life cycle assessment	Literature review	Varied	Varied	BIPV orientation and shadow consideration affect the life cycle assessment of a BIPV system.
Wang et al., 2017	Harbin, Beijing, Changsha, Kunming, Hong Kong, China	Varied	Office building	PV window	a-Si	Thermal, daylight, and energy	To assess the energy performance of PV double skin façade (PV-DSF) and PV insulating glass unit (PV-IGU)	Reference building, 3D model and simulation, field measurement	Energy Plus, laboratory tests	Periodical analysis	The overall energy-saving potential of two glazing systems is defined as 28.4% and 30%.
Jayathissa et al., 2017	Zurich, Germany	Temperate	Office building	PV shading	CIGS	Thermal, daylight, and energy	To propose an adaptive and dynamic PV shading system for better energy performance	Reference building, 3D model, and simulation	Rhino, Grasshopper, Ladybug, Honeybee	Periodical analysis	The proposed dynamic model report 20-80% energy saving.
Martellotta et al., 2017	Los Angeles, USA	Warm Mediterranean	Office building	PV window	a-Si and perovskite	Energy performance	To compare two different PV solar cells' energy performance	Reference building, 3D model, and simulation	Energy Plus	Periodical analysis	A-si PV module saves more energy than perovskite-based cells. PCs have a better daylight performance.

(cont. on the next page)



Appendix A. (cont.)

Zhang et al., 2017	Hong Kong, China	Subtropical	Office building	PV shading	Polycrystalline silicon	Thermal, daylight, and energy	To optimize the tilt angle of PV shading for better daylight and energy performance	Reference building, 3D model and simulation, field measurements	Energy Plus	Periodical analysis	Optimized PV shading element on south façade with 20° tilt angle is proposed.
Budhiyanto et al., 2017	Jakarta, Indonesia	Monsoon	Office building	PV shading	Undefined	Energy	To compare energy models of various PV shading devices	Reference building, 3D model, and simulation	Energy Plus, mathematical formulas	Periodical analysis	Fewer panel installation with greater distance provides better performance than more close-distance panels.
Shukla et al., 2017	Varied	Varied	Varied	BIPV review	Varied	Life cycle assessment, economically	To present a comprehensive review of BIPV technologies	Literature review	Varied	Varied	Large monocrystalline PV modules have the highest energy payback time compared to thin-film cells.
Nundy et al., 2018	Cornwall, UK	Temperate oceanic	-	PV window	Polycrystalline	Thermal and daylight	To offer hybrid smart glazing to control excessive solar gain, thermal and visual comfort	Numerical models, field experiments	UV-VIS-NIR spectrophotometer	Steady-state	Multicrystalline-based combined PV-vacuum glazing with different transparencies ranged between 35%, and 42% is produced.
Sun et al., 2018	Harbin, Beijing, Shanghai, Guangzhou, Kunming, China	Varied	Office building	PV window	CdTe	Daylight and energy	To understand the energy and daylight performance of thin-film CdTe PV glazing	Reference building, 3D model, and simulation	Energy Plus, RADIANCE	Periodical analysis	Thin-film CdTe PV glazing improves daylight performance and saves energy when the WWR is high.
Cheng et al., 2018	Taiyuan, China	Cold	Office building	PV window	a-Si	Daylight and energy	To assess daylight and energy performance of PV glazing considering variables as transmittance, orientation, window-to-wall ratio	Experimental measurements, reference building, 3D model and simulation, numerical model	DAYSIM, Energy Plus, Optics, field measurement equipment	Periodical analysis/ steady-state	Glazing transmittance and WWR should be 50-60% and 40-50%, respectively, to satisfy both energy and daylighting performance.

(cont. on the next page)

Appendix A. (cont.)

Gao et al., 2018	Shanghai, New York, Tokyo, Beijing, London, Los Angeles, Toronto, Paris, Berlin	Varied	Office building	PV window	monocrystalline silicon	Daylight and energy	To evaluate the daylight and energy performance of PV glazing integrated with shading elements	Reference building, 3D model, and simulation	MATLAB, MATLAB Simulink, Sketch-Up, Rhinoceros DIVA, and Grasshopper	Periodical analysis	Annual energy generation covers 27.4% of the total energy demand of the building.
Gao et al., 2018	Undefined	Undefined	Office building	PV window	Undefined	Daylight and energy	To test the potential of PV windows with shading devices for maximum solar energy harvesting	Reference building, 3D model, and simulation	Rhinoceros DIVA and Grasshopper	Periodical analysis	Dynamic and static PV shading elements can reduce glare risks.
Asfour 2018	Saudi Arabia	Hot desert	Office building	PV shading	Undefined	Thermal and daylight	To assess the daylight and thermal performance of various shading devices with different incline angles	Reference building, numerical model, simulation	Design-Builder, Energy Plus, analysis programs such as IES VE and Ecotect Analysis 2011	Periodical analysis	Horizontal BIPV shading device with 45° incline angle has the highest annual solar radiation by providing an effective shading of 96%.
Piccoli et al., 2018	Athens/Greece, Milan/Italy, Copenhagen	Mediterranean	-	PV shading	Undefined	Daylight	To assess a BIPV shading device for better daylight and energy performance	Reference building, 3D model and simulation	Energy Plus, MATLAB, Window,	Periodical analysis	
Agathokleous et al., 2018	Limassol, Cyprus	Coastal	-	Facade	Undefined	Energy	To analyze a BIPV system's energy performance theoretically and experimentally	Numerical and experimental model	Mathematical equations and measuring instruments	Periodical analysis	The system's energy saving potential varies between 26.5-33.5%, while energy efficiency varies between 13-16%.
Zhang et al., 2018	Varied	Varied	Varied	BIPV review	Varied	Energy	To review the evaluation and progress of recent developments in BIPV systems	Literature review	Undefined	-	Energy payback time and greenhouse-gas emissions are discussed.
He et al., 2018	Wuhan, China	Temperate	Undefined	Facade	Undefined	Daylight	To propose a daylight performance evaluation method for BIPV	Reference building, 3D model, and simulation, numerical model	Rhino, Grasshopper, DIVA, Energy Plus	Steady-state	Results present similar values between simulation and numerical models.

(cont. on the next page)

Appendix A. (cont.)

Zhang et al., 2018	Varied	Varied	Varied	PV shading review	Varied	Energy, thermal, and daylight	To analyze PV shading implementations in terms of overall energy performance	Varied	Varied	Varied	Comprehensive literature is grouped according to PV materials, orientations, tilt angles, building types, and research approaches.
Zhang et al., 2019	Harbin, Beijing, Shanghai, Hong Kong, Kunming, China	Varied	Office building	PV window	a-Si	Daylight and energy	To evaluate the energy and daylight performance of PV glass in different climates	Experimental measurements, reference building, 3D model, and simulation	Laser Comp FOX heat flow meter, OPTICS, Berkeley Lab WINDOW, Energy Plus	Periodical analysis	Although the glazing increases lighting loads, it still proposes better daylight performance due to reducing glare risks.
Mesloub et al., 2019	Algeria	Semi-arid	Office building	PV window	a-Si	Daylight and energy	To understand the energy and daylight performance of PV window	Experimental measurements, Reference building, 3D model, and simulation	Energy Plus, Open Studio, Integrated Environment Solution-Virtual environment (IES-VE)	Periodical analysis	Cooling load and glare reduction are minimized. PV window provided a uniform distribution of daylight by keeping illuminance levels between 300- and 700 lux.
Chinazzo et al., 2019	Geneva, Casablanca, Helsinki, Morocco	Temperate, hot-arid, cold	Office building	PV window	Undefined	Thermal, daylight, and energy	To explore thermal and visual comfort and overall energy performance	Reference building, 3D model and simulation, field measurements	Ladybug, Honeybee, Energy Plus, DAYSIM, RADIANCE, MATLAB	Periodical analysis	Results proposed the best design alternation for Geneva and Helsinki with 50% transmittance and Casablanca with 20% transmittance.
Alrashidi 2019	Penryn, UK	Cold	Office building	PV shading	CdTe	Thermal, daylight and energy	To investigate the thermal, daylight, and energy performance of different types of CdTe thin-film based PV glazing	Reference building, field measurements, data analysis, mathematical equations	Measuring tools	Periodical analysis/ steady-state	BISTS enhance daylight performance by reducing glare and increasing UDI. They provide 85% of hot water and 20% of heating and cooling demand.

(cont. on the next page)

Appendix A. (cont.)

Taveres-Cachat et al., 2019	Oslo, Norway	Nordic	Office building	PV shading	Undefined	Thermal, daylight and energy	To optimize the performance of shading elements for overall performance	Reference building, 3D model and simulation, optimization	Rhino with Grasshopper, plug-ins of Ladybug with Honeybee and Energy Plus, Octopus	Periodical analysis	The authors propose an optimized model for the building's daylight, thermal, and energy performance.
Lee 2019	Seoul, Korea	humid continental	Office building	PV shading	monocrystalline silicon	Daylight and energy	Developing a light shelf covers only some part of the shading element to evaluate daylighting and energy generation at the same time	Reference building, scale model, field tests	Scale model and field test	Steady-state	The optimum incline angle is different for light shelves with or without PV implementation. The uniform distribution of daylight decreases when the PV area changes.
Bennouna et al., 2019	Morocco	Varied	Undefined	PV window	a-Si, monocrystalline, and polycrystalline silicon	Energy	To evaluate the energy performance of different PV glazing systems on various sites	Reference building, field measurements	Measurement tools	Periodical analysis	There occurred a difference in energy performance between seaside and continental cities.
Piccoli et al., 2019	Milan, Italy	Temperate	Office building	PV shading	monocrystalline	Energy	To assess the energy performance of the BIPV shading device	Numerical and 3D simulation model	Window LBNL software, Energy Plus, mathematical formulas	Periodical analysis	BIPV shading device can improve glare risks with proper solar control performance.
Aelenei et al., 2019	Lisbon, Portugal	Temperate	Office building	Façade and roof	Polycrystalline and a-Si	Energy	To evaluate the energy performance of two BIPV systems on the roof and façade.	Using a reference building, 3D model and simulation, numerical model	Mathematical equations and measuring instruments	Periodical analysis	BESS's energy flexibility can improve metrics such as load matching and grid interaction.
Yoo 2019	Seoul, Korea	Humid continental	Community center	PV shading	Monocrystalline	Energy and thermal comfort	To assess the thermal and energy performance of a BIPV shading device	Using a reference building, 3D model and simulation	SolCel 19, TRNSYS 17	Periodical analysis	Parameters are optimized for better energy performance and thermal comfort.

(cont. on the next page)

Appendix A. (cont.)

Jakica et al., 2019	Varied	Varied	Varied	BIPV review	Varied	Energy, thermal, and daylight	To present tools and methods for BIPV design and performance modeling	Simulation	RET Screen, Homer Pro, Sunnulator, SAM, Polysun, PV Sol, PV-GIS, Skelion, Ladybug, PVsyst, PVwatts, Revit, PV-GIS, Grasshopper Plug-ins	Varied	The study comprehensively analyzes the tools used to make a BIPV performance analysis.
Saretta et al., 2019	Varied	Varied	Varied	BIPV review	Varied	Varied	A comprehensive review of BIPV systems in terms of approaches, methods, tools, and characteristics	Literature review	Varied	Varied	BIPVs can develop the overall energy performance of a building in a significant manner.
Sarkar et al., 2019	Varied	Varied	Varied	BIPV review	Varied	Development and recent trends	To evaluate recent development and trends on BIPV energy generation	-	-	-	A systematic review is conducted on the recent technologies of BIPV.
Chan 2019	Varied	Varied	Commercial building	Façade	Varied	Energy	To assess the effect of shading on BIPV system's energy performance	Reference building, 3D model, and simulation	Energy Plus	Periodical analysis	Correlation between energy generation ratio and sky view factors is conducted.
Qiu et al., 2020	Beijing, Wuhan, Hong Kong, and Kunming, China	Varied	-	PV window	Undefined	Thermal, daylight, and energy	To see how PV vacuum glazing affects thermal, daylight, and energy performance in various climatic zones	Measurements, real-time tests, 3D modeling, and simulation	Spectrophotometer, Rhino, Ladybug with Honeybee and DAYSIM, Energy Plus	Periodical analysis/ steady-state	In four climatic zones, PV vacuum glazing reduces energy consumption by 43.4%, 66.0%, 48.8%, and 35.0%, respectively. In hot and temperate areas, they raise cooling demand.

(cont. on the next page)

Appendix A. (cont.)

Liu et al., 2020	Birmingham, UK	Temperate maritime climate	Office building	PV window	CdTe	Daylight	To test the effect of varied transmittance of CdTe on daylight performance	Field measurement, simulation	RADIANCE	Periodical analysis	CdTe PV glazing helped improve the uniform distribution of daylight and overall performance.
Mesloub et al., 2020	Riyadh, London, Kuala Lumpur, Algiers	Varied	Office building	PV window	a-Si	Energy and daylight	Assess double-glazing Low-E STPV glazing and double glazed Low-E argon filled a clear glass with interior light shelves for energy and daylight performance	Reference building, 3D model, and simulation	Energy Plus, Rhino with Grasshopper, Diva plug-in of Grasshopper	Periodical analysis	a-Si STPV glazing could not improve daylight performance for east and west, but it contributed to energy saving.
Qiu et al., 2020	Hong Kong, China	Subtropical	Office building	PV window	CdTe	Energy and daylight	To examine the energy and daylight performance of vacuum CdTe PV windows	Reference building, 3D model and simulation, field measurements	RADIANCE simulation, ANN model, spectrophotometer	Periodical analysis	The proposed model presents a more accurate daylight performance result for this hybrid glazing.
Sun et al., 2020	Harbin, Shanghai and Guangzhou, China	Varied	Office building	PV window	CdTe and monocrystalline silicon	Daylight	To explore the daylight performance of various PV glazing options under multiple circumstances and performance measures	Reference building, scale model, field tests, 3D model, and simulation	RADIANCE	Periodical analysis	If crystalline silicon cells and CCPC optics are used together, they can enhance daylight performance.
Alrashidi et al., 2020	UK	Temperate	Office building	PV window	CdTe	Energy	To understand the effect of PV window's orientation and transmittance on reducing cooling loads	Using a reference building, field tests, simulation	Measuring tools, data logger, AAA solar simulator	Steady-state	PV glazing achieved an energy saving of 20%.
Mesloub et al., 2020	Algeria	Semi-arid	Office building	PV window	a-Si	Daylight and energy	To assess PV window's daylight and energy performance	Reference building, 3D model and simulation, field measurements,	Energy Plus, Open Studio, Sketch-Up, RADIANCE, measuring instruments	Periodical analysis	Double-glazing PV modules with a 20% window-to-wall ratio are considered optimal PV windows. They provide 60% energy saving for the south façade.

(cont. on the next page)

Appendix A. (cont.)

Nundy et al., 2020	Undefined	Temperate	Undefined	PV window	undefined	Thermal and daylight	To evaluate thermal and visual comfort of SPD vacuum glazing	Reference building, field measurements	Outdoor test cell, non-calorimetric, PMV, and PPD methods	Periodical analysis	The opaque state did not provide proper daylighting on the overcast sky.
Mesloub et al., 2020	Ha'il, Saudi Arabia	Hot desert	Office building	PV shading	Undefined	Thermal, daylight, and energy	To understand the effects of light shelves' configurations on building performance	Reference building, 3D model, and simulation	Rhino, Diva, and DAYSIM plug-ins of Grasshopper	Periodical analysis	The best configuration for energy and daylight performance is proposed.
Megahed et al., 2020	Mansoura, Egypt	Desert	Residential building	Roof	polycrystalline silicon	Energy, thermal, and cost	To develop a PV system for supplying some of the building's energy demand	Reference building, numerical and simulation model	Mathematical formulas, ANSYS Fluent 19.2	Periodical analysis	PV system with a coolant flow rate (2 L/min) module can produce the maximum electrical energy with satisfied thermal energy.
Ghosh 2020	Varied	Varied	Varied	BIPV review	Varied	Energy, thermal, daylight	To conduct a comprehensive review on BIPV and (BAPV)	Literature review	-	-	Obstacles that produce shading on PV systems may obstruct PV installation.
Li et al., 2020	Tianjin, China	Monsoon	Educational building	Facade	monocrystalline	Energy	To understand the effect of shading conditions on a BIPV system's overall performance	3D model and simulation, numerical model, field measurements	ANSYS, COMSOL Multiphysics, mathematical formulas, measuring instruments	Steady-state	Shading and masking conditions are effective in the performance of a PV.

(cont. on the next page)

Appendix A. (cont.)

Ramanan et al., 2020	Tamil Nadu, India	Hot and humid	Education al building	Facade	polycrystalline	Energy	To evaluate the effect of orientation and incline angle on the performance of the BIPV system	Field experiments, 3D model, and simulation	HOMER, mathematical formulas, measuring instruments	Periodical analysis	The East façade is the optimum orientation for BIPV implementation. South orientation is the best performed one for pitched roofs.
Paydar 2020	Tehran, Iran	Cold semi-arid	Undefined	PV shading	Undefined	Energy	To assess the energy performance of a BIPV shading device with different incline angles	Reference building	Energy Plus and MATLAB	Periodical analysis	The optimum PV system is proposed. Movable shading devices performed better than fixed ones in energy generation and thermal loads.
Jung et al., 2020	Michigan, USA	Continental	Office building	PV shading	Undefined	Energy and daylight	To develop a BIPV shading device model to save energy and enhance visual comfort	Reference building, numerical and experimental model	ANN model, scale model, measuring instruments	Periodical analysis	Results present a consistency between the ANN model and experiment results in energy and daylight performance.
Yadav et al., 2020	Delhi, India	Humid subtropical	Two stories small building	Roof	Undefined	Thermal	To evaluate the thermal performance of a semi-transparent BIPV on a building roof	Reference building, numerical and experimental model	Mathematical equations and measuring instruments	Periodical analysis	On the 15th of May, rooms have the highest indoor temperature values as 47.3°C and 42.6°C.
Alrashidi et al., 2020	Penryn, UK	Temperate	Education building	PV window	CdTe	Thermal	To develop an experimental model to test a PV system's thermal performance	Experimental measurements	UV-Vis-NIR, Class AAA+, AM 1.5, NI logging system, K-type thermocouple sensors, Pyrheliometer and Pyranometer	Steady-state	The overall heat transfer coefficient (U-value) of the PV module was found as 2.7 W/m <sup>2</sup> K
Yahya et al., 2020	Baghdad, Iraq	Hot desert	Office building	PV shading	Undefined	Energy	To evaluate the energy generation capacity of a PV shading device on façade	Reference building, 3D model and simulation, statistical data analysis	Autocad, Sketch-Up, ModelIT-IES, IES-VE, LBNL Window 7.5,	Periodical analysis	A systematic approach is needed for the further development of the BIPV system.

(cont. on the next page)



Appendix A. (cont.)

Roy et al., 2020	Varied	Varied	Varied	BIPV review	Perovskite		To discuss challenges and current situation of perovskite-based cell technology in the industry	Literature review	-	Varied	Perovskite-based cell challenges, potential, current situation, and knowledge are discussed.
Gosh et al., 2021	Riyadh, Saudi Arabia	Hot desert	-	PV window	Perovskite	Daylight	To understand the effect of perovskite BIPV windows on visual comfort and proper daylight performance	Reference building, 3D model, and simulation	Rhino with Grasshopper, Diva plug-in of Grasshopper		For a south-facing façade, optimum glazing transmittance should be between 50-and 70%. Transmittance should be around 90% for improved color rendering, which may create glare problems.
Lee et al., 2021	Undefined	Undefined	Office building	PV shading	Polycrystalline silicon	Energy	To develop a scale model to estimate the BIPV shading elements' thermal and daylight performance	Reference building, scale model and field tests, numerical model	Monitoring by sensors, math formulas	Periodical analysis	Light shelf incline angle and PV module installation area effectively affect daylight uniformity and thermal performance.
Gholami et al., 2021	Stavanger/ Norway, Bern /Switzerland, Rome/Italy, and Dubai/UAE	Varied	Undefined	Facade	Varied	Energy and daylight	To understand the effect of climate and weather on solar radiation, BIPV's performance	Reference building, field measurements	Measurement tools	Periodical analysis	Solar radiation of whole façade is higher than average radiation on the east and west facades. Also, there found a correlation between the performance of solar cells and climate
Gonçalves et al., 2021	Leuven, Belgium	Temperate	Undefined	Facade	Undefined	Thermal	To propose a combination of CFD with a multi-physics BIPV model to assess its thermal performance	Reference building, 3D model and simulation, field measurement	openIDEAS/Mo delica mathematical formulas,	Steady-state	eCHTC variations may change cell temperatures up to 17%. Also, near-edge zones have lower temperatures while bottom and center zones have higher.

(cont. on the next page)

Appendix A. (cont.)

Li et al., 2021	Chengdu, China	Temperate	Undefined	PV window	monocrystalline	Energy and daylight	To develop a BIPV and improve its daylight and energy performance	Reference building, field measurement, 3D model, and simulation	Scale model,	Steady-state and periodical	The daylight performance of a PV façade can be improved with good design. The highest energy saving of 26.5% is achieved during the winter months.
Maghrabie et al., 2021	Varied	Varied	Varied	BIPV review	Varied	Varied	To conduct a comprehensive review on the application and challenges of BIPV systems	Literature review	-	Varied	Challenges and motivations with prospects of BIPV systems are presented due to the study.
Azami et al., 2021	Tabriz, Iran	Temperate climate	Office building	Facade	monocrystalline	Energy	To understand the role of building envelope for energy performance of BIPV systems with a parametric model	Using a reference building, numerical and 3D simulation model	DesignBuilder, mathematical formulas	Periodical analysis	Results imply a correlation between energy generation and form configuration with orientation.
Kuhn et al., 2021	Varied	Varied	Varied	BIPV review	Varied	Technology	To present widely analyzed BIPV systems in terms of technological opportunities	Literature review	-	Varied	The paper presents several design options for structural integration of the BIPV system on the building envelope.
Weerasinghe et al., 2021	Varied	Varied	Non-domestic	BIPV review	Varied	Cost	To review the economic feasibility of BIPV systems in different regions	Literature review	-	Varied	Economic analysis of built projects shows that BIPV is economically feasible.
Syafaruddin et al., 2021	Varied	Varied	Varied	BIPV review	Varied	Technology, cost, energy	To review the current technology and situation of BIPV systems	Literature review	-	Varied	New trends, opportunities, and challenges are discussed in the study.
Singh et al., 2021	Varied	Varied	Varied	BIPV review	Varied	Cost and thermal	To discuss the applicability and performance of phase-change materials in BIPV	Literature review	-	Varied	PSM decreases module and building envelope temperatures.

(cont. on the next page)

Appendix A. (cont.)

Liu et al., 2021	Varied	Varied	Varied	BIPV review	Varied	Energy, aesthetic value	To review the feasibility of BIPV systems to increase their utilization in areas with high solar irradiation	Literature review	-	Varied	An optimum system is emphasized based on the factors that affect BIPV performance.
Rababah et al., 2021	Southeast Asia	Tropical	Varied	BIPV review	Varied	Overall performance and cost	To define the effects and challenges of BIPV application considering cost, climate, and government policy	Literature review	-	Varied	Climate and government policy substantially affect BIPV performance, efficiency, and technology improvement.
Rajoria et al., 2021	Varied	Varied	Varied	BIPV/T review	Varied	Energy and thermal	To review current developments of BIPV/T systems on building performance	Literature review	-	Varied	BIPV/T performance strongly depends on the climate and building design variables.
Martín-Chivelet et al., 2022	Varied	Varied	Varied	BIPV review	Varied	Thermal, energy, and daylight	To review thermal, solar, optical, and electrical aspects of BIPV systems	Literature review	-	Varied	The study presented knowledge of BIPV's thermal, solar, optical, and electrical aspects.
Pillai et al., 2022	Varied	Varied	Varied	BIPV review	Varied	Technology, life cycle assessment, and outdoor testing	To analyze outdoor test systems, technological improvement, and life cycle assessment of BIPV	Literature review	-	Varied	Different test systems are reviewed and presented for future improvements in the BIPV industry.
Chen et al., 2022	Phoenix, USA	Hot desert	High rise residential tower	PV window	a-Si	Thermal, daylight, and energy	To investigate building parameters and urban landscape's effect on PV window performance	Monitoring, numerical model	BEM-SLUCM model, mathematical equations,	Steady-state and periodical	The optical and thermal aspects of PW windows do not significantly affect urban microclimate.
Alrashidi et al., 2022	Penryn, UK	Temperate	Office building	PV window	CdTe	Thermal and energy	To understand window-based variables' effect on thermal and energy performance	Reference building, outdoor experiment, numerical model	Class AAA+, AM 1.5, mathematical equations	Steady-state and periodical	The relationship between window-based variables and building thermal and energy performance are discussed.

(cont. on the next page)

Appendix A. (cont.)

Pabasara Upalakshi Wijeratne et al., 2022	Melbourne, Australia	Subtropical	Commercial	Roof and skylight	Varied	Energy and cost	To optimize BIPV envelope parameters, high energy generation and low life cycle cost	Reference building, 3D model and simulation, optimization	NSGA II, mathematical equations, Revit	Steady-state and periodical	Results present optimum roof sheet and skylight solutions for higher energy generation and lower life cycle costs.
Samarasinghalage 2022	Australia	Subtropical	Undefined	Roof, canopy, and cladding	Undefined	Energy and cost	To optimize BIPV energy generation and life cycle cost together with building envelope parameters and BIPV application type	Reference building, 3D model and simulation, optimization	Revit, NSGA II, Python, PyCharm IDE	Steady-state and periodical	In the early design stage, multi-objective optimization is effective.
Singh et al., 2022	Indore, India	Tropical	Education building	Roof	Polycrystalline silicon	Thermal	To compare the thermal performance of insulated and non-insulated BIPV roofs	Reference building, scale model, numerical model	K-type thermocouple, Keithley 2700 Datalogger, mathematical formula	Steady-state and periodical	Heat gain, heat loss and module temperature changes due to different insulation materials applied on BIPV.
Zhang et al., 2022	Hefei, China	Humid subtropical	Undefined	PV window	CdTe	Thermal and energy	Compare different PV glazing types' thermal and energy performance	Reference building, numerical model	Dataloggers, thermocouples, mathematical formula	Steady-state and periodical	Vacuum glazing improves the thermal performance of PV double-skin windows due to a lower U-value.
Kirimtat et al., 2022	Varied	Varied	Varied	PV shading	Varied	Cost and energy	To conduct comprehensive research on PV integrated shading devices and their cost and energy behavior	Literature review	-	Varied	A detailed analysis of current literature is presented regarding PV integrated shading devices.

## APPENDIX B. GRASSHOPPER SCRIPT FOR DAYLIGHT AND ENERGY SIMULATIONS

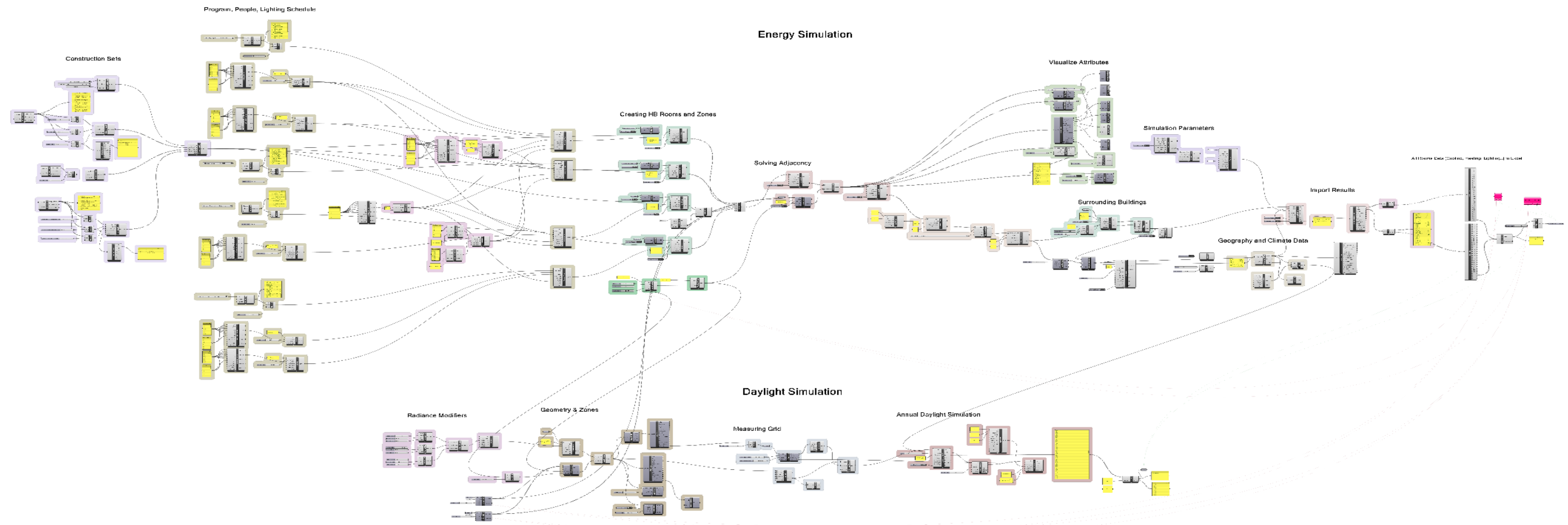
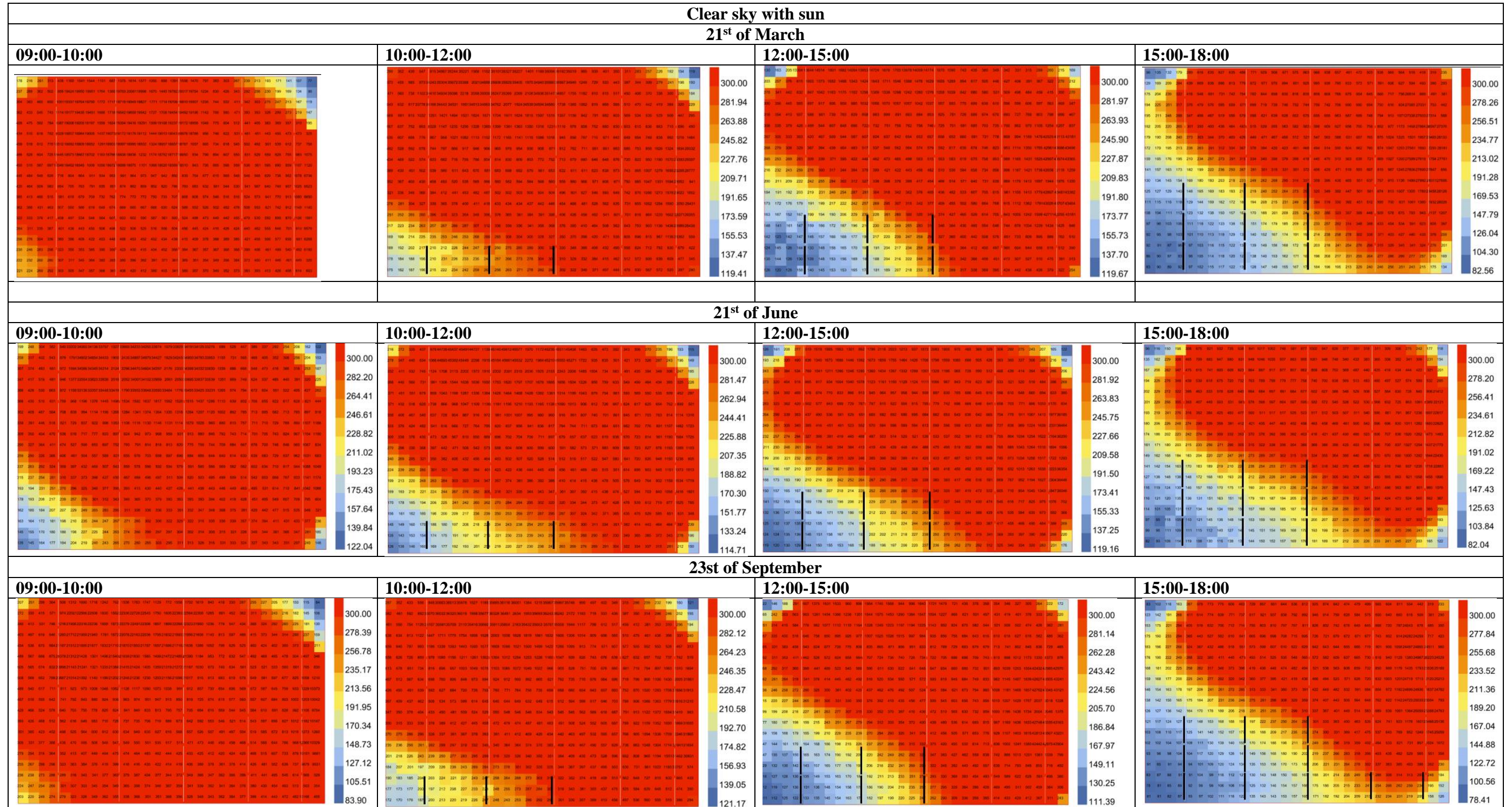


Figure A.1. Grasshopper script for daylight and energy simulations.

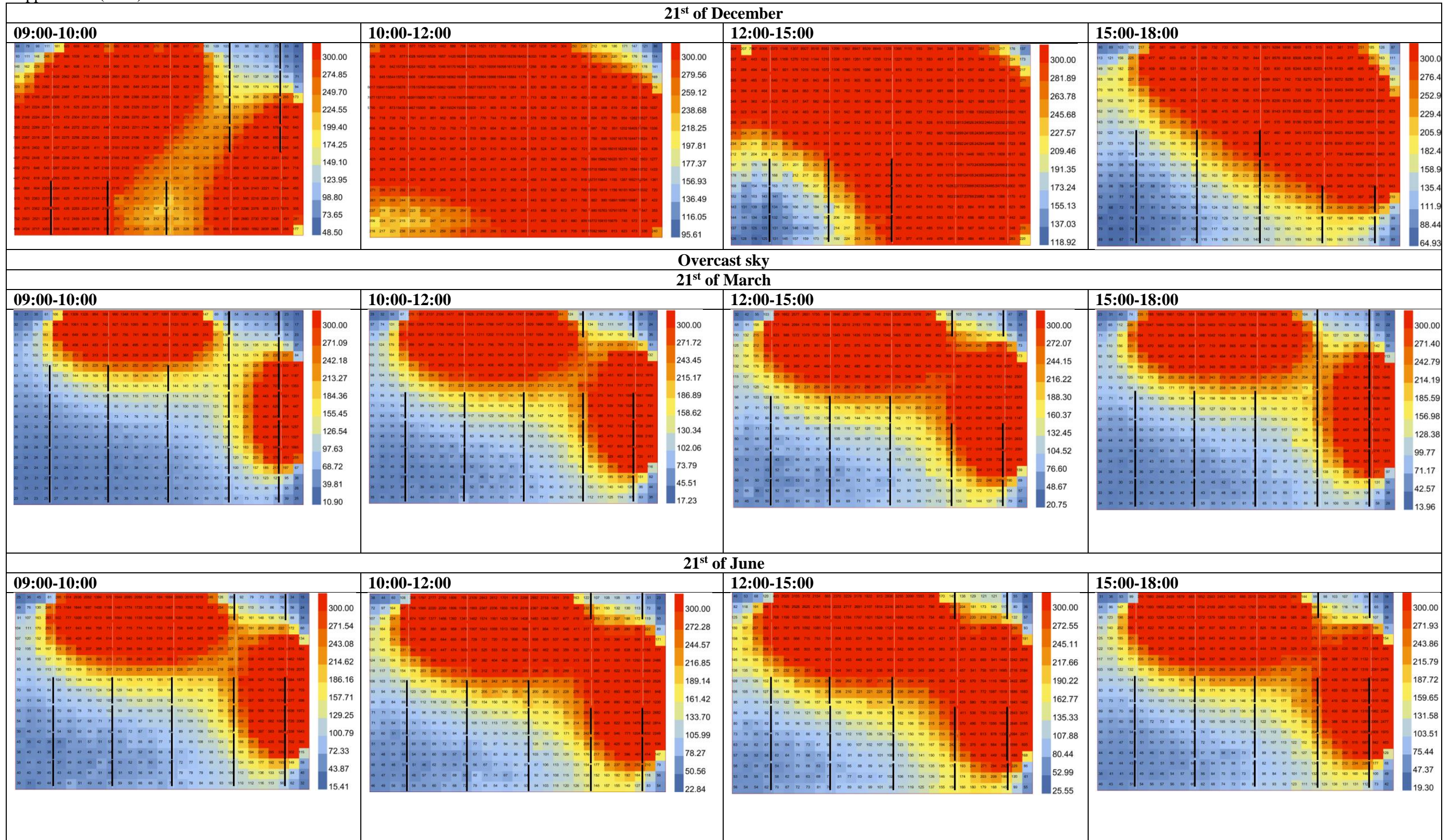
## APPENDIX C. POINT-IN-TIME DAYLIGHT ANALYSIS OF BASE CASE UNDER CLEAR SKY WITH SUN AND OVERCAST SKY CONDITIONS

Table A.2. Point-in-time daylight analysis of base case under clear sky with sun and overcast sky conditions (the black lines represent artificial lighting fixtures to illuminate areas below 300 lux. 1 line=1 fixture).



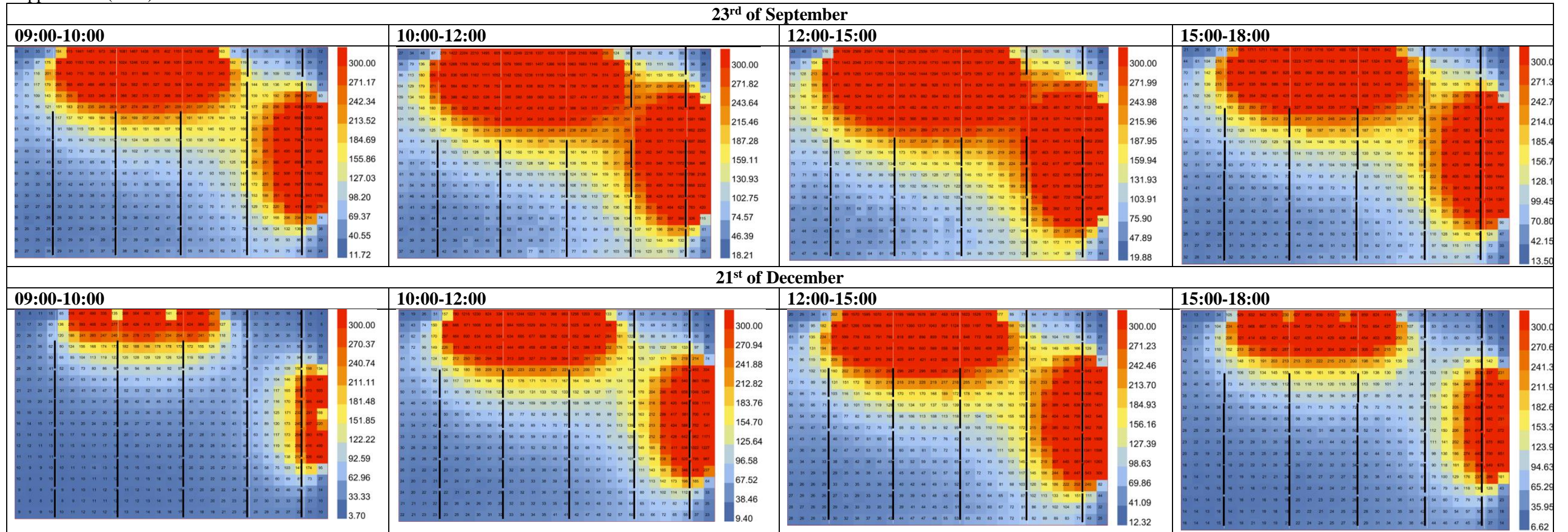
(cont. on the next page)

Appendix C (cont.)



(cont. on the next page)

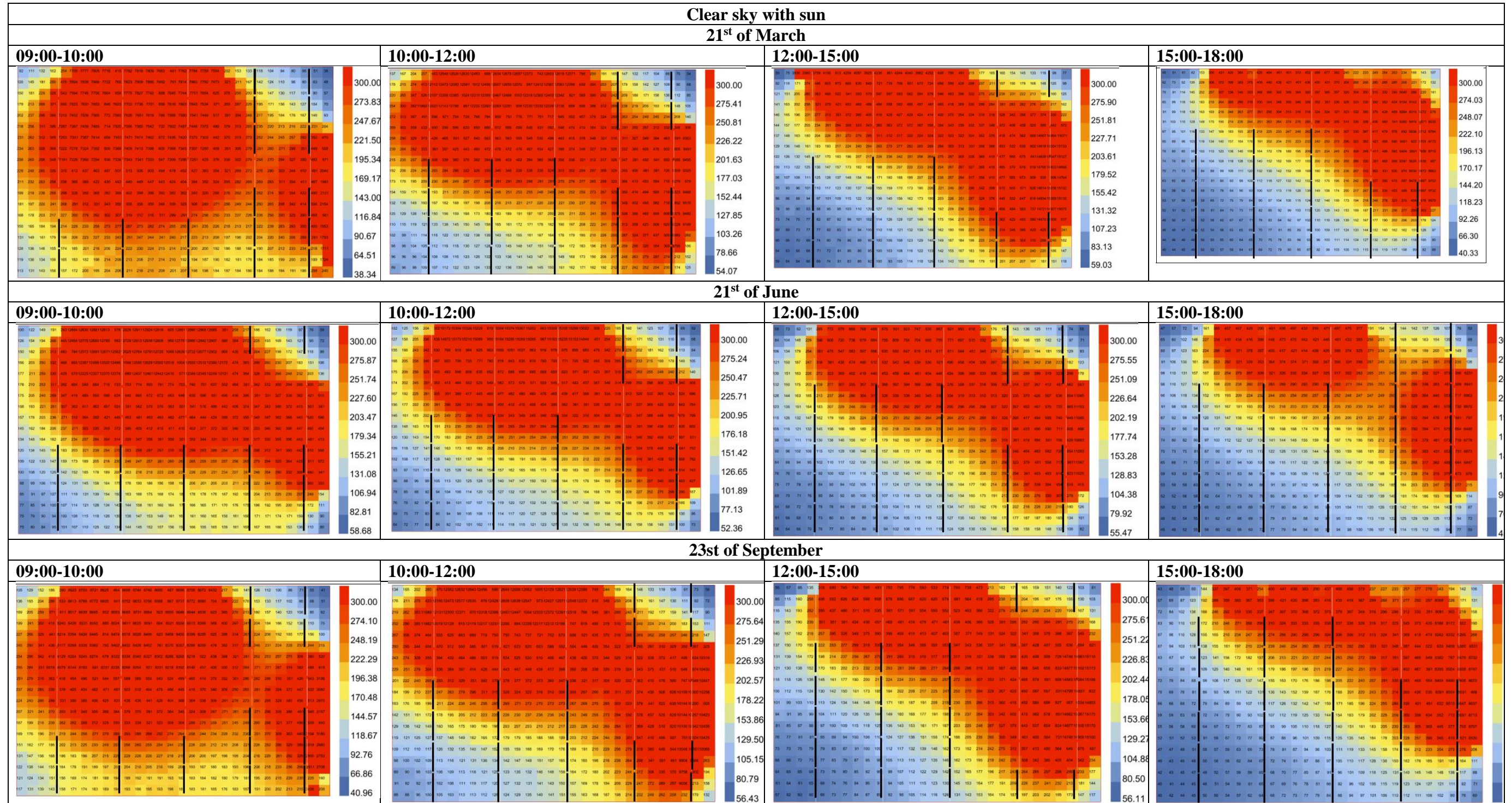
Appendix C (cont.)





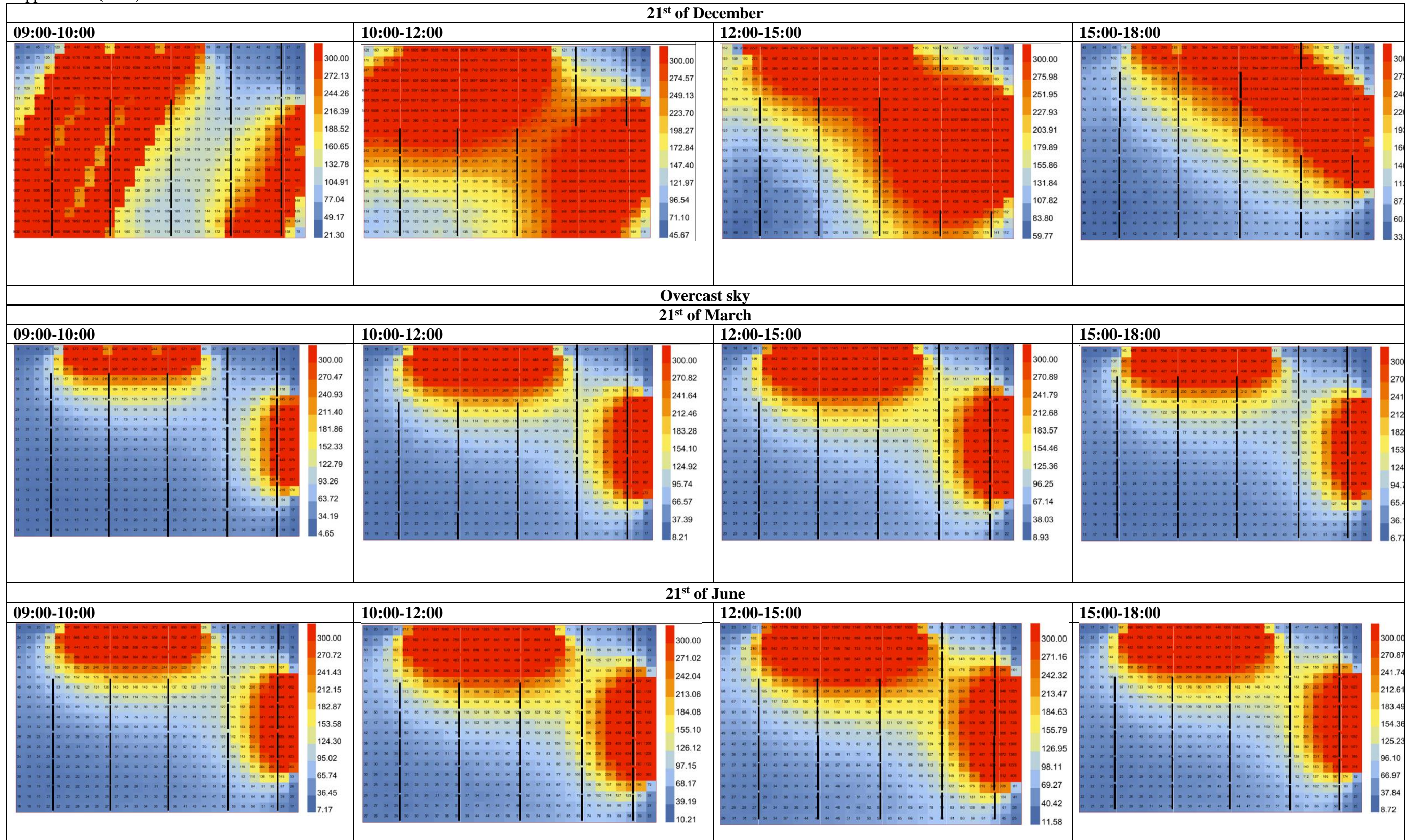
# APPENDIX D. POINT-IN-TIME DAYLIGHT ANALYSIS OF 30% TRANSMITTANCE PV WINDOW UNDER CLEAR SKY WITH SUN AND OVERCAST SKY CONDITIONS

Table A.3. Point-in-time daylight analysis of 30% transmittance PV window under clear sky with sun and overcast sky conditions

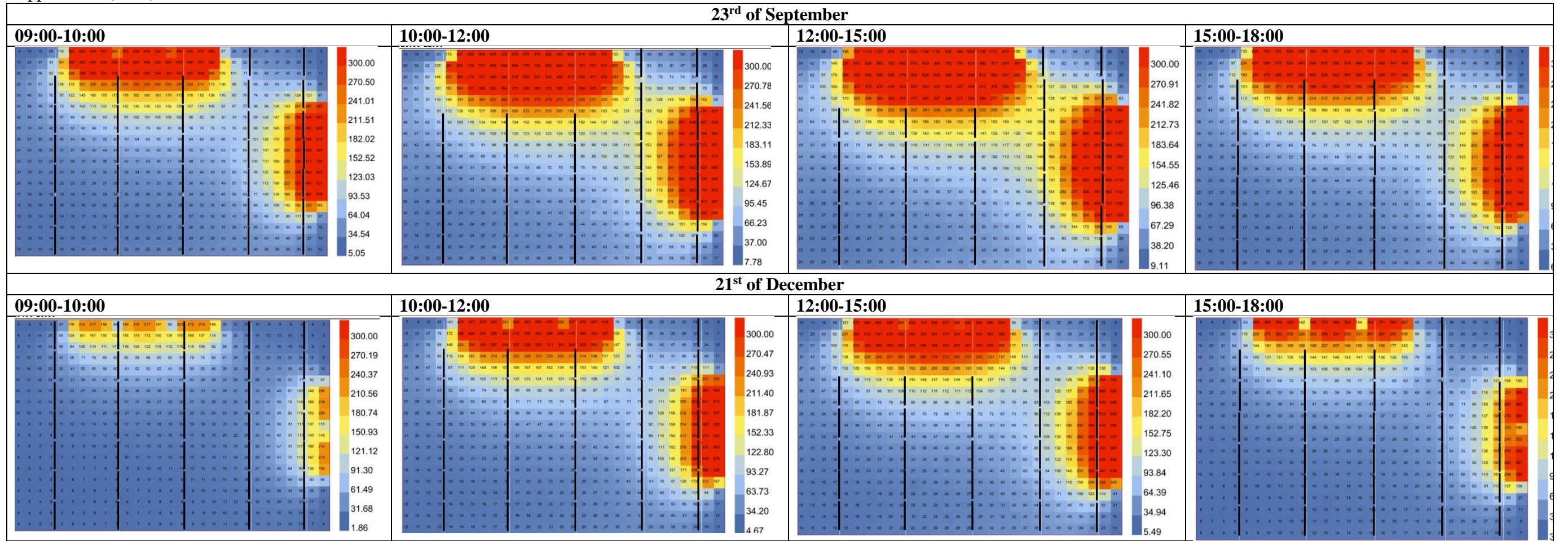


(cont. on the next page)

Appendix D (cont.)

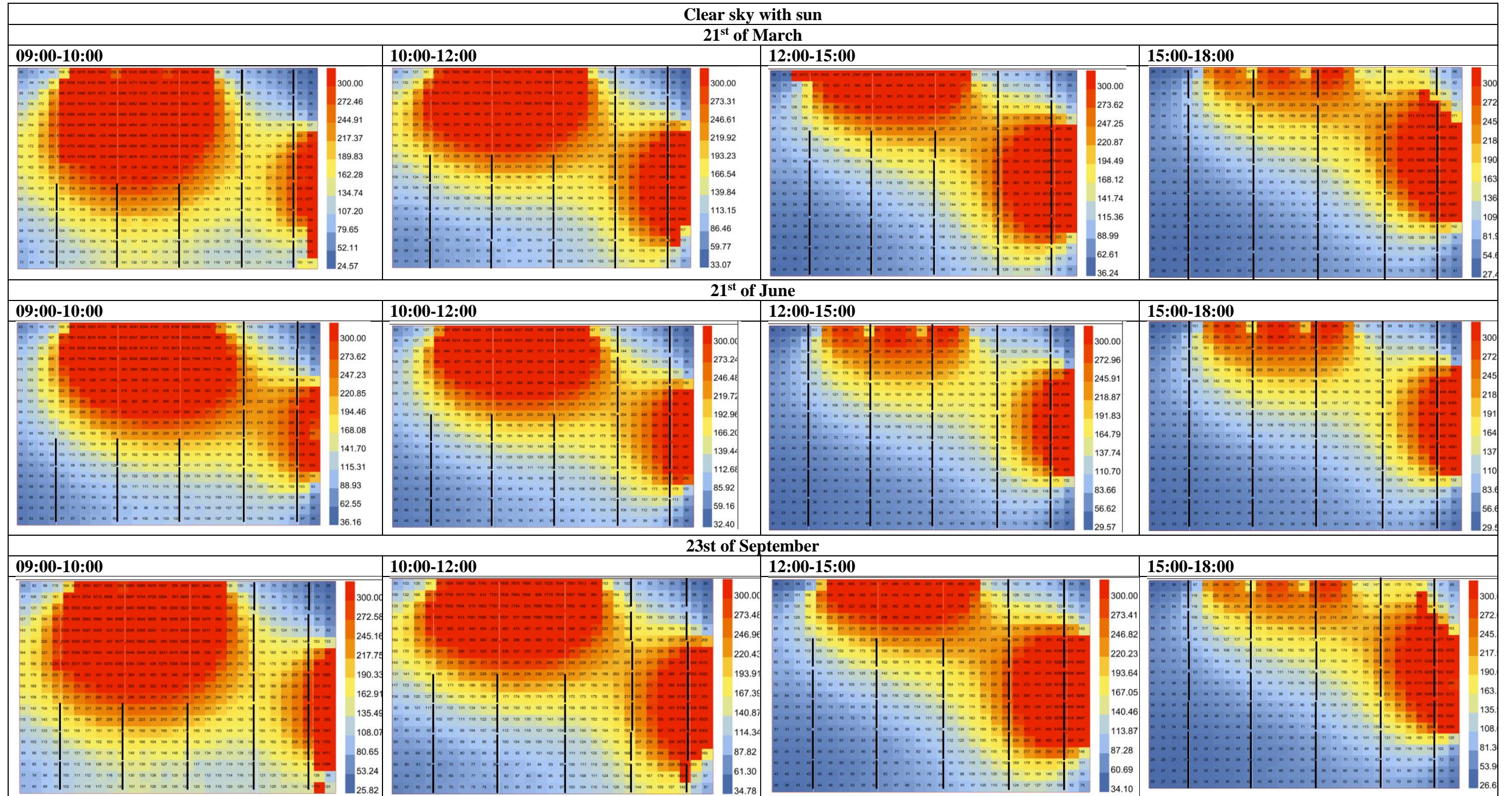


(cont. on the next page)



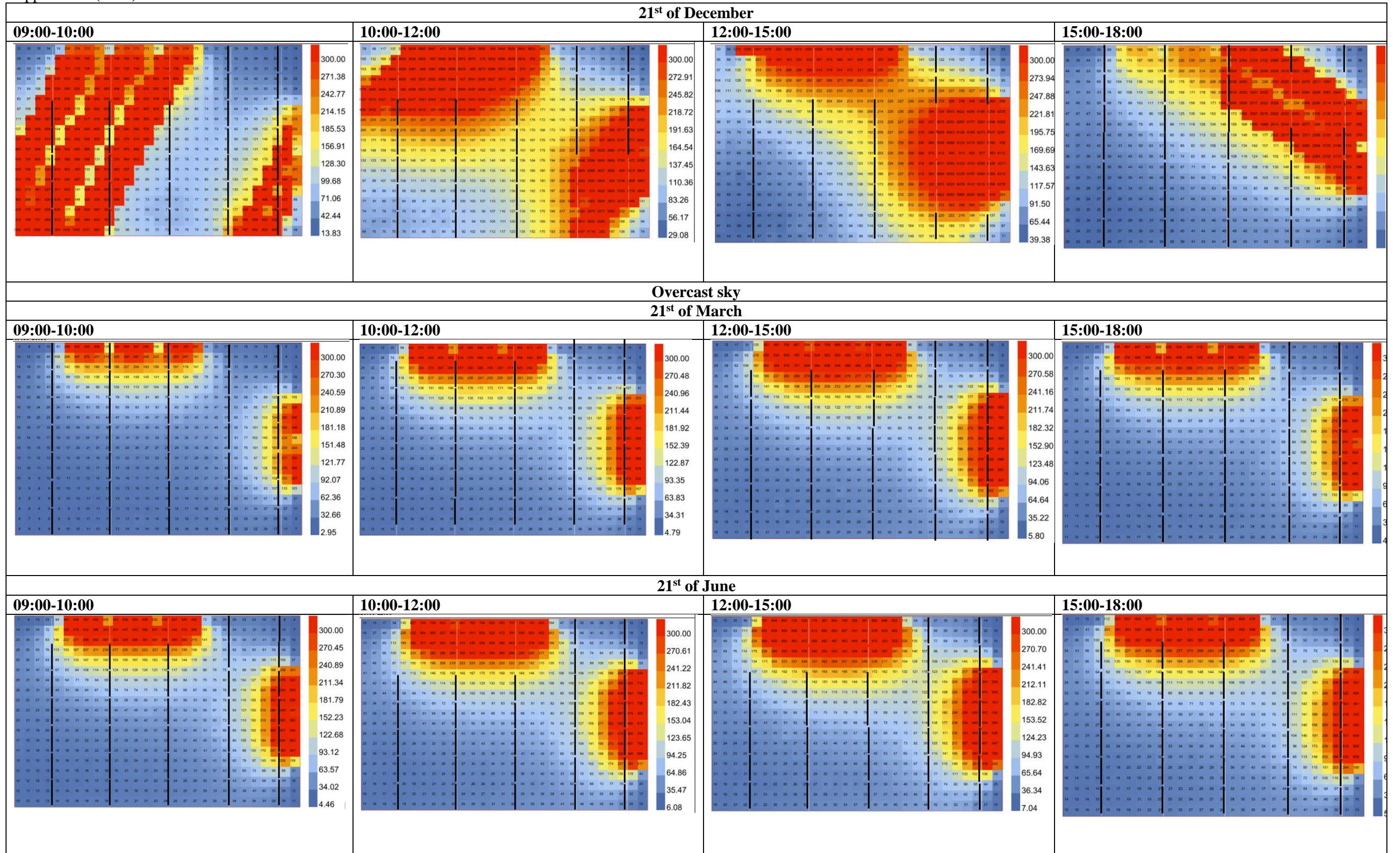
# APPENDIX E. POINT-IN-TIME DAYLIGHT ANALYSIS OF 20% TRANSPARENT PV WINDOW UNDER CLEAR SKY WITH SUN AND OVERCAST SKY CONDITIONS

Table A.4. Point-in-time daylight analysis of 20% transmittance PV window under clear sky with sun and overcast sky conditions



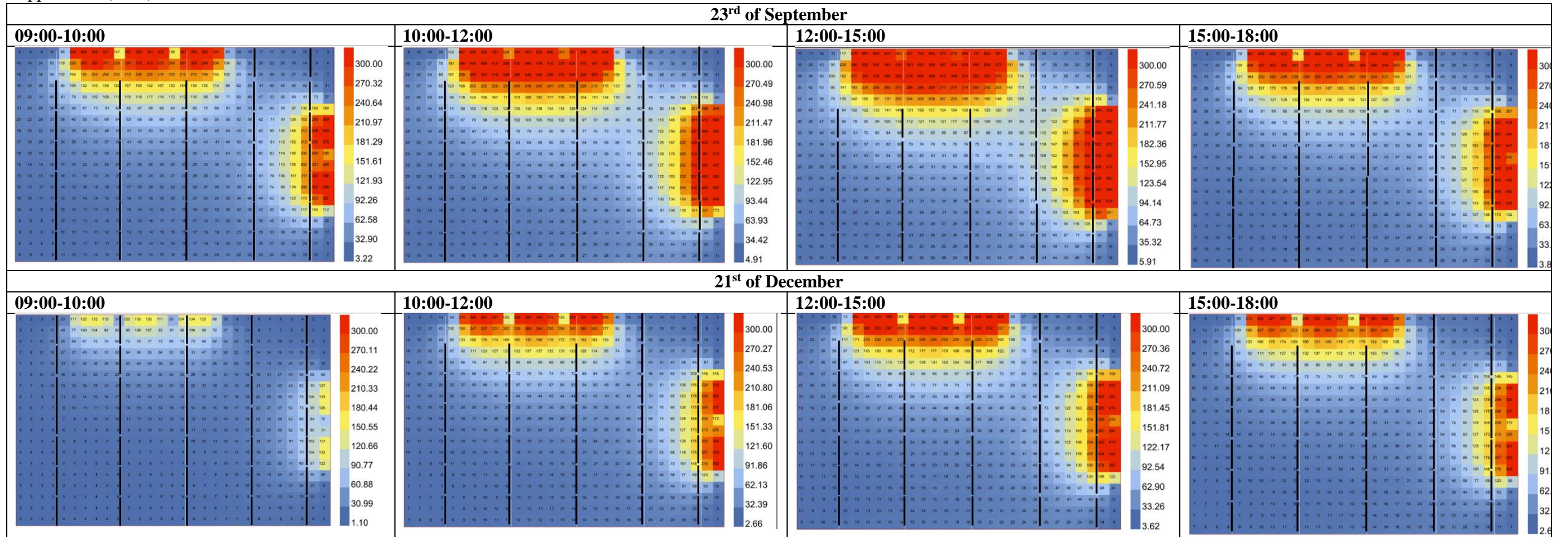
(cont. on the next page)

Appendix E (cont.)



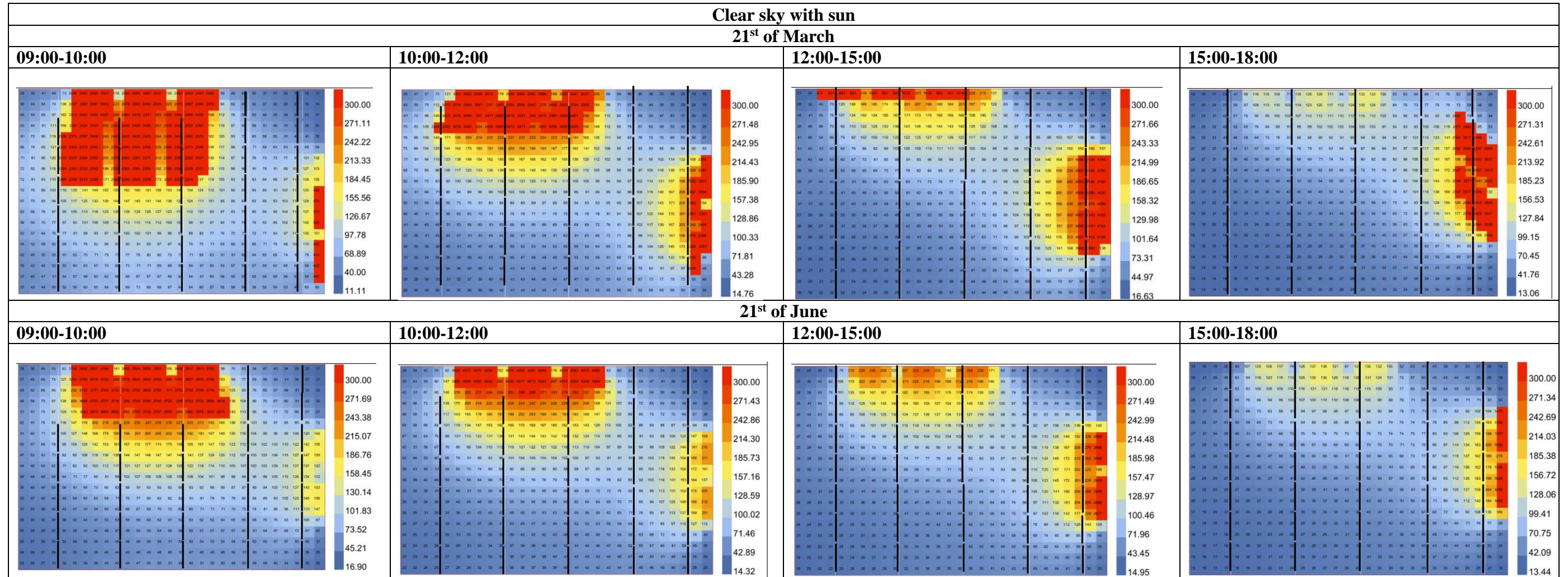
(cont. on the next page)

Appendix E (cont.)

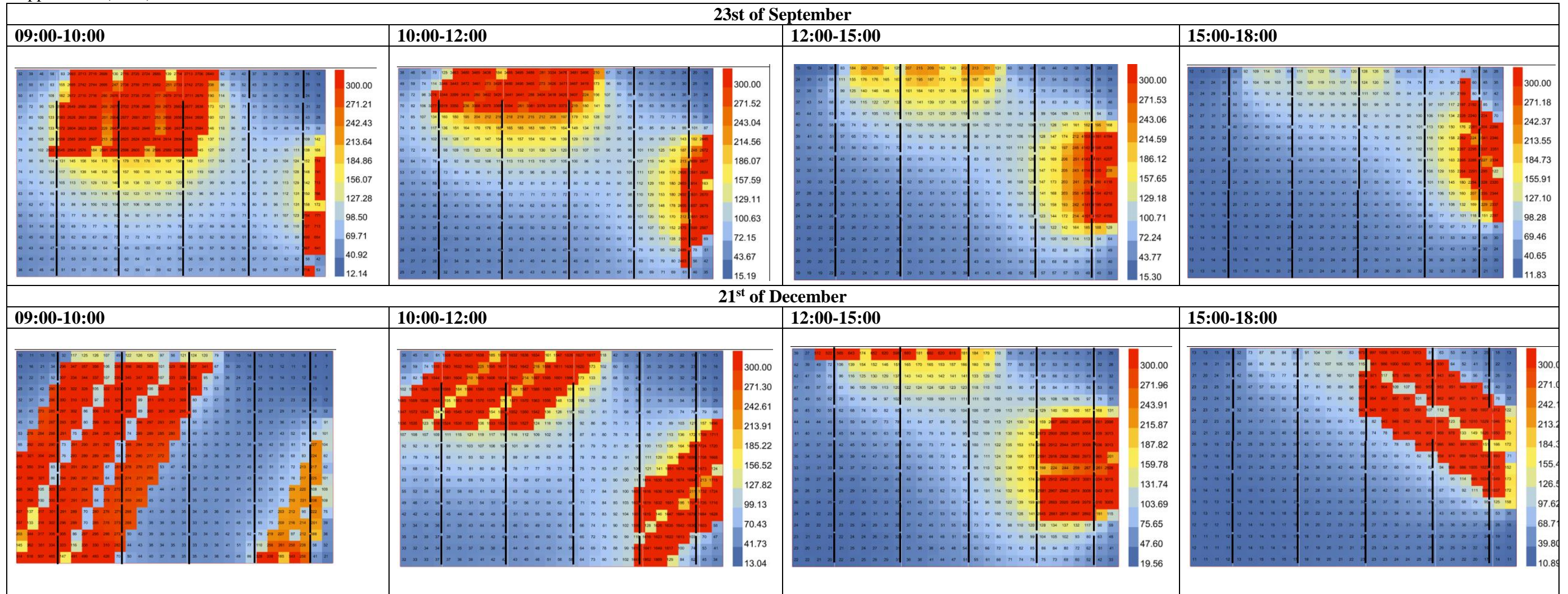


# APPENDIX F. POINT-IN-TIME DAYLIGHT ANALYSIS OF 10% TRANSPARENT PV WINDOW UNDER CLEAR SKY WITH SUN AND OVERCAST SKY CONDITIONS

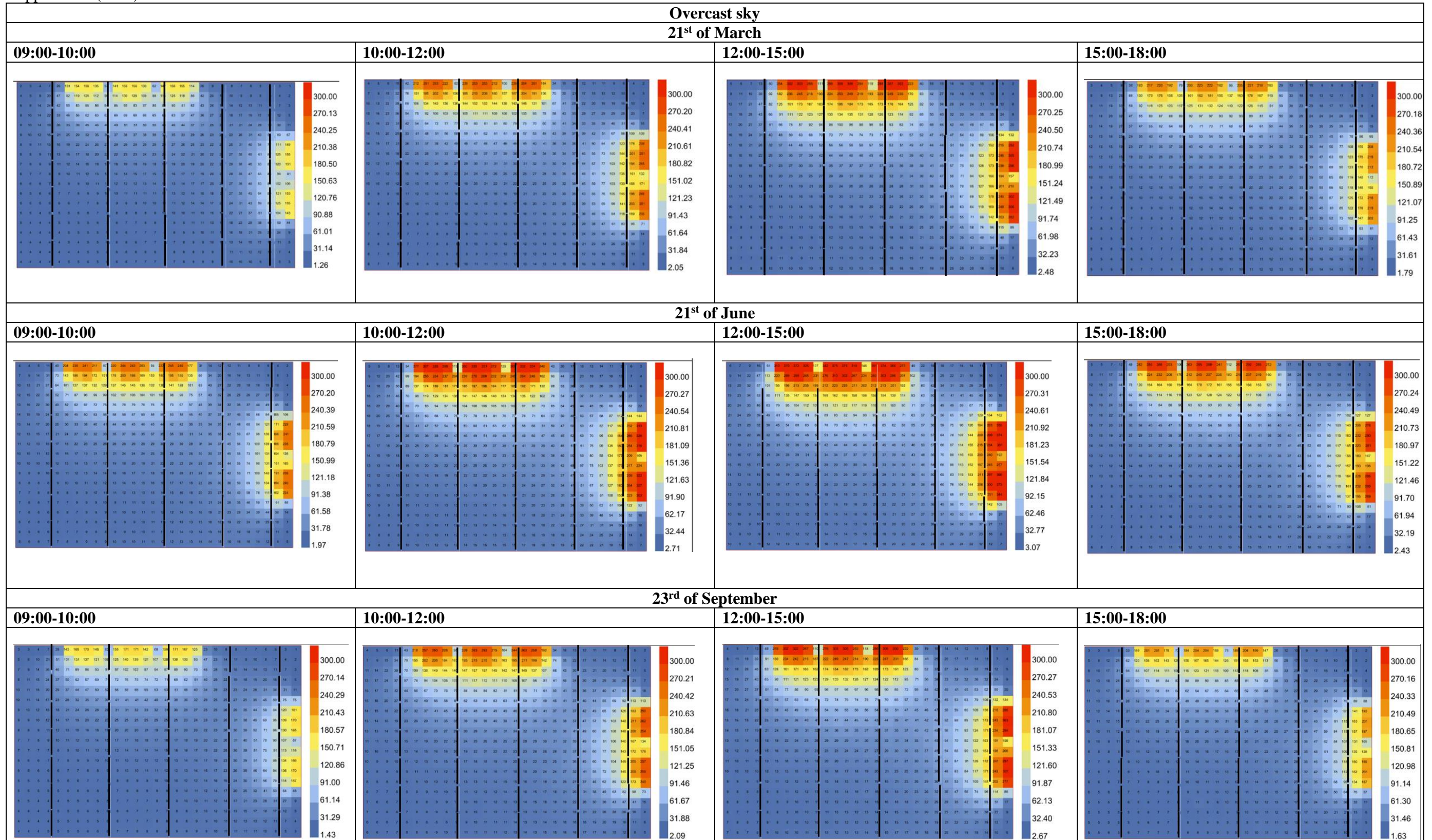
Table A.5. Point-in-time daylight analysis of 10% transmittance PV window under clear sky with sun and overcast sky conditions



(cont. on the next page)







Appendix F (cont.)

